LBL-16559
UC-94cd

Lawrence Berkeley Laboratory
UNIVERSITY OF CALIFORNIA

APPLIED SCIENCE DIVISION

RECEIVED
LAWRENCE
BERKELEY LABORATORY
NOV 1 1983
LIBRARY AND
DOCUMENTS SECTION

FUELS AND CHEMICALS FROM BIOMASS DEPOLARIZED WATER ELECTROLYSIS

M.R. St. John and A.J. Furgala

July 1983

TWO-WEEK LOAN COPY
This is a Library Circulating Copy which may be borrowed for two weeks. For a personal retention copy, call Tech. Info. Division, Ext. 6782.

APPLIED SCIENCE DIVISION

Prepared for the U.S. Department of Energy under Contract DE-AC03-76SF00098

LBL-16559 c.2

DISCLAIMER

This document was prepared as an account of work sponsored by the United States Government. While this document is believed to contain correct information, neither the United States Government nor any agency thereof, nor the Regents of the University of California, nor any of their employees, makes any warranty, express or implied, or assumes any legal responsibility for the accuracy, completeness, or usefulness of any information, apparatus, product, or process disclosed, or represents that its use would not infringe privately owned rights. Reference herein to any specific commercial product, process, or service by its trade name, trademark, manufacturer, or otherwise, does not necessarily constitute or imply its endorsement, recommendation, or favoring by the United States Government or any agency thereof, or the Regents of the University of California. The views and opinions of authors expressed herein do not necessarily state or reflect those of the United States Government or any agency thereof or the Regents of the University of California.

LBL-16559
DOE/CE/90032-13

FUELS AND CHEMICALS FROM BIOMASS DEPOLARIZED WATER ELECTROLYSIS*

Institute of Gas Technology
IIT Center, 3424 S. State Street
Chicago, Illinois 60616

Michael R. St. John
Alan J. Furgala

For the period September 28, 1981 through November 30, 1982

Submitted to:

U.S. Department of Energy
Technology Base Research Project for Electrochemical Storage
Lawrence Berkeley Laboratory
University of California, Berkeley
Berkeley, California 94720

July 1983

* This work was supported by the Assistant Secretary for Conservation and Renewable Energy, Office of Energy Systems Research, Energy Storage Division of the U.S. Department of Energy under Contract No. DE-AC03-76SF00098 and No. DE-AC02-81CE-90032.

ABSTRACT

The program's principal objective was to identify anode depolarizers derivable from biomass sources capable of reducing the overall cell voltage for electrolytic processes, in particular hydrogen generation, by replacing the oxygen evolution reaction by the thermodynamically more favorable electro-oxidation of biomass materials. A second objective was to identify the anodic reactions of the biomass materials. Two beneficial outcomes of the biomass electrooxidation were envisioned: 1) the synthesis of a desirable organic chemical from a biomass feedstock and 2) the complete electrooxidation of the biomass to CO_2, which could be used as a method of removal of unwanted or waste biomass from water. These beneficial anodic reactions would, of course, occur along with a desirable cathodic reaction such as hydrogen generation.

The biomass-derivable materials selected for investigation were chosen from the two most abundant biomass materials groups, carbohydrates and lignins. In particular, glucose, its derivatives, and its polymers were considered to be representative of the carbohydrate group and were explored. Lignins selected were those derived from the two principal pulping processes, sulfite and kraft.

These materials were surveyed for electrooxidative activity under varying experimental conditions of electrolyte (pH), anode material, and temperature. This variation in experimental conditions resulted in a great diversity of electrochemical behavior for biomass materials selected and made generalizations difficult. However, all the biomass materials examined showed some anodic activity under some set of experimental conditions at potentials prior to oxygen evolution. In fact, only very few conditions showed no activity at all. The electrooxidations were always irreversible. Several reactions were often detected under a given set of conditions; these reactions occurred at potentials ranging from +200 to +1200 mV versus RHE and exhibited current densities from a few microamperes to hundreds of milliamperes per square centimeter. Alkaline electrolytes showed the greatest electrochemical activity, followed by acid, and then neutral. Anode material had the greatest effect on the biomass electrochemical activity, indicating the catalytic nature of the reactions.

The largest current densities for carbohydrate electrooxidation were obtained with palladium, nickel, and lead ruthenate anodes, on the order of

200 mA/cm^2, which makes them likely candiates for depolarizing anode materials. The short-term data suggest that cells generating hydrogen, which were carbohydrate or lignin depolarized, could operate in the range of 600 to 1100 mV.

Reaction product analysis of glucose electrooxidation was carried out on platinum only and was found to be highly nonspecific. Electrooxidation of carbohydrates to carbon dioxide appeared possible on platinum and lead ruthenate anodes.

The program clearly identified experimental conditions at which electrochemical oxidation occurred for both carbohydrates and lignins at potentials more negative than oxygen evolution. This demonstrated that the biomass materials can depolarize the oxygen anode to some extent, but preliminary continuous electrooxidation experiments revealed continuously declining currents indicative of electrode passivation. Further work required includes the identification of reaction products, effects of concentration, and the sustainability of acceptable current densities over time. In addition, further work on the identification of suitable anode materials or electrocatalysts for biomass and organic electrooxidation is desirable because significant improvements in oxidation potentials and currents may be expected.

6H/RPE/bio-elec3

TABLE OF CONTENTS

	Page
INTRODUCTION	1
TASK 1. SELECTION OF DEPOLARIZING AGENTS	5
TASK 2. ELECTROCHEMICAL CHARACTERIZATION OF NATURAL PRODUCTS	13
General Experimental Procedures	13
Electrooxidation of Glucose	14
Platinum Anode — Platinized	18
Platinum Anode — Shiny	48
Platinum Anode — Shiny with Underpotentially Deposited Metals	49
Palladium Anode	54
Nickel Anode	59
Rhodium Anode	63
Lead Anode	65
Vitreous Carbon Anode	69
Lead Ruthenate Anode	70
Ruthenized Titanium Anode	74
Electrooxidation of Glucose Derivatives	76
Gluconic Acid Results	76
Glucaric Acid Results	81
Glucuronic Acid Results	84
Glucitol Results	88
α-Methyl-D-Glucoside Results	92
Discussion and Conclusions	95
Electrooxidation of Dextrin	98
Electrooxidation of Lignosulfonic Acid Salts	98
Platinum Anode — Shiny	101
Platinum Anode — Platinized	108
Lead Anode	112
Vitreous Carbon Anode	116
Conclusions	116

TABLE OF CONTENTS, Cont.

	Page
Electrooxidation of Other Lignin Materials	117
Kraft Lignin	117
Black Liquor	119
TASK 3. CHARACTERIZATION OF ANODIC OXIDATIONS	123
Electrooxidation of Glucose	123
Platinum Anode — Platinized	123
Lead Ruthenate Anode	140
Electrooxidation of Lignosulfonic Acid	
TASKS 4 AND 5	143
SUMMARY	145
REFERENCES CITED	149

LIST OF FIGURES

Figure No.		Page
1	Open-Chain Structures of Three Monosaccharides	7
2	Glucose and its Derivatives Related by Oxidation and Reduction	9
3	Prominent Structures of Softwood Lignin Comprising 16 Phenylpropane Units	10
4	Equilibrium Forms of D-Glucose and Their Percentages in Pure Water	16
5	Cycle Voltammogram of Platinized Platinum Specifying the Different Surface Regions of the Electrode in 1.00M H_2SO_4 at 25°C	23
6	Comparison of Cyclic Voltammograms With and Without 0.50M Glucose Present. Experimental Conditions: Electrolyte, 1.0M H_2SO_4 (pH = 0.0); Working Electrode, Platinized Pt (a) 940 cm^2 and (b) 830 cm^2; Scan Rate, 5 mV/s; Temperature, (a) 23°C and (b) 69°C.	25
7	Comparison of Cyclic Voltammograms With and Without 0.50M Glucose Present. Experimental Conditions: Electrolyte, 0.50M $HClO_4$ (pH = 0.3); Working Electrode, Platinized Pt (a) 900 cm^2 and (b) 830 cm^2; Scan Rate, 5 mV/s; Temperature, (a) 23°C and (b) 66°C.	26
8	Comparison of Cyclic Voltammograms With and Without 0.50M Glucose Present. Experimental Conditions: Electrolyte, 0.20M $NaHSO_4$/0.80M Na_2SO_4 (pH = 1.8); Working Electrode, Platinized Pt (a) 835 cm^2 and (b) 820 cm^2; Scan Rate, 5 mV/s; Temperature, (a) 23°C and (b) 66°C.	27
9	Comparison of Cyclic Voltammograms With and Without 0.50M Glucose Present. Experimental Conditions: Electrolyte, 0.22M H_3PO_4/0.77M NaH_2PO_4 (pH = 2.4); Working Electrode, Platinized Pt,(a) 888 cm^2 and (b) 813 cm^2; Scan Rate, 5 mV/s; Temperature, (a) 23°C and (b) 65°C.	28
10	Comparison of Cyclic Voltammograms With and Without 0.50M Glucose Present. Experimental Conditions: Electrolyte, 0.50M Na_2HPO_4/0.50M NaH_2PO_4 (pH = 6.6); Working Electrode, Platinized Pt (a) 872 cm^2 and (b) 830 cm^2; Scan Rate, 5 mV/s; Temperature, (a) 23°C and (b) 67°C.	29

LIST OF FIGURES, Cont.

Figure No.		Page
11	Comparison of Cyclic Voltammograms With and Without 0.50M Glucose Present. Experimental Conditions: Electrolyte, 0.30M Na_2HPO_4/0.70M Na_3PO_4 (pH = 11.7); Working Electrode, Platinized Pt (a) 889 cm^2 and (b) 813 cm^2; Scan Rate, 5 mV/s; Temperature, (a) 23°C and (b) 64°C.	30
12	Comparison of Cyclic Voltammograms With and Without 0.50M Glucose Present. Experimental Conditions: Electrolyte, 6.1M KOH (pH =14.8); Working Electrode, Platinized Pt (a) 889 cm^2 and (b) 810 cm^2; Scan Rate, 5 mV/s; Temperature, (a) 23°C and (b) 68°C.	31
13	Peak Potentials Versus pH for Glucose Electrooxidation on Platinized Pt in the Forward Scan at 23°C.	35
14	Peak Current Densities Versus pH for Glucose Electro-oxidation on Platinized Pt's H and DL Regions for the Forward Scan at 23°C	36
15	Peak Potentials Versus pH for Glucose Electrooxidation on Platinized Pt in the Forward Scan at 66°C.	39
16	Comparison of Cyclic Voltammograms of 0.50M Glucose Recorded Using Pretreatment I and Pretreatment III Experimental Conditions: Electrolyte, 1.00M H_2SO_4 (pH = 0.0); Working Electrode, Platinized Pt (898 cm^2); Scan Rate, 5 mV/s; Temperature, 22°C.	45
17	Comparison of Cyclic Voltammograms on Shiny Pt (1 cm^2) in a) 0.50M $HClO_4$ and b) 0.50M $HClO_4$/0.50M Glucose; Scan Rate, 50 mV/s; Temperature, 23°C.	51
18	Comparison of Cyclic Voltammograms on Shiny Pt (1 cm^2) in a) 0.50M $HClO_4$, b) 0.50M $HClO_4$/1.0 X 10^3M $Pb(NO_3)_2$, and c) 0.50M $HClO_4$/1.0 X 10^3M $Pb(NO_3)_2$/0.50M Glucose; Scan Rate, 50 mV/s; Temperature, 23°C.	52
19	Comparison of Cyclic Voltammograms on Shiny Pt (1 cm^2) in a) 0.50M $HClO_4$, b) 0.50M $HClO_4$/1.0 X 10^3M $Bi(NO_3)_3$, and c) 0.50M $HClO_4$/1.0 X 10^{-3}M $Bi(NO_3)_3$/0.50M Glucose; Scan Rate, 50 mV/s; Temperature, 21°C	53
20	Comparison of Cyclic Voltammograms on Shiny Pt (1 cm^2) in a) 0.50M $HClO_4$, b) 0.50M $HCLO_4$/1.3 X 10^{-3}M $TlNO_3$, and c) 0.50M $HClO_4$/1.3 X 10^{-3}M $TlNO_3$/0.50M Glucose; Scan Rate, 50 mV/s; Temperature, 21°C	55
21	Cyclic Voltammogram of 0.50M Glucose in 6.1M KOH on a Shiny Pd (1 cm^2) Anode at a 5 mV/s Scan Rate and 28°C	57

LIST OF FIGURES, Cont.

Figure No.		Page
22	Cyclic Voltammogram of Shiny Pd (1 cm^2) in 6.1M KOH Alone at a 5 mV/s Scan Rate and 23°C. Surface Reactions are Similar to Those of Pt.	58
23	Comparison of Cyclic Voltammograms With and Without 0.50M Glucose Present. Experimental Conditions: Electrolyte, 6.1M KOH (pH = 14.8); Working Electrode, Nickel (1 cm^2); Scan Rate, 5 mV/s; Temperature, (a) 22°C and (b) 67°C.	60
24	Cyclic Voltammogram of Ni (1 cm^2) in 6.1M KOH at 24°C With 5 mV/s Scan Rate	62
25	Comparison of Cyclic Voltammograms With and Without 0.50M Glucose Present. Experimental Conditions: Electrolyte, 6.1M KOH (pH = 14.8); Working Electrode, Shiny Rh (1 cm^2); Scan Rate, 5 mV/s; Temperature, 66°C.	64
26	Cyclic Voltammogram of Pb (1 cm^2) in 1.00M H_2SO_4 at a 5 mV/s Scan Rate and 23°C	66
27	Comparison of Cyclic Voltammograms With and Without 0.50M Glucose Present. Experimental Conditions: Electrolyte, 1.00M H_2SO_4 (pH = 0.0); Working Electrode, Pb (1 cm^2); Scan Rate, 5 mV/s; Temperature, 66°C.	67
28	Comparison of Cyclic Voltammograms With and Without 0.50M Glucose Present. Experimental Conditions: Electrolyte, 6.1M KOH (pH = 14.8); Working Electrode, Pb (1 cm^2); Scan Rate, 5 mV/s; Temperature, 23°C.	68
29	Comparison of Cyclic Voltammograms With and Without 0.50M Glucose Present. Experimental Conditions: Electrolyte, 6.1M KOH (pH = 14.8); Working Electrode, Vitreous Carbon (1 cm^2); Scan Rate 5 mV/s; Temperature, (a) 23°C and (b) 63°C.	71
30	Steady-State Current-Potential Curves for a Teflon-Bonded Lead Ruthenate Electrode in 1.00M H_2SO_4 With and Without 0.50M Glucose at 61°C. Potential Stepped 6 steps/min With 10 mV/step.	73
31	Steady-State Current-Potential Curves for a Teflon-Bonded Lead Ruthenate Electrode in 6.1M KOH With and Without 0.50M Glucose at 25°C. Potential Stepped 6 step/min With 10 mV/step.	75
32	Steady-State Current-Potential Curves for a Ruthenized Titantium Working Electrode in 6.1M KOH With and Without 0.50M Glucose at 25°C. Potential Stepped 3 steps/min With 10 mV/step.	77

LIST OF FIGURES, Cont.

Figure No.		Page
33	Comparison of Cyclic Voltammograms With and Without 0.50M Potassium Gluconate Present. Experimental Conditions: Electrolyte, 1.33M H_2SO_4; Working Electrode, Platinized Pt (788 cm^2); Scan Rate, 5 mV/s; Temperature, (a) 23°C and (b) 67°C.	79
34	Comparison of Cyclic Voltammograms With and Without 0.50M Potassium Gluconate Present. Experimental Conditions: Electrolyte, 6.1M KOH; Working Electrode, Platinized Pt (484 cm^2); Scan Rate, 5 mV/s; Temperature, (a) 23°C and (b) 60°C.	82
35	Comparison of Cyclic Voltammograms With and Without 0.50M Monopotassium Glucarate Present. Experimental Conditions: Electrolyte 1.26M H_2SO_4; Working Electrode, Platinized Pt (801 cm^2); Scan Rate, 5 mV/s; Temperature, (a) 28°C and (b) 61°C.	85
36	Comparison of Cyclic Voltammograms With and Without 0.50M Monopotassium Glucarate Present. Experimental Conditions: Electrolyte, 6.1M KOH; Working Electrode, Platinized Pt (746 cm^2); Scan Rate, 5 mV/s; Temperature, (a) 26°C and (b) 62°C.	86
37	Comparison of Cyclic Voltammograms With and Without 0.50M Glucuronic Acid, 6,4 Lactone Present. Experimental Conditions: Electrolyte, 1.00M H_2SO_4; Working Electrode, Platinized Pt (728 cm^2); Scan Rate, 5 mV/s; Temperature, 23°C.	89
38	Comparison of Cyclic Voltammograms With and Without 0.50M Glucitol Present. Experimental Conditions: Electrolyte, 1.00M H_2SO_4; Working Electrode, Platinized Pt (825 cm^2); Scan Rate, 5 mV/s; Temperature, (a) 23°C and (b) 64°C.	90
39	Comparison of Cyclic Voltammograms With and Without 0.50M Glucitol Present. Experimental Conditions: Electrolyte, 0.50M NaH_2PO_4/0.50M Na_2HPO_4 (pH =6.6); Working Electrode, Platinized Pt (825 cm^2); Scan Rate, 5 mV/s; Temperature, (a) 24°C and (b) 65°C.	93
40	Glucose and its Derivatives Shown to Emphasize the Differences in Terminal Carbon Groups	96
41	Comparison of Cyclic Voltammograms With and Without 100 g/L Dextrin Present. Experimental Conditions: Electrolyte, 1.00M H_2SO_4; Working Electrode, Platinized Pt (801 cm^2); Scan Rate, 5 mV/s; Temperature, (a) 24°C and (b) 61°C.	99

LIST OF FIGURES, Cont.

Figure No.		Page
42	Comparison of Cyclic Voltammograms With and Without 100 g/L Dextrin Present. Experimental Conditions: Electrolyte, 6.1M KOH; Working Electrode, Platinized Pt (764 cm^2); Scan Rate, 5 mV/s; Temperature, (a) 22°C and (b) 62°C.	100
43	Comparison of Cyclic Voltammograms With and Without 100 g/L Lignosulfonic Acid, Na Salt. Experimental Conditions: Electrolyte, 1.00M H_2SO_4 (pH = 0.0); Working Electrode, Shiny Pt (1 cm^2); Scan Rate, 5 mV/s; Temperature, 24°C.	102
44	Comparison of Cyclic Voltammograms With and Without 100 g/L Lignosilfonic Acid, Na Salt Present. Experimental Conditions: Electrolyte, 1.00M H_2SO_4; Working Electrode, Shiny Pt (1 cm^2); Scan Rate, 5 mV/s; Temperature, (a) 23°C and (b) 62°C.	105
45	Comparison of Cyclic Voltammograms With and Without 100 g/L Lignosulfonic Acid, Na Salt Present. Experimental Conditions: Electrolyte, 0.50M NaH_2PO_4/0.50M Na_2HPO_4 (pH = 6.6); Working Electrode, Shiny Pt (1 cm^2); Scan Rate, 5 mV/s; Temperature, 24°C.	106
46	Comparison of Cyclic Voltammograms With and Without 100 g/L Lignosulfonic Acid, Na Salt Present. Experimental Conditions: Electrolyte, 6.1M KOH (pH =14.8); Working Electrode, Shiny Pt (1 cm^2); Scan Rate, 5 mV/s; Temperature, (a) 26°C and (b) 64°C.	107
47	Comparison of Cyclic Voltammograms With and Without 100 g /L Lignosulfonic Acid, Na Salt Present. Experimental Conditions: Electrolyte, 1.00M H_2SO_4 (pH = 0.0); Working Electrode, Platinized Pt (1200 cm^2); Scan Rate, 5 mV/s; Temperature, (a) 24°C and (b) 65°C.	110
48	Schematic Illustration of a Lignin Fragment Approaching a Platinized Pt Electrode	114
49	Comparison of Cyclic Voltammograms With and Without 100 g/L Lignosulfonic Acid, Na Salt (Pfaltz & Bauer) Present. Experimental Conditions: Electrolyte, 0.50M H_2SO_4; Working Electrode, Pb (1 cm^2); Scan Rate, 5 mV/s; Temperature, 23°C.	115
50	Comparison of Cyclic Voltammograms With and Without 100 g/L Kraft Lignin. Experimental Conditions: Electrolute, 6.1M KOH; Working Electrode, Shiny Pt (1 cm^2 Geometrical); Scan Rate, 5 mV/s; Temperature, a) 24°C and b) 64°C	118

LIST OF FIGURES, Cont.

Figure No.		Page
51	Cyclic Voltammograms of Weak Black Liquor on Shiny Pt (1 cm^2) Immediately After Receipt and After Exposure to the Atmosphere for ~20 Hours; Scan Rate, 5 mV/s; Temperature, 23°C.	120
52	Chronoamperogram of Glucose Oxidation at +450 mV Versus SCE. Experimental Conditions: Electrolyte, 0.50 Glucose/1.00M H_2SO_4; Anode, Platinized Platinum (428 cm^2); Temperature, 68° ± 3°C; Error Bars Indicate Standard Deviation for 3 Measurements.	125
53	Potential-Time Curve for the Oxidation of Glucose in Acid at a Constant Current of 5 mA	128

LIST OF TABLES

Table No.		Page
1	Anode Depolarizing Reactions and Their E°'s	3
2	Biomass Materials Investigated	12
3	Anode Materials Investigated for Glucose Electrooxidation	17
4	Compositions and pH's of Electrolytes Used in the Voltammetry Study of the Electrooxidation of Glucose	17
5	Anodic Peak Potentials and Current Densities From the Cyclic Voltammograms for the Electrooxidation of Glucose on Platinized Platinum at Ambient Temperature and Variable pH	32
6	Anodic Peak Potentials and Current Densities From the Cyclic Voltammograms for the Electrooxidation of Glucose on Platinized Platinum at Elevated Temperature and Variable pH	33
7	Comparisons of Peak Potentials and Current Densities in the Cyclic Voltammograms for the Oxidation of Glucose on Platinized Platinum and Shiny Platinum	49
8	Peak Potentials and Peak Current Densities for the Cyclic Voltammetry of Glucose in 6.1M KOH on a Rh Electrode at 65° C	64
9	Potential Required to Attain 2 mA/cm^2 in the Cyclic Voltammetry of Glucose in Phosphate Buffer at 5 mV/s in Vitreous Carbon	70
10	Anodic Peak Potentials and Current Densities in the Cyclic Voltammograms for the Electrooxidation of 0.5M Potassium Gluconate in 1.33M H_2SO_4 at Variable Temperature	80
11	Anodic Peak Potentials and Current Densities From the Cyclic Voltammograms for the Electrooxidation of 0.43M Potassium Gluconate in 6.1M KOH at Variable Temperature	83
12	Peak Potentials and Current Densities in the Cyclic Voltammograms for the Electrooxidation of Glucaric Acid on Platinized Pt in 6.1M KOH	87
13	Anodic Peak Potentials and Current Densities in the Cyclic Voltammograms for the Electrooxidation of 0.50M Glucitol in 1.00M H_2SO_4 at Variable Temperature	91

LIST OF TABLES, Cont.

Table No.		Page
14	Anodic Peak Potentials and Current Densities From the Cyclic Voltammograms for the Electrooxidation of 0.50M Glucitol in 0.50M NaH_2PO_4/0.50M Na_2HP_4O at Variable Temperature	94
15	Lignosulfonic Acid Salts and Selected Properties	101
16	Peak Potentials and Current Densities for the Lignosulfonic Acid Salts Listed in Table 15	104
17	Cyclic Voltammetric Potentials and Current Densities for the Electrooxidation of Lignosulfonic Acid, Na Salt in 6.1M KOH on Shiny Platinum	109
18	Real and Geometric Current Densities for the Lignosulfonic Acids at +725 and 1210 mV vs. SCE at 26° and 62°C	111
19	Effect of Pt Electrode Roughness Factor on the Cyclic Voltammmetry Geometric and Real Current Densities for Electrooxidation of Lignosulfonic Acid	113
20	Typical Composition of the Organic Material in Pine Kraft Spent Liquor	120
21	Chronoamperometry Results: Charge Passed per 60 min and Selected Current Density Under Varying Conditions on Platinized Platinum Anode	126
22	5-mA Chronopotentiometry of Fresh Glucose Solutions	130
23	Comparison of Low Potential Plateau Data for Variable Current	130
24	Consecutive 5-mA Chronopotentiometry in the Same Glucose Solution	131
25	Potentials at Selected Times During the Electrolysis of Glucose in H_2SO_4 on Platinized Platinum at 65°C	131
26	Plateau Data of the Potential-Time Curve for the Electrooxidation of 0.50M KOH at 10 mA/cm^2 and 25°C	133
27	Charge Passed in 1.0 Hours by Various Electrolysis Schemes for the Electrooxidation of Glucose	136
28	Results of Glucose Electrolyses in 1.00 H_2SO_4 on Platinized Pt	137

INTRODUCTION

This program was directed at the investigation of the anodic reactions of materials originating from biomass sources. Several purposes for such an investigation can be enumerated. The primary emphasis was on the identification of depolarizing agents derivable from biomass sources whose electrochemical oxidation occurs at potentials more negative than oxygen evolution. In this manner, the substitution of the biomass electrooxidation for the oxygen evolution reaction in those electrolyses in which it is the anodic reaction will lead to a reduction in cell voltage and, thereby, lower power consumption. The cathodic reaction of greatest interest here, and whose overall power requirements are to be reduced by depolarization of the anode, was electrochemical H_2 generation, but other desirable reductions carried out in aqueous electrolytes such as metal electrowinning could also be considered.

The incentive behind the use of a depolarizing agent can be readily appreciated by analyzing the components contributing to the total cell potential for an electrolysis:

$$E_{cell} = E^0 + \eta_A + \eta_C + \eta_{IR} \qquad (1)$$

where —

E° = thermodynamic reversible potential

η_A = anodic overpotential

η_C = cathodic overpotential

η_{IR} = ohmic overpotential

E° is the minimum cell potential required for the electrolysis and is entirely fixed by the overall reaction of interest. The ohmic overpotential will be present in any cell, but it is subject to minimization by proper cell design. The anodic and cathodic overpotentials are a function of the kinetics for the particular cathodic and anodic reactions and are subject to manipulation only through the difficult task of identifying suitable electrocatalysts which can lower the activation energy for reaction.

In the case of conventional water electrolysis great effort has been expended on the reduction of the overpotentials, particularly at the anode. Although progress has been made in identifying electrocatalysts to reduce the overpotentials, they still account for an appreciable fraction of the total

cell potential. Typically they account for 0.4 to 0.6 V out of a total cell potential of 1.8 to 2.0 V at acceptable reaction rates. The largest component of the total cell potential in conventional water electrolyses is E°, which under standard conditions amounts to 1.23 V. As noted earlier, no reduction in this value is possible for the particular overall reaction considered. Any large reduction in cell potential will by necessity require a change in the overall reaction, which is capable of reducing E°. For a fixed, desirable cathodic reaction like H_2 generation, this means a change in the anodic reaction or depolarization of the anode.

Anode depolarization reactions that have drawn recent attention are given in Table 1. In each case the E° obtained using one of the depolarizing half reactions is reduced by greater than 1.0 V with the oxidation of hexoses, such as glucose, yielding the most favorable value. One view of the depolarizer is that its oxidation provides energy for splitting the water molecule, thereby resulting in attractively small E° values. The depolarizer should meet the following criteria: 1) abundant, 2) low cost, which is usually associated with abundance, 3) fuel-like in character, which yields favorable thermodynamics via its oxidation, and 4) rapid electrode kinetics, which is of course desirable for any electrochemical reaction. The biomass-derivable materials under consideration here are believed to meet criteria 1 through 3 while virtually nothing was previously known about the fourth. This general group of materials has the additional advantage of originating from nonfossil fuel, renewable sources which are often found as wastes.

Although substantial reduction in cell potential for cathodic reactions of interest, such as H_2 generation, is in itself valuable, the existence of a complementary anode reaction carrying out something beneficial would be very advantageous and perhaps even necessary for the overall success of this type of electrolysis process. Possible beneficial anode reactions envisioned are the removal of unwanted biomass-derived materials from aqueous waste streams by complete electrooxidations to CO_2 or the electro-synthesis of desirable organic chemicals from these materials. In recognition of this fact, the identification of the reaction products generated by electrooxidation of the biomass-derivable materials was an important second purpose of the program.

Data gathered during the course of the program also provided general scientific information on the electrochemical oxidation of the organic

Table 1. ANODE DEPOLARIZING REACTIONS AND THEIR E°'s

Anodic Half Reactions	E°, V[c,d]	References
$C(s)^a + 2H_2O(l) \rightarrow CO_2(g) + 4H^+(aq) + 4e^-$	-0.21	1-6
$SO_2(g) + 2H_2O(l) \rightarrow SO_4^{2-}(aq) + 4H^+(aq) + 2e^-$	-0.14	7,8
$C_6H_{12}O_6(s)^b + 6H_2O(l) \rightarrow 6CO_2(g) + 2rH^+(aq) + 24e^-$	+0.01	9, this work
$2H_2O(l) \rightarrow O_2(g) + 4H^+(aq) + 4e^-$	-1.23	

a. Carbon or coal.

b. Hexose sugars.

c. Calculated by coupling the anodic half rreaction given. With the cathodic half reaction, $2H^+ + 2e^- \rightarrow H_2$.

d. A positive sign denotes a spontaneous reaction whereas a negative sign is not.

materials available in biomass which could have application in other areas. For example, electrochemical sensors for biomass materials (such as glucose) and fuel cells operating by oxidation of biomass molecules are of interest in medicine. Thus, a third and indirect purpose was the generation of useful scientific knowledge on organic electrochemistry — particularly of those organic materials which can be derived from a biomass source.

The program was organized along the following lines. The first task was to identify and acquire those chemicals for experimentation which have been loosely referred to as biomass-derivable materials in the earlier text. As the second task, those chemicals selected in Task 1 were surveyed by appropriate potential sweep methods for identification of any anodic electrochemical reactivity under experimental conditions of variable anode material, electrolyte composition, and temperature. Those promising materials and experimental conditions identified in Task 2 were investigated further in Task 3 by conducting actual bulk electrolyses. These electrolyses allowed identification of reaction products and any difficulties associated with decline in electrode performance. In the event that a potentially attractive electrolysis reaction was identified in the prior task work, methods of product isolation and their economic viability were to be addressed in Tasks 4 and 5, respectively.

TASK 1. SELECTION OF DEPOLARIZATION AGENTS

The biomass-derivable materials considered here to be of greatest interest are those which are the most abundant or available as waste materials. These two groups are most often the same because wastes originate from abundant materials in most instances. On the basis of organic carbon, nearly all plant biomass can be found in two general material groups, carbohydrates and lignins. Consequently, these materials and substances derivable from them were selected for investigation as possible anode depolarizers.

Carbohydrates constitute the largest segment of biomass and exhibit well-defined, simple chemical structures consisting of single monossaccharides (simple sugars), oligosaccharides, and their polymers, polysaccharides.[10-13] By far the most prevalent carbohydrate found in nature is the polysaccharide, cellulose. It is built up of the single, simple monosaccharide, glucose, which may be obtained by chemical or biological degradation of cellulose.[14]

The other major constituent of naturally occurring carbohydrates is hemicellulose. Like cellulose, hemicellulose is a polymer constructed from simple monosaccharides linked together. However, more than one type of monosaccharide is found in the hemicellulose structure. In addition to glucose, the other hexoses (galactose, mannose) and pentoses (xylose, arbinose) are prevalent.[15-17]

Because monosaccharides are the principal and simplest molecular units of the carbohydrate group, they were selected for initial investigation as anode depolarizers. Also, from an electrochemical point of view, the monosaccharides would be preferred over the polysaccharides on a steric and solubility basis. Another reason for the selection of monosaccharides was that prior literature reports of electrochemical oxidation of glucose and other monosaccharides existed.[18-22] This literature is, in general, rather old and the data gathered have not been concerned with the dependency of anode potential on the particular electrooxidation occurring, largely because experiments were conducted using constant current rather than controlled potential. Of course, the knowledge of potential is critical for the depolarizing questions. This lack of attention to potential is a serious defect in the organic electrochemical literature with either anode potentials not being reported at all or very large potentials, e.g. 50 V, being applied in order to maintain the desired reaction rate (current). In addition, this

prior work provided little information on the role either of anode material or electrolyte composition on the electrochemical oxidation of the monosaccharide, and actual product analysis was minimal.

Emphasis was placed on the electrooxidation of glucose for several reasons. First, it is the most abundant monosaccharide. Second, because of the common structural elements among monosaccharides and oligosacharides, glucose may be expected to act as a prototype for this group of compounds. Figure 1 gives the open-chain structures of the hexoses, glucose and mannose, and the pentose, xylose, which illustrate the dominant alcoholic nature of their functionality and the structural similarity among monosaccharides. After base data on the electrochemical oxidation of glucose have been collected, differences in the electrooxidation properties among the soluble carbohydrates will be of great interest.

Third, prior literature demonstrated that, at least under some circumstances, some electrochemical oxidation of glucose was possible. This literature may be divided into two chronological periods. The early period, prior to 1945, is almost exclusively devoted to the oxidation of glucose to gluconate, and an industrial process for the production of calcium gluconate was actually adopted for awhile.[23,24] In this early work glucose was not electrochemically oxidized directly, but was oxidized indirectly by hypobromite ions produced electrochemically from bromide ions present in catalytic amounts. Here the electrochemical reaction is essentially bromide oxidation, and no information on direct glucose oxidation is available. It does, however, offer another avenue of approach to the oxidation of glucose via an electrochemically reactive redox couple; no effort was expended on this approach, however.

Interest in the oxidation of glucose and other carbohydrates that began in the late 1960's has been associated with medical applications, which include the development of an <u>in-situ</u> fuel cell that uses glucose as the fuel for pacemakers and a glucose sensor for diabetic applications.[25-40] Because of their intended medical applications, most of these studies were experimentally very restricted in terms of electrolyte and anode material. Platinum was nearly always the anode material, and a near-neutral physiological buffer was the electrolyte. This limited the scope of these studies because the chemical entities and reactivity of glucose solutions depend on the components

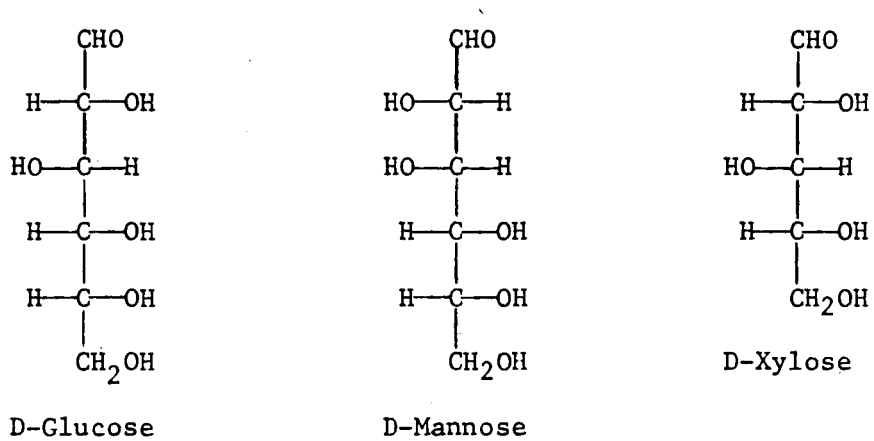

Figure 1. OPEN-CHAIN STRUCTURES OF THREE MONOSACCHARIDES

of the solution, or in this case the electrolyte.[41-43] Although considerable data were available on the electrochemical oxidation of glucose under physiological conditions, this data had only limited application to the work presented here. In addition, results obtained from the literature were not entirely consistent, and possible reasons for this will be discussed in Task 2.

Prior experimentation at IGT conducted before the beginning of this program was in the area of glucose electrooxidation[9] and a fourth, more practical reason to pursue glucose was to allow continuity with this previous effort. For these reasons, the majority of the work performed in the program was directed at the investigation of glucose electrooxidation under a variety of experimental conditions to be discussed in the tasks that follow.

Derivatives of glucose that are related by oxidation or reduction were also selected for investigation, and these included gluconic acid, glucaric (saccharic) acid, and glucitol as shown in Figure 2. These glucose derivatives were of interest because the partially oxidized derivatives are also found in biomass sources,[44] particularly processed or waste biomass, and their investigation yields valuable information on the continued oxidation of glucose.

The heterogeneous carbohydrate substance, dextrin, was also chosen for study. Dextrin is a mixture of glucose monomers and soluble glucose polymeric units produced by the hydrolysis of starch and, as such, was considered to be representative of a more realistic sample in which the soluble carbohydrates are derived from hydrolysis of an insoluble glucose polymer.

The other major biomass constituent of interest is lignin, which is chemically a much less well-defined entity in comparison to the carbohydrates. Soluble lignins are a myriad of fragments derived from the parent lignin polymer via a given degradation or extraction process.[13,45-49] Consequently, no finite number of chemical structures can be defined for the lignins, and their properties are, in part, dependent on the process by which the lignin was prepared. Nonetheless, the polymeric units are constructed from phenylpropane-type units which are bonded together in a finite number of ways and dominate the chemistry.[13] Figure 3 illustrates a partial structure proposed for softwood lignin. Lignin typically accounts for around 25% of the dry weight of woody biomass and is the portion put to the least use.

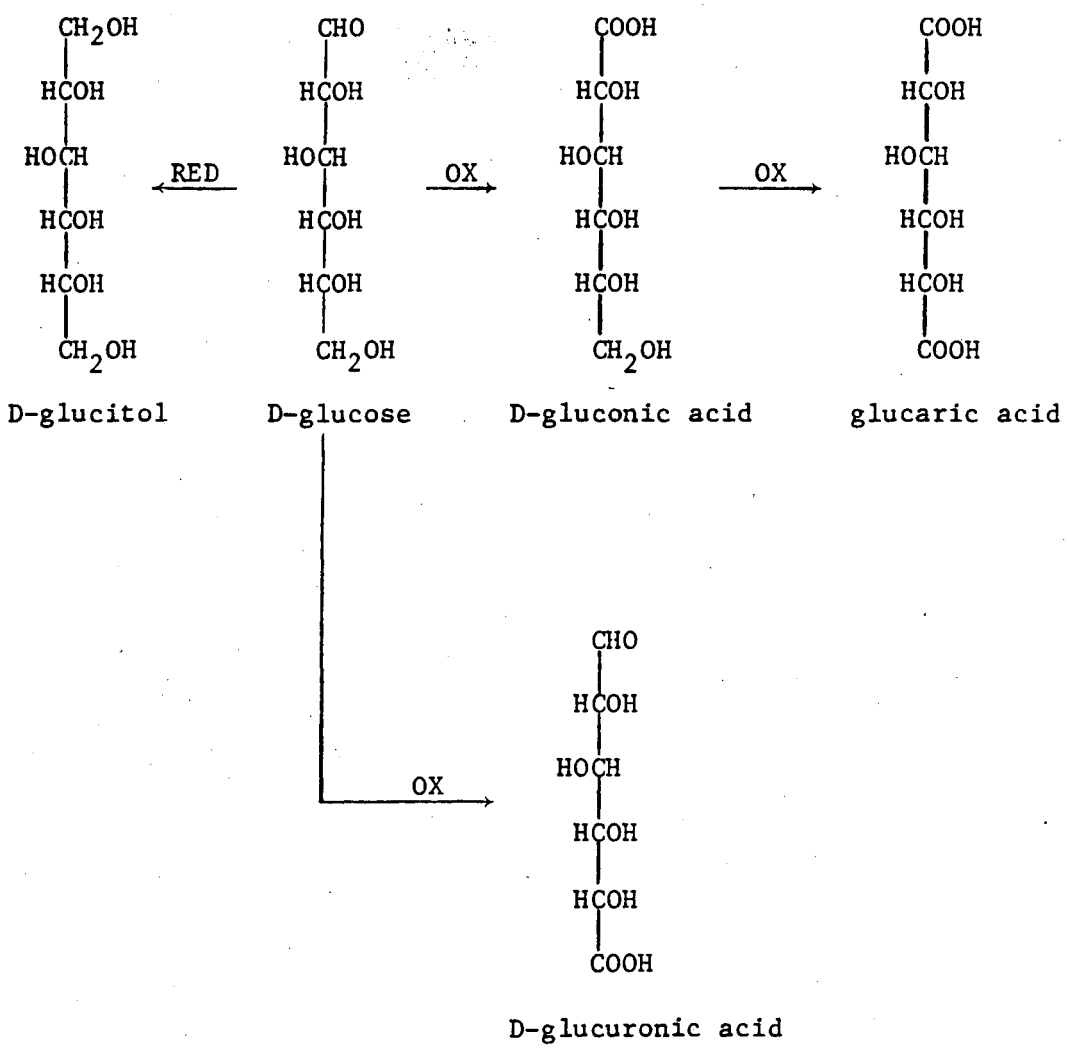

Figure 2. GLUCOSE AND ITS DERIVATIVES RELATED BY OXIDATION AND REDUCTION

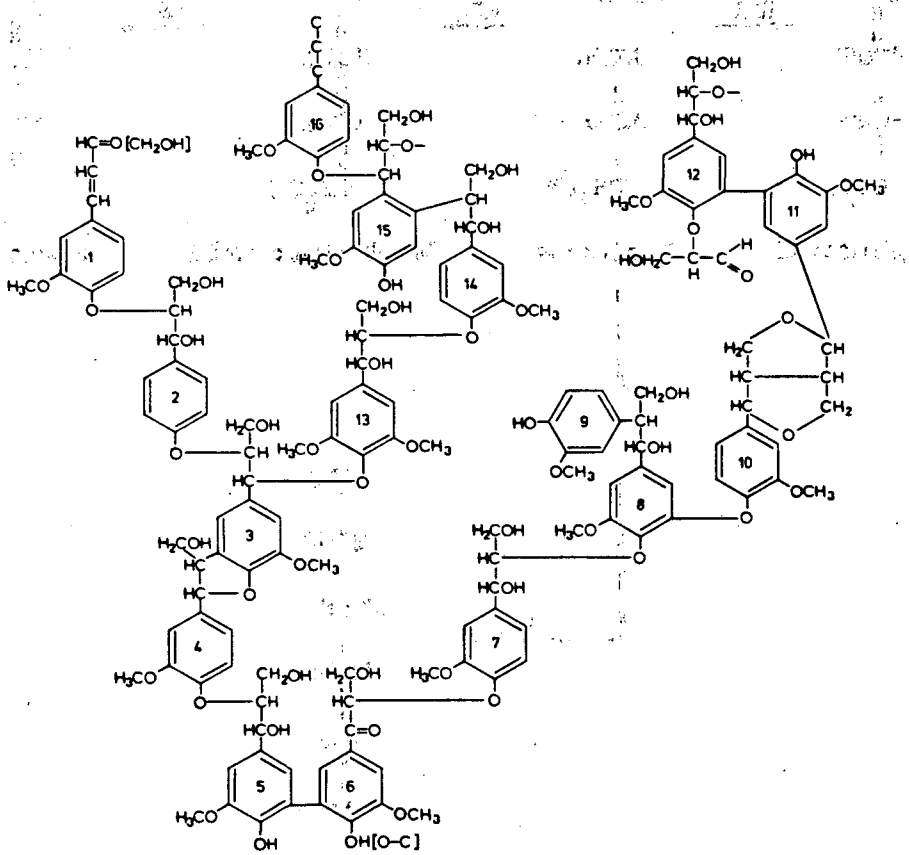

Figure 3. PROMINENT STRUCTURES OF SOFTWOOD LIGNIN COMPRISING 16 PHENYLPROPANE UNITS (From Reference 13)

Therefore identification of ways to better utilize lignins would be of great value. The aromatic structures contained in the lignin could potentially be a valuable source of this type of compound if selected bond cleavages could be performed.

Existing information on the electrochemical oxidation of lignin is even more meager than on the carbohydrates[50-55] and consists of some recent Russian reports [51-55] and work on model compounds.[56-60] Although this information had little direct applicability to the work performed here, it did show the possibility of lignin electrooxidation and suggested possible products.

A selection of lignosulfonates from the sulfite pulping process were suggested and provided by the pulp and paper industry for testing. The lignin materials provided were Orzan A (an ammonium lignosulfonate), Orzan S (an acidic sodium lignosulfonate), Orzan LS (an alkaline sodium lignosulfonate), and Product 1120 (a calcium lignosulfonate).

Two types of lignin materials derived from the kraft pulping process were tested. One was the heterogeneous raw spent pulping liquid, the black liquor, and the other was kraft lignin precipitated from the black liquor by acidification. Thus the materials derived from the two major pulping processes could be investigated.

In addition the lignins (conidendrins and conidendrols) were provided. These are dimeric phenylpropane-type units which may be useful as model compounds for the lignin structures.

Table 2 is a list of the biomass-derivable materials on which some experimental data were obtained.

Table 2. BIOMASS MATERIALS INVESTIGATED

- Carbohydrates and Related Compounds
  - Glucose
  - Glucose Derivatives
    - Glucitol
    - Gluconic Acid
    - Glucaric (Saccharic) Acid
    - Glucuronic Acid
    - α-Methyl Glucoside
  - Dextrin
- Lignins
  - Lignosulfonic Acid Salts
  - Kraft Lignin
  - Pulping Black Liquor

TASK 2. ELECTROCHEMICAL CHARACTERIZATION OF NATURAL PRODUCTS

There is general lack of available literature on the electrochemistry of biomass-derived materials. Consequently, this deficiency dictated that a general investigation to identify experimental conditions showing electro-oxidative activity of the biomass materials be performed as a necessary first step. Such an investigation was the purpose of this task and was performed using voltammetric procedures. In this manner, reaction conditions could be rapidly identified that were worthy of further study. The major effort of the program was expended on this task. The variables explored for a given biomass material were electrolyte (pH), anode material, and temperature. The diversity of the biomass materials' electrooxidative behavior upon changing these variables was found to be extraordinarily great. As the results will show, the variable exhibiting the greatest effect on the electrooxidations was the anode material. This result highlights the importance of electrocatalysis in the electrooxidation of biomass-derived materials. After a brief description of the general experimental procedures used, the voltammetric results and their discussion will be presented under the heading of each biomass material.

General Experimental Procedures

Cyclic voltammetry was the method most often used in surveying the selected biomass materials for electrooxidation under varying conditions of electrolyte composition, anode material, and temperature. A PAR 173 Potentiostat equipped with a PAR 376 Logarithmic Current Converter and potential control by a PAR 175 Universal Programmer provided the necessary electronics for recording cyclic voltammograms. Data were recorded at a scan rate of 5 mV/s under all experimental conditions. This relatively slow rate allowed quasi-steady-state currents to be attained. Higher scan rates, 100 and 1000 mV/s, were occasionally used in attempts to gain insight into the electrochemical processes, but the 5 mV/s rate proved the most informative. The cyclic voltammograms were always recorded over the entire potential range available to the electrolyte starting at the most negative potential, near H_2 evolution, and scanning to more positive potentials, near O_2 evolution. The scan from the most negative potential to the most positive potential will be referred to as the forward scan, and the return from positive to negative potentials will be referred to as the reverse scan. In most instances a PAR

K0047 Corrosion Cell was employed as the electrochemical cell, and working electrodes were flat plates held in a PAR K105 Flat Specimen Holder, which exposed an electrode geometric area of 1 cm^2. In all electrolytes except strong alkaline, either a saturated calomel electrode (SCE) or a mercury/mercurous sulfate electrode (MSE) was used as the reference. The use of MSE as the reference was found to be necessary for recording accurate cyclic voltammograms with Pt anodes because of the interfering effect of Cl^- when the SCE was used. The SCE and MSE were separated from the reaction solution by vycor tips. A mercury/mercuric oxide (Hg/HgO) electrode with an asbestos separator was used as the reference in strong alkaline electrolytes. A graphite rod separated from the electrolyte by a fine glass frit served as the counter electrode. The electrolyte was deaerated by purging with high-purity N_2 prior to recording of voltammograms, except in those few experiments in which the effect of O_2 was investigated. All chemicals were used as received without additional purification. In general, electrolytes were chosen to span a range of pH from strongly acidic to strongly alkaline whenever possible. A limited temperature survey was conducted under all conditions by recording voltammograms at ambient temperature (23° ± 3°C) and 65° ± 4°C. The elevated temperature was attained by placement of the reaction cell in a water bath regulated by an Omega Model 4001 temperature controller.

Cyclic voltammograms recorded with metal oxide anodes at a 5 mV/s scan rate were not very informative because of the large background currents, typically 10 to 30 mA. At a fixed potential these currents would disappear in 5 to 30 seconds, and consequently, information was obtained by recording steady-state current potential (I-V) or log I-potential (log I-V) curves. This was accomplished by stepping the working electrode potential at an appropriate rate (typically 6 steps/min with 10 mV/step) through the desired potential range with a Wenking SMP72 Scanning Potentiometer while recording either I or log I.

In all cases, evidence of biomass electrooxidation was determined by comparing either cyclic voltammograms or I-V curves in the electrolyte alone with those containing the electrolyte plus the biomass material of interest.

Electrooxidation of Glucose

During the program a wide range of experimental conditions that employed different anode materials, temperatures, and electrolytes were surveyed for

glucose electrooxidation. Those anode materials investigated are listed in Table 3. Electrolytes were chosen to cover a range of pH from strong acid to strong base; a listing of the electrolytes used for the glucose study is given in Table 4. Over this range of pH the solution chemistry of glucose, as well as other monosaccharides, is quite diverse,[41-43] and although the term glucose will be used throughout, it should always be recognized that this term refers to the collection of molecular species derivable from glucose when it is placed in a particular aqueous environment. For example, even in the simplest case when glucose is dissolved in pure water, it exists as an equilibrium mixture of three forms: the α- and β-ring structures and the open-chain structure of D-glucose as shown in Figure 4.[43] Even though the α and β anomers differ only by the orientation at the number one carbon, large differences have been observed in the rates of chemical oxidation of the anomers,[61] and a report observing similar behavior during electrochemical oxidation also exists.[26] Thus even small changes in the molecular structure may lead to significant reactivity changes, and detailed descriptions of the electrooxidation process become exceedingly difficult.

The glucose concentration used throughout was 0.50M. The sources of the glucose used in the experiments were Baker anhydrous dextrose (D-glucose) and Sigma α-D-glucose. The vast majority of work was performed with the Baker glucose. Gas chromatography/mass spectrometry (GC/MS) of the trimethylsilated solids revealed that the two sources were essentially identical and were composed predominantly of the α form with a few percent β. No other chromatographically detectable signals were observed, which indicated that the sources were pure, at least to the 0.1% level. The concentration of glucose used in the voltammetric work was relatively high, 0.50M, and as will be seen, real current densities were often small, differing greatly from values anticipated on the basis of diffusion of bulk glucose. These circumstances of high concentration and low currents could lead to signals derived from impurities of the sample. To insure against such a possibility, high-purity D-glucose (Baker Ultrex) was acquired, and cyclic voltammograms were recorded with it using Pretreatment I (to be discussed) in 1.00M H_2SO_4 and 6.1M KOH on platinized Pt. In the acid electrolyte, cyclic voltammograms obtained from the Ultrex and regular glucose were alike in every way. Cyclic voltammograms recorded with the Ultrex glucose in KOH exhibited the same qualitative features as before although with somewhat greater resolution of peaks.

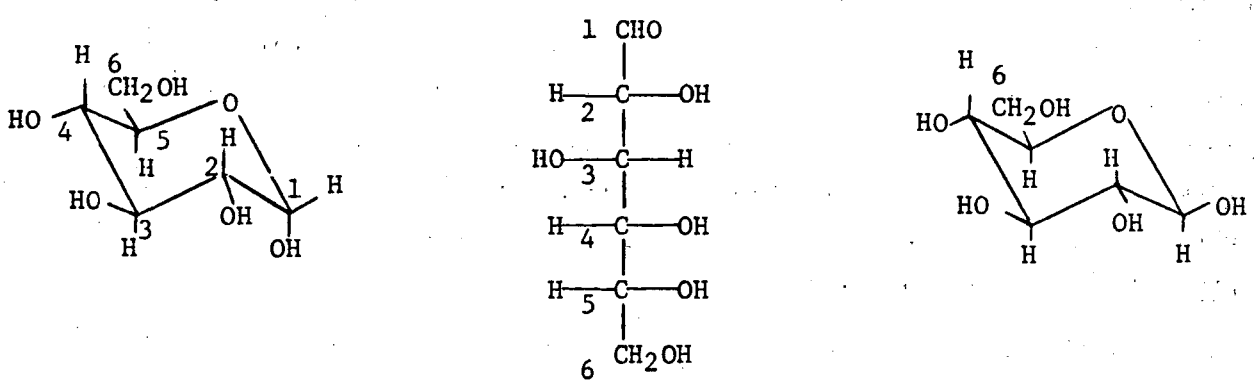

α	γ (Open Chain)	β
37%	0.003%	63%

Figure 4. EQUILIBRIUM FORMS OF D-GLUCOSE AND THEIR PERCENTAGES IN PURE WATER. THE CARBON NUMBERING SCHEME IS SHOWN FOR THE α AND γ FORMS

Table 3. ANODE MATERIALS INVESTIGATED FOR GLUCOSE ELECTROOXIDATION

Platinum (Pt) - Shiny
Platinized
Underpotential Deposited Bi, Tl, and Pb
Palladium (Pd)
Nickel (Ni)
Rhodium (Rh)
Lead (Pb)
Vitreous Carbon
Lead Rutenate ($Pb_2[Ru_{2-x}Pb_x]O_{7-y}$)
Ruthenized Titanium (RuO_x/Ti)

Table 4. COMPOSITIONS AND pH's OF ELECTROLYTES USED IN THE VOLTAMMETRY STUDY OF THE ELECTROOXIDATION OF GLUCOSE

No.	Electrolyte Composition	pH
1	1.00M H_2SO_4	0.0
2	0.50M $HClO_4$	0.3
3	0.20M $NaHaSO_4$/0.80M Na_2SO_4	1.8
4	0.22M H_3PO_4/0.77M NaH_2PO_4	2.4
5	0.50M NaH_2PO_4/0.50M Na_2HPO_4	6.6
6	0.30M Na_2HPO_4/0.70M Na_3PO_4	11.7
7	6.1M KOH	14.8

These results obtained with high-purity glucose indicate that the normal glucose used was electrochemically pure, and information obtained with it arises only from glucose electrooxidation.

Because the solid glucose was not in the equilibrium proportions of α and β forms found in aqueous solutions, as given in Figure 4, some time is required for it to be attained upon dissolution, a process referred to as mutarotation. Mutarotation is catalyzed by acid and base and is slowest in neutral solutions. An effort was made to detect a time dependence associated with mutarotation at pH = 6.6 on platinized Pt by periodic recording of cyclic

voltammograms but none was ever observed. Therefore, equilibrium mixtures of glucose species were believed to exist in all solutions except where specifically noted.

As chemical degradation of the glucose may occur with time especially in strong acid or base,[41,42] a limited number of stability tests were conducted. These tests consisted of comparing cyclic voltammograms of glucose recorded on platinized Pt at different time intervals and glucose analysis by high-pressure liquid chromatography (HPLC). At pH = 0.0, no changes were obtained between a voltammogram recorded for a solution left at ambient temperature overnight and the original solution. HPLC results of 0.50M glucose solutions at this pH, which were heated at 65°C for periods from 16 to 18 hours, showed no decline in glucose concentration within 5 wt %, indicating that no bulk degradation occurred. Ambient temperature solutions always remained clear, although solutions heated to 65°C acquired a slight yellow tinge after several hours. Heating a solution at 58°C for 18 hours using the pH = 6.6 electrolyte also resulted in a negligible change in the voltammograms recorded before and after this time period.

Ambient temperature solutions of glucose prepared with the pH = 14.8 electrolyte became yellowed immediately, and heating to 60°C turned the solution a dark, opaque brown. Cyclic voltammograms recorded during this color change significantly changed. In addition, no glucose signal was detected by HPLC for a pH = 14.8 sample that was heated at 65°C for 4 hours. These results indicate that the bulk of the glucose is stable under the experimental conditions used except when a pH = 14.8 electrolyte is heated, in which case complete degradation of the glucose occurs.

Further specific discussion of the glucose electrooxidation results will be organized according to anode material.

Platinum Anode — Platinized

The capability of electrooxidizing glucose on platinized Pt anodes was surveyed using cyclic voltammetry. Results obtained with this anode material were the most extensive because Pt is one of the most important anode materials and because it provided a common point of interest with prior literature. Substantial difficulty was encountered in recording reproducible cyclic voltammograms of glucose on platinized Pt, and special procedures were

developed during the course of the program which eventually gave good reproducibility.

Experimental. Experimentally platinized Pt anodes were prepared by platinizing the 1-cm^2 geometric area exposed by the electrode holder in a standard manner as described in Reference 62. To stabilize the platinized Pt anodes toward area changes, they were cycled in 1.00M H_2SO_4 between oxygen and hydrogen evolution until further cycling resulted in negligible area change. Real areas from 600 to 1200 cm^2 per 1 cm^2 of geometric area were obtained.

The true electrode areas were determined at regular intervals by measuring the charge necessary to cathodically strip the adsorbed hydrogen from the electrode in an electrolyte of 1.00M H_2SO_4 as described in Reference 63. The charge was determined by graphically integrating the current-potential curve in the hydrogen region and dividing by the scan rate, typically 200 mV/s. The conversion factor used to convert charge to area was 210 $\mu C/cm^2$.[64]

Cyclic voltammograms of glucose were recorded with the platinized Pt anode in all the electrolytes listed in Table 4. Recording cyclic voltammograms is often highly dependent on the initial condition of the electrode surface which is determined by the electrode pretreatment. This is particularly true of electrode materials like Pt, which adsorbs molecules strongly. Thus, reproducible cyclic voltammograms require experimental procedures which yield the same starting surface for the electrode; obtaining such a surface on Pt with its great ability to adsorb substances is very difficult. Several procedures were explored, and the most frequently used are given below.

Platinized Pt Electrode Pretreatments

Pretreatment I

A. External Pretreatment (performed in a cell external to the reaction cell)

1. Electrode surface cleaning by anodic and cathodic galvanostatic cycling in 1.00M H_2SO_4

33 seconds at 300 mA cathodic	
33 seconds at 300 mA anodic	3 times
33 seconds at 300 mA cathodic	

2. Stripping of hydrogen layer

Potentiostatted at +300 mV versus SCE
until I <0.1 mA

B. Transfer Procedure to Reaction Cell

1. Rinsed throughly in Millipore water

2. Inserted into reaction cell containing 0.50M glucose and electrolyte

C. Internal Pretreatment (performed in reaction cell)

1. Electrode held at open-circuit potential with stirring for 5.0 minutes

2. Electrode held at start potential for 5.0 minutes and scan begun.

Pretreatment II

A. External Pretreatment — same as Pretreatment I

B. Transfer Procedure to Reaction Cell — same as Pretreatment I

C. Internal Pretreatment

1. Electrode held at start potential for 10 minutes (electrode exposed to glucose at open circuit momentarily upon insertion)

Pretreatment III

A. External Pretreatment — same as Pretreatment I

B. Transfer Procedure to Reaction Cell

1. Rinsed thoroughly in Millipore water

2. Inserted into reaction cell containing only electrolyte

C. Internal Treatment

1. Electrode held at start potential for 10 minutes

2. Cyclic voltammogram of electrolyte recorded — this checks the condition of the Pt surface

3. Glucose concentrate added to electrolyte with electrode at start potential

4. Electrode held at start potential for 10 minutes and scan begun.

In Step C3 of Pretreatment III, the concentrated glucose solution was 3.00M containing the same salt concentrations as the electrolyte, and 100 mL of the concentrate was added to 500 mL of electrolyte from a separatory funnel in a period less than 20 seconds. The pretreatments are listed in the order of their development. Pretreatment III was the final version which gave good reproducible results.

Initially, cyclic voltammograms were recorded between potentials defined by the appearance of hydrogen evolution at the negative end to oxygen evolution at the positive end in order to cover the whole potential range available to the electrolyte. Most of the cyclic voltammograms were recorded using this potential criteria for the boundaries. However, because of concern for the effect that the presence of hydrogen may have on the reproducibility of the voltammogram, the following procedure was adopted in defining the start potential so that no hydrogen interference would be possible. The electrode was potentiostatted negatively in the electrolyte of interest, and an I-V curve was generated in the region where significant H_2 evolution occurred. The initial linear portion of the curve would be extrapolated to zero current, and the potential would be determined. The start potential was then determined by adding +50 mV to the extrapolated value in order to insure that no H_2 would be evolved. The potential was then swept 1.5 or 1.6 V in the positive direction. Those cyclic voltammograms that gave the most reproducible results had their scan range defined in this manner.

Early work recorded cyclic voltammograms at scan rates of 5, 100 and 1000 mV/s in hopes of acquiring information available from the variation of peak potential and current as a function of this experimental variable. However, the most informative voltammograms were recorded at the 5 mV/s scan rate. They exhibited the clearest definiton of individual peaks and also approximated steady-state currents more accurately. Faster scan rates broadened features severely and shifted potentials to more positive values, as expected for irreversible reactions, although lack of IR compensations may have been a factor in this distortion as well. At the 1000 mV/s scan rate no distinct features were visible at all; the voltammograms showed only gradually rising currents as a function of potential. Consequently, the higher scan rates were abandoned, and only results obtained at the 5 mV/s scan rate will be considered here.

The SCE was used as the reference electrode for most of the work, but the MSE was employed in order to avoid the presence of Cl^- for the recording of the final, best results. In strong alkaline electrolyte, 6.1M KOH, the Hg/HgO electrode provided the reference.

The electrolyte was deaerated by purging with high purity N_2 prior to recording cyclic voltammograms, except in those few experiments in which the effect of O_2 was investigated.

Results and Discussion. In aqueous electrolyte the Pt electrode is not inert over the potential range available, but exhibits a well-known series of surface reactions as the potential is changed.[65,66] The electrocatalytic properties of the different surfaces presented are often found to be distinct, and it is convenient to discuss the Pt electrode results in terms of the potential regions corresponding to each particular surface. Figure 5 illustrates this behavior showing the division of the regions in 1.00M H_2SO_4. The basic form of the cyclic voltammogram remains essentially unchanged with pH except for a shifting of the potentials. Temperature also has little effect on the Pt surface voltammogram. The different regions correspond to different surfaces at the Pt electrolyte interface, which often control the electrochemical processes. The hydrogen (H) region represents a surface composed of Pt metal and adsorbed hydrogen. In the double-layer (DL) region only the Pt metal surface is exposed. In the third region called the "Pt-oxide" (Pt-O), the surface consists of a platinum-oxygen complex or "Pt-oxide." These designations will be used in the discussion of the glucose electrooxidation.

The cyclic voltammetric results obtained during the course of the work on the electrooxidation of glucose on platinized Pt demonstrated that this electrode is extraordinarily temperamental for this application. The unpredictable behavior observed is believed to result from the complex adsorption phenomena associated with the adsorption of glucose and its oxidative products on the Pt surface. Consequently, the methods of Pt surface preparation and of glucose adsorption on that surface are critical if consistent results are desired.

Before considering the subtleties of the electrode pretreatment phenomena, the reproducible results obtained using Pretreatment III will be presented in order to establish a basis for further discussion. This pre-

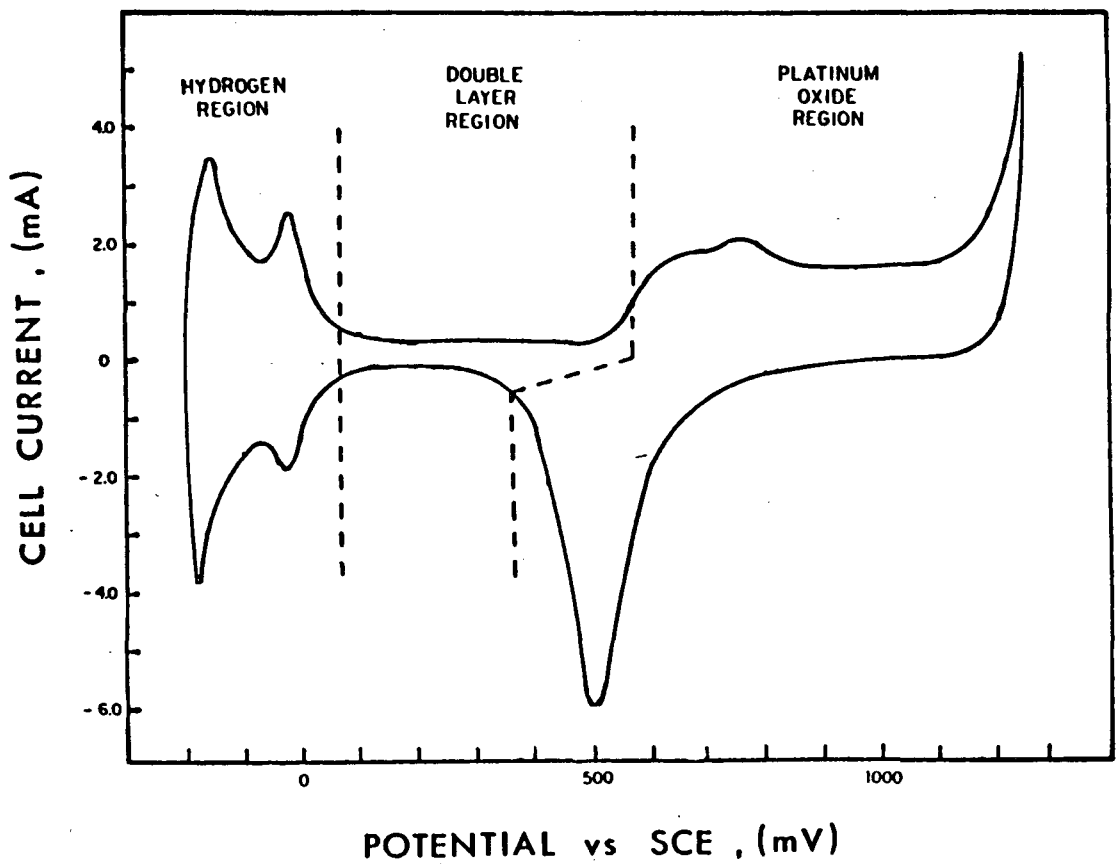

Figure 5. CYCLIC VOLTAMMOGRAM OF PLATINIZED PLATINUM SPECIFYING THE DIFFERENT SURFACE REGIONS OF THE ELECTRODE IN 1.00M H_2SO_4 AT 25°C

61060

treatment procedure was found to yield highly reproducible cyclic voltammograms of glucose under all experimental conditions. The high degree of reproducibility was attributed to precise control of the electrode starting condition. Standard deviations at ambient temperature for peak potentials were at most 20 mV, with 10 mV or less being typical. For peak current densities, standard deviations were at most 1 $\mu A/cm^2$, with 0.50 $\mu A/cm^2$ or less being typical. At elevated temperatures (~66°C) the standard deviations were roughly double those calculated at ambient temperature. These values were within the experimental error of the measurements.

Figures 6 through 12 show representative cyclic voltammograms of glucose on platinized Pt recorded using Pretreatment III in all seven electrolytes listed in Table 4 and at the two temperatures. The peak potentials and current densities based on real area for the cyclic voltammograms presented in Figures 6 through 12 are given in Tables 5 and 6 for the two temperatures, 23° and 65°C, respectively.

General inspection of the cyclic voltammograms in this series shows that the pH, electrolyte anion, and temperature have both quantitative and qualitative effects on the results. Although some changes would surely be expected as a function of the specified variables, the frequency of qualitative changes in the voltammogram structure is thought to be somewhat surprising. In spite of the rather large diversity in the results found, some common features do exist among all the cyclic voltammograms:

1. The glucose electrooxidations are always found to be totally irreversible for the experimental time frames used.

2. Some amount of glucose electrooxidation occurs over the entire potential range available to the electrolyte. (This situation is believed to contribute to the problem of obtaining reproducible results.)

3. Glucose electrooxidation is found to occur on the reverse potential scan after the Pt-O surface has been reduced.

Consider first the behavior in the H-region. At ambient temperature in the presence of glucose, a single anodic peak replaces the hydrogen desorption peaks which would be observed in the electrolyte alone, with one exception. The total charge passed, as indicated by the area under the peak, and the peak current densities are larger than the hydrogen desorption peaks, indicating that a glucose reaction is involved. The peak potentials of the glucose

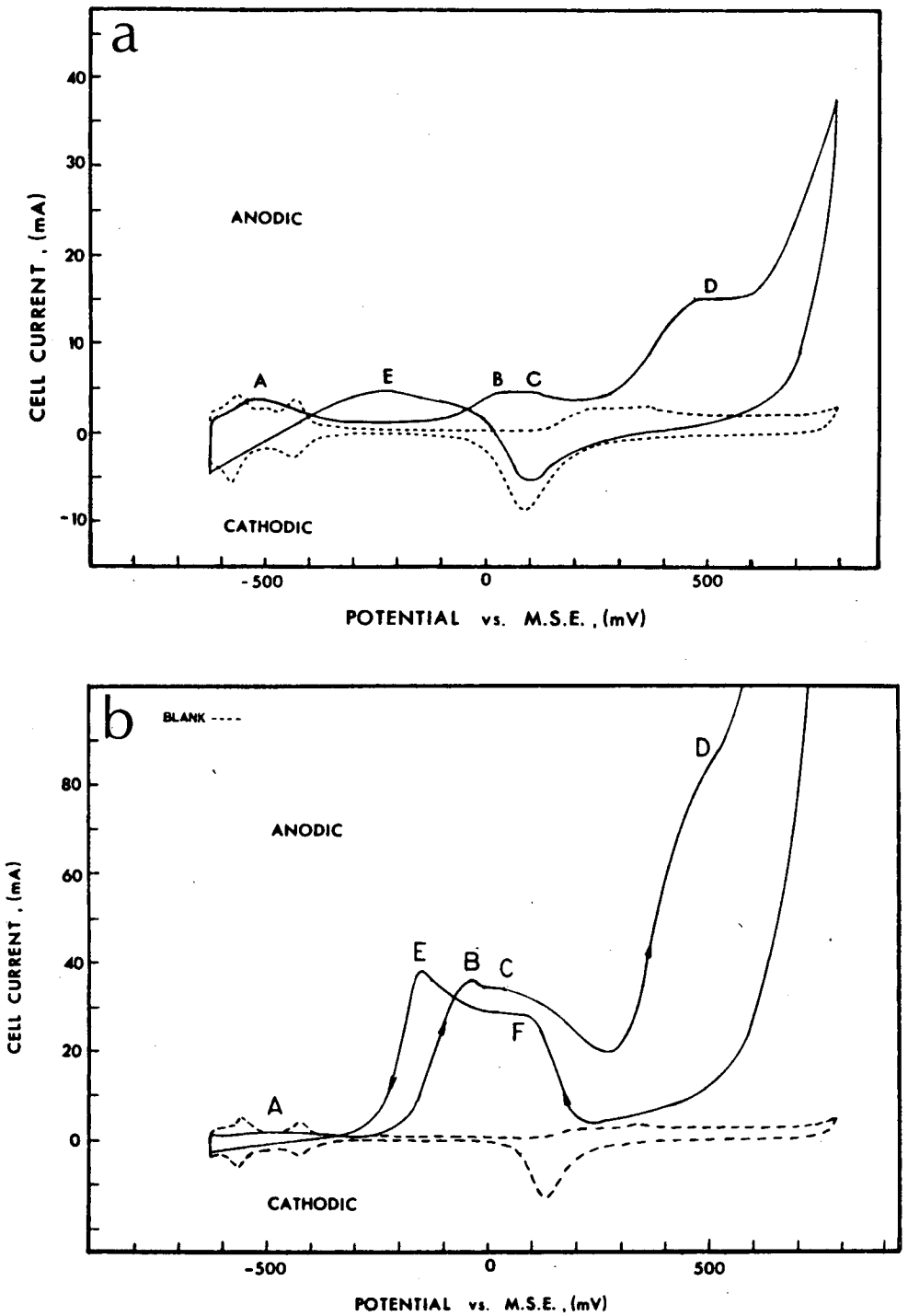

Figure 6. COMPARISON OF CYCLIC VOLTAMMOGRAMS WITH (Solid Line) AND WITHOUT (Dashed Line) 0.50M GLUCOSE PRESENT. EXPERIMENTAL CONDITIONS: ELECTROLYTE, 1.0M H_2SO_4 (pH = 0.0); WORKING ELECTRODE, PLATINIZED Pt (a) 940 cm^2 AND (b) 830 cm^2; SCAN RATE, 5 mV/s; TEMPERATURE, (a) 23°C AND (b) 69°C.

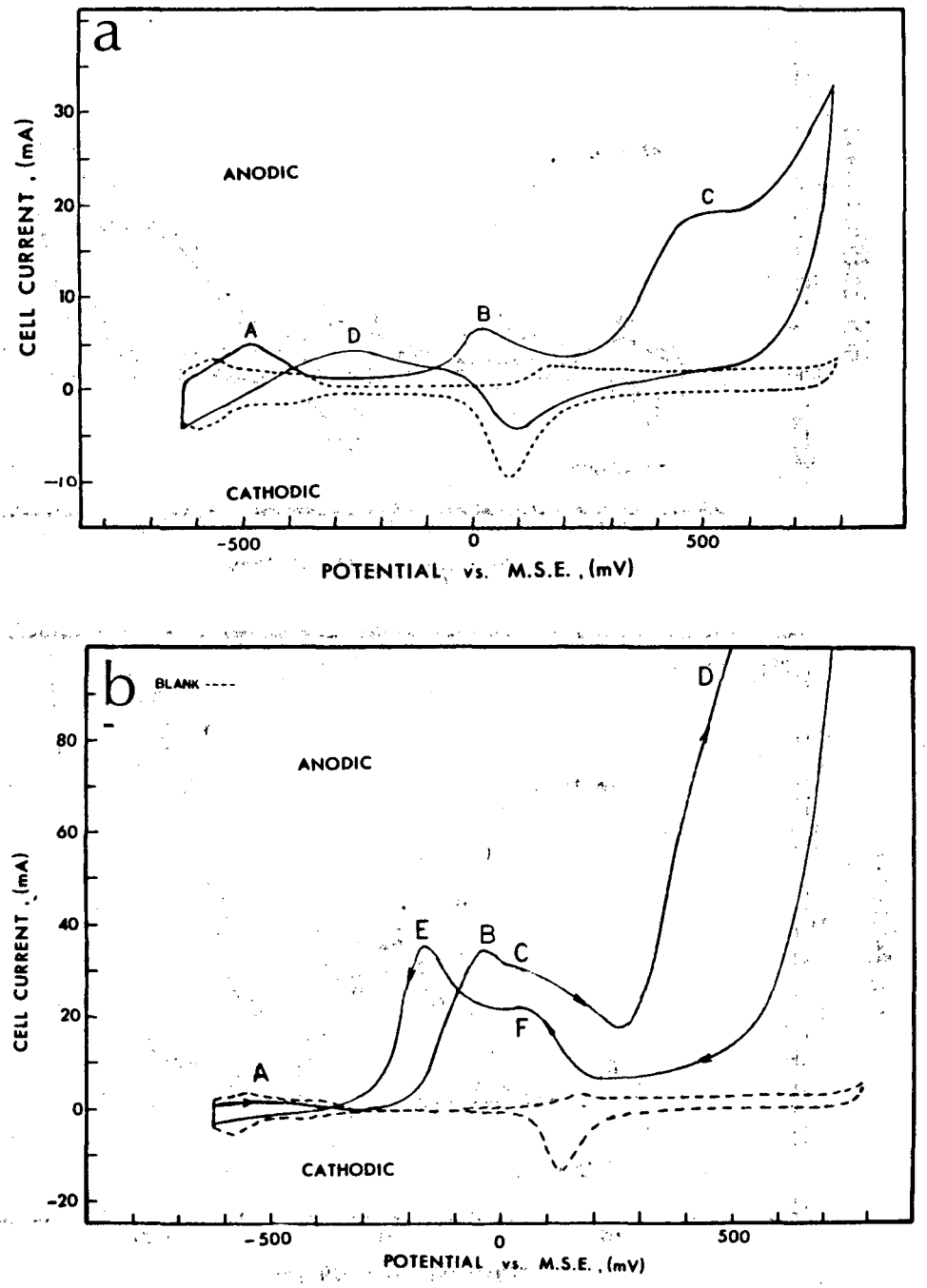

Figure 7. COMPARISON OF CYCLIC VOLTAMMOGRAMS WITH (Solid Line) AND WITHOUT (Dashed Line) 0.50M GLUCOSE PRESENT. EXPERIMENTAL CONDITIONS: ELECTROLYTE, 0.50M $HClO_4$ (pH = 0.3); WORKING ELECTRODE, PLATINIZED Pt (a) 900 cm^2 AND (b) 830 cm^2; SCAN RATE, 5 mV/s; TEMPERATURE, (a) 23°C AND (b) 66°C.

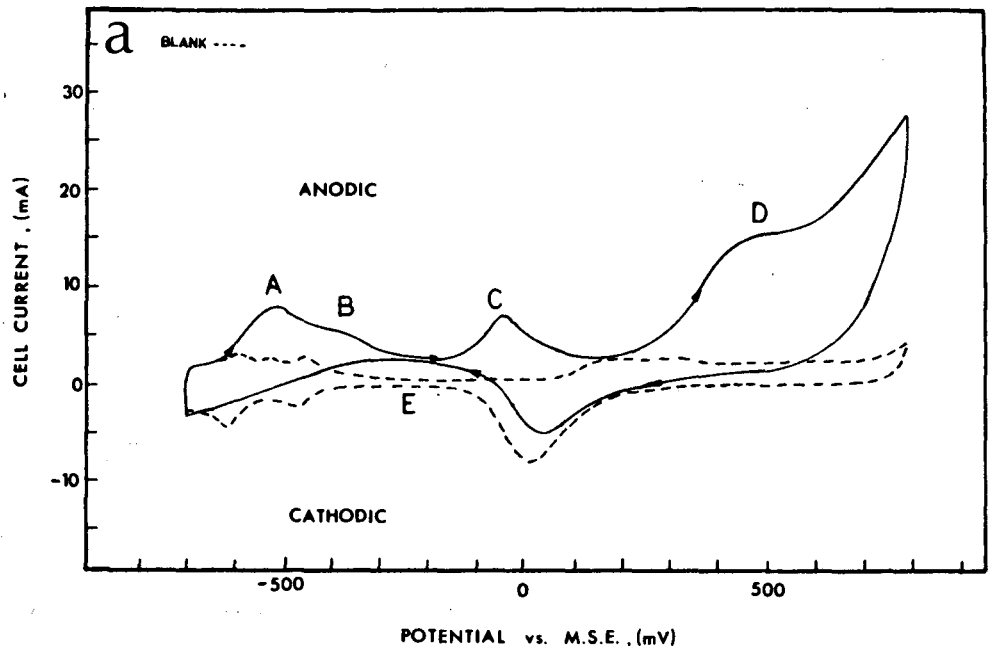

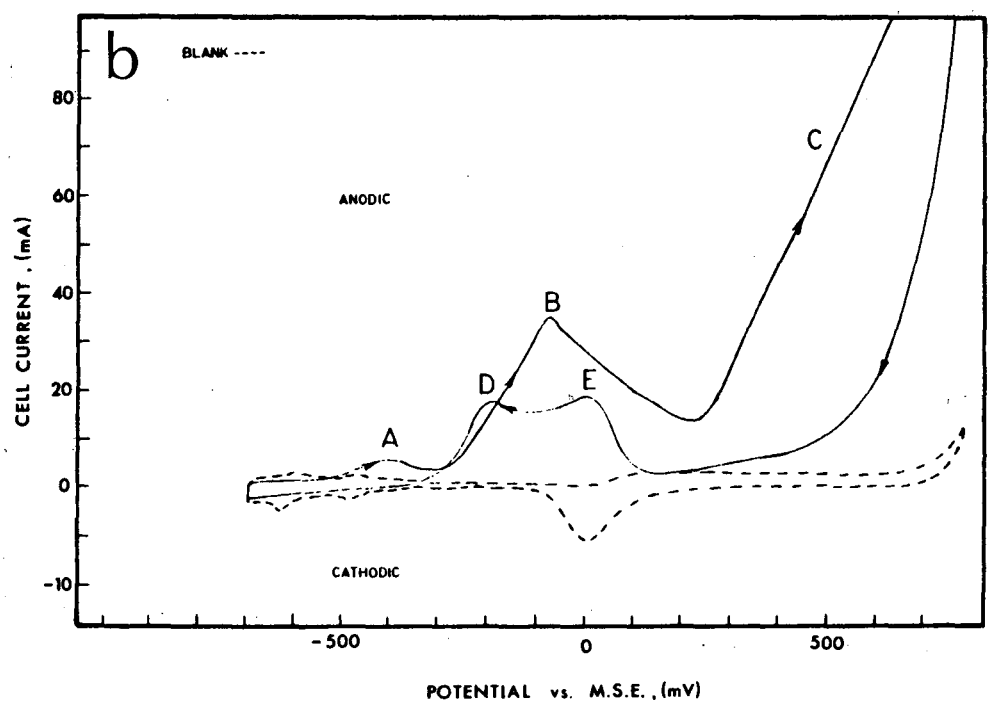

Figure 8. COMPARISON OF CYCLIC VOLTAMMOGRAMS WITH (Solid Line) AND WITHOUT (Dashed Line) 0.50M GLUCOSE PRESENT. EXPERIMENTAL CONDITIONS: ELECTROLYTE, 0.20M $NaHSO_4$/0.80M Na_2SO_4 (pH = 1.8); WORKING ELECTRODE, PLATINIZED Pt (a) 835 cm^2 AND (b) 820 cm^2; SCAN RATE, 5 mV/s; TEMPERATURE, (a) 23°C AND (b) 66°C.

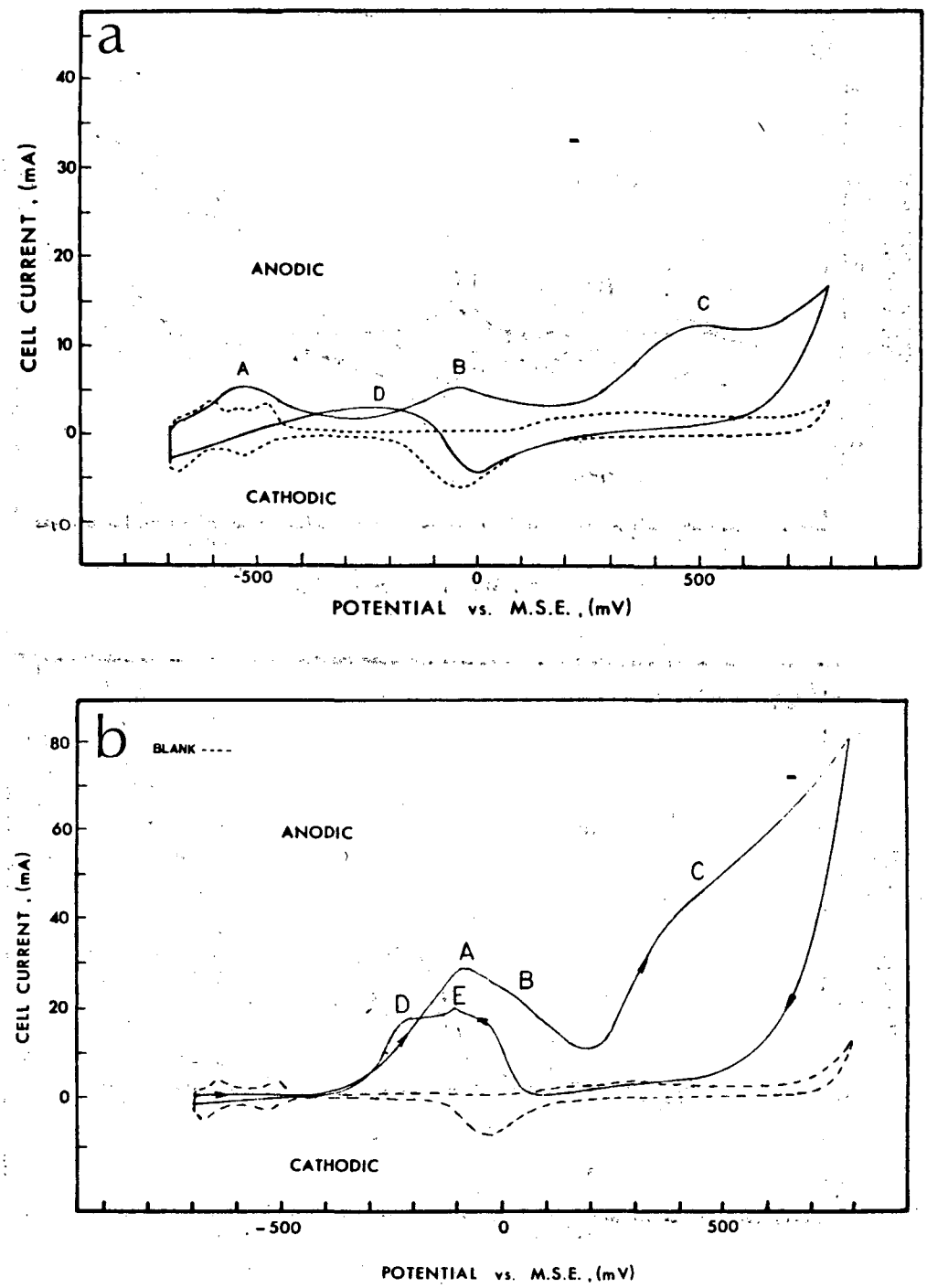

Figure 9. COMPARISON OF CYCLIC VOLTAMMOGRAMS WITH (Solid Line) AND WITHOUT (Dashed Line) 0.50M GLUCOSE PRESENT. EXPERIMENTAL CONDITIONS: ELECTROLYTE, 0.22M H_3PO_4/0.77M NaH_2PO_4 (pH = 2.4); WORKING ELECTRODE, PLATINIZED Pt, (a) 888 cm^2 AND (b) 813 cm^2; SCAN RATE, 5 mV/s; TEMPERATURE, (a) 23°C AND (b) 65°C.

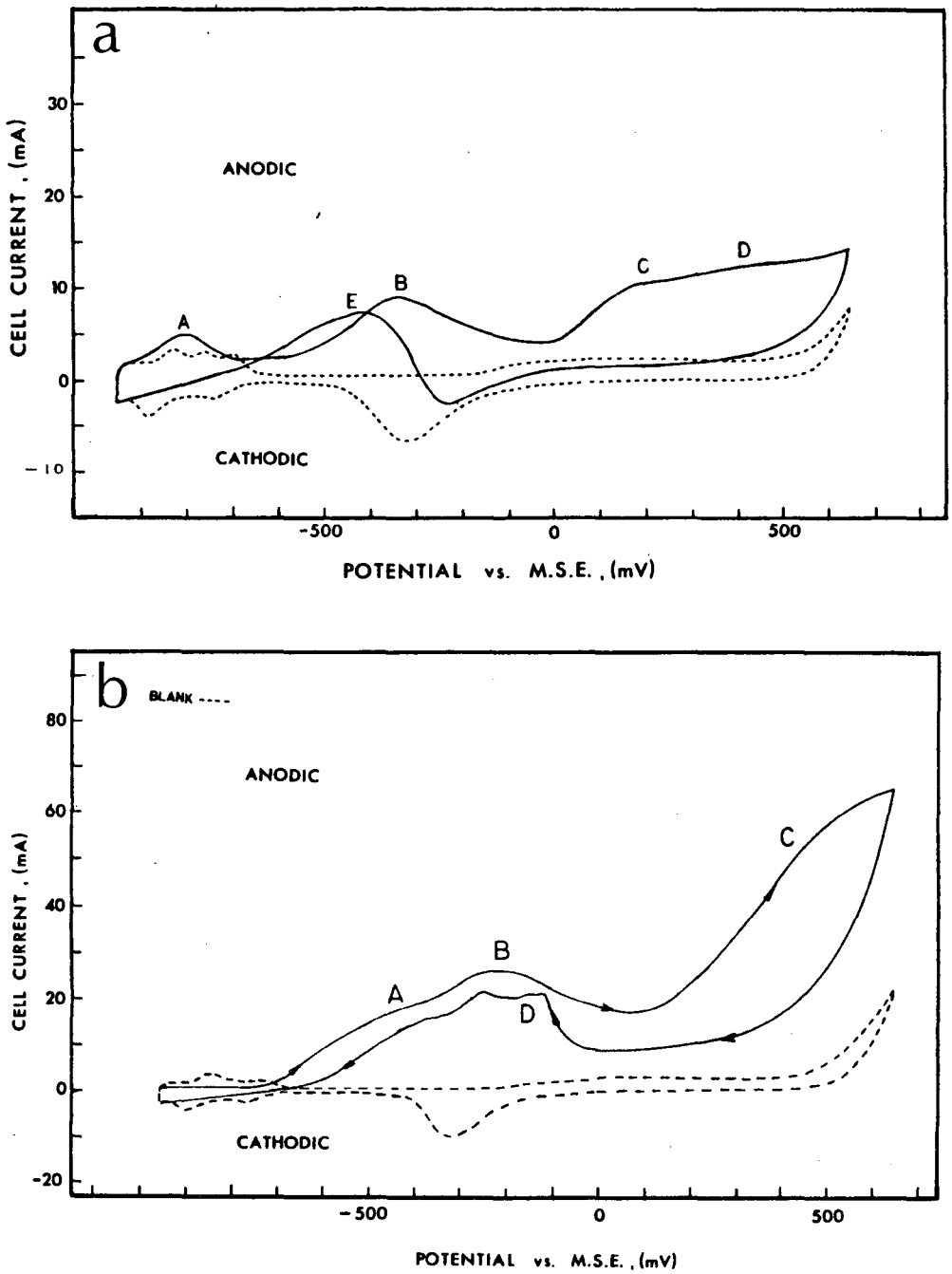

Figure 10. COMPARISON OF CYCLIC VOLTAMMOGRAMS WITH (Solid Line) AND WITHOUT (Dashed Line) 0.50M GLUCOSE PRESENT. EXPERIMENTAL CONDITIONS: ELECTROLYTE, 0.50M Na_2HPO_4/0.50M NaH_2PO_4 (pH = 6.6); WORKING ELECTRODE, PLATINIZED Pt (a) 872 cm^2 AND (b) 830 cm^2; SCAN RATE, 5 mV/s; TEMPERATURE, (a) 23°C AND (b) 67°C.

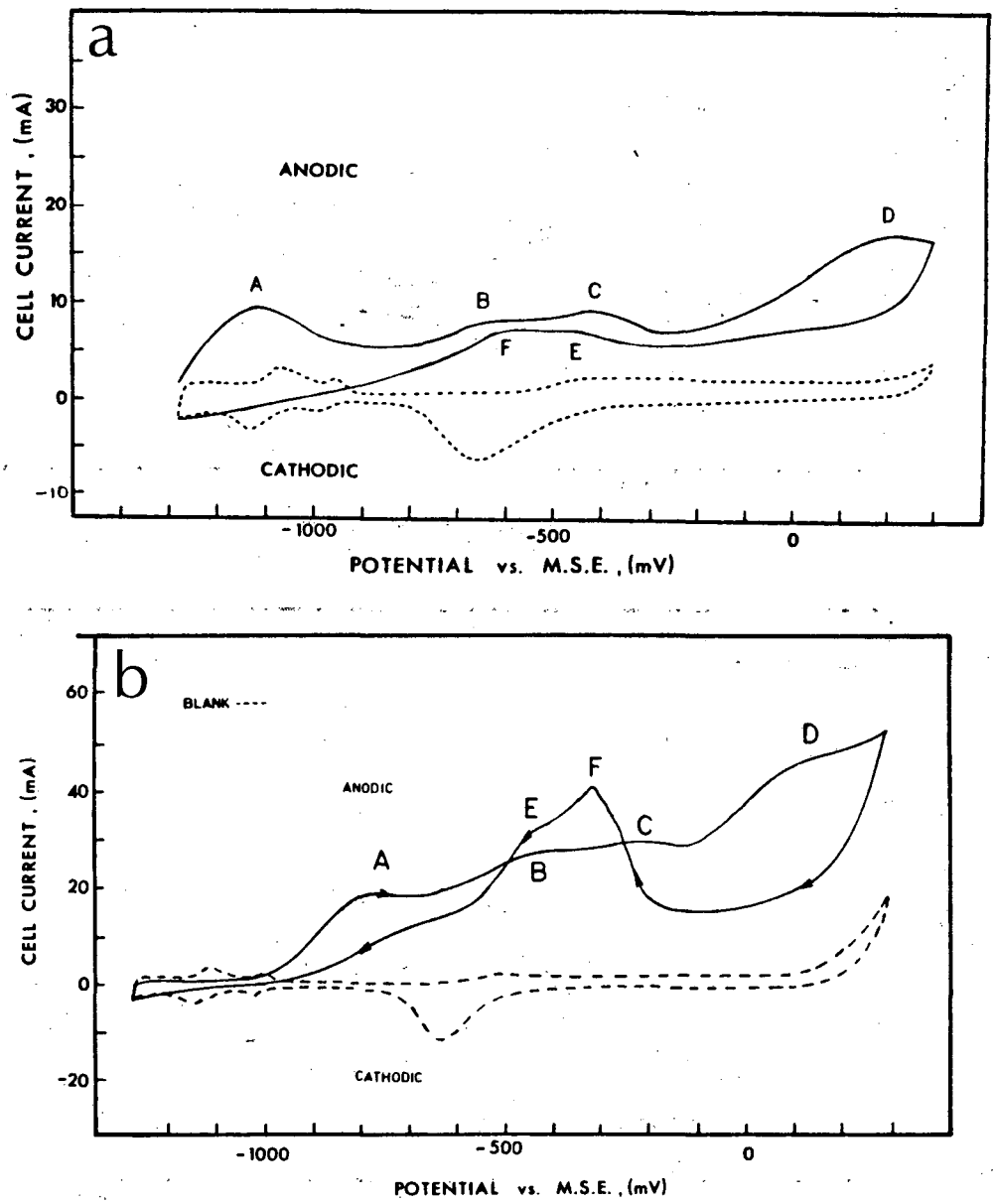

Figure 11. COMPARISON OF CYCLIC VOLTAMMOGRAMS WITH (Solid Line) AND WITHOUT (Dashed Line) 0.50M GLUCOSE PRESENT. EXPERIMENTAL CONDITIONS: ELECTROLYTE, 0.30M Na_2HPO_4/0.70M Na_3PO_4 (pH - 11.7); WORKING ELECTRODE, PLATINIZED Pt (a) 889 cm^2 AND (b) 813 cm^2; SCAN RATE, 5 mV/s; TEMPERATURE, (a) 23°C AND (b) 64°C.

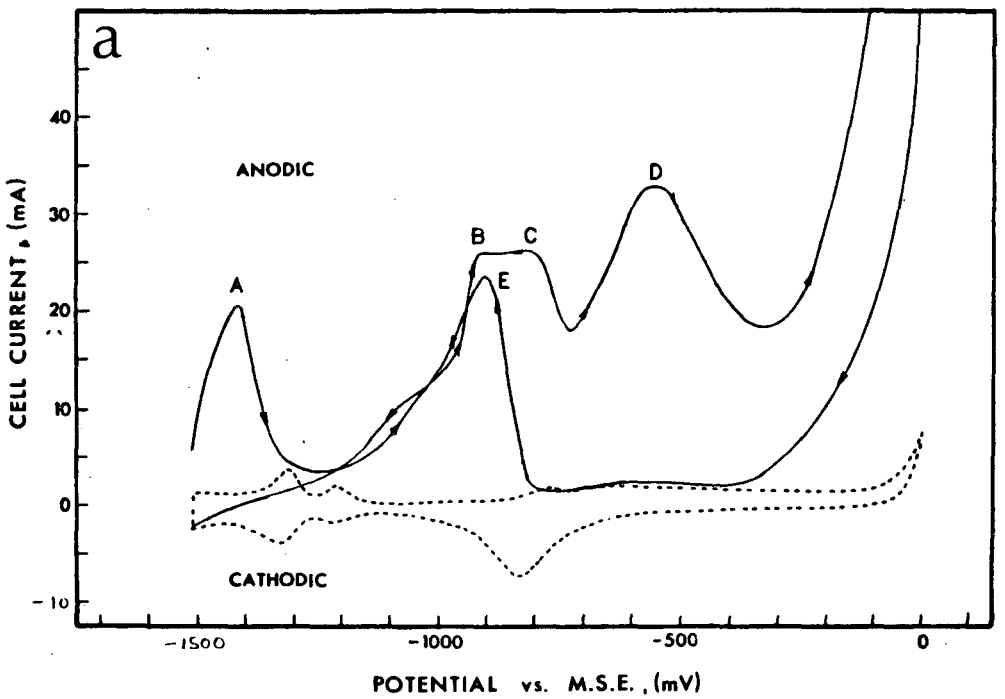

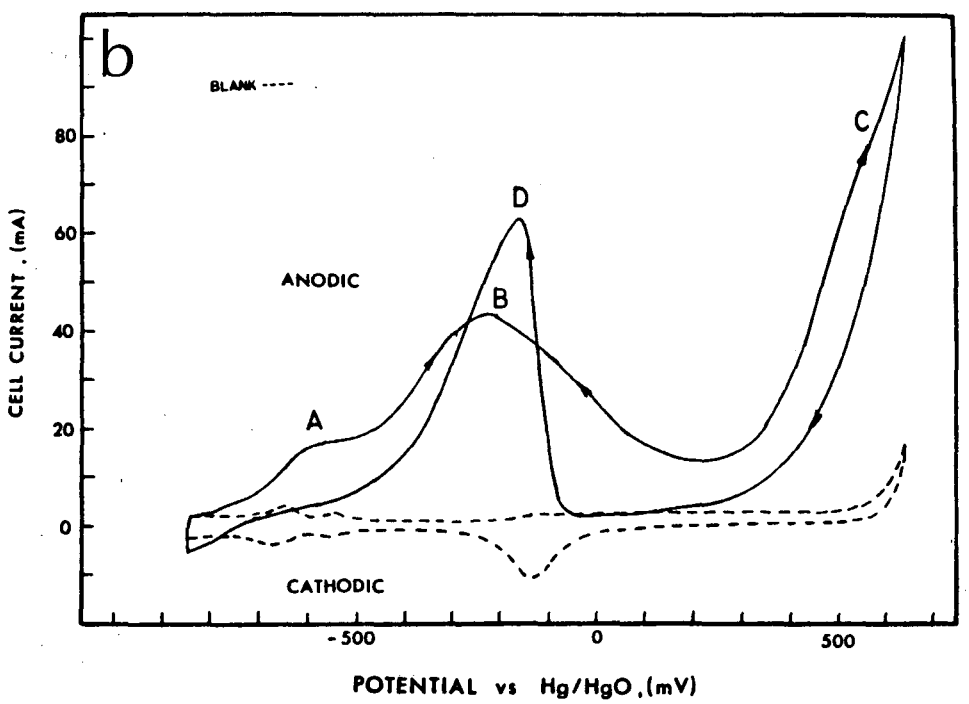

Figure 12. COMPARISON OF CYCLIC VOLTAMMOGRAMS WITH (Solid Line) AND WITHOUT (Dashed Line) 0.50M GLUCOSE PRESENT. EXPERIMENTAL CONDITIONS: ELECTROLYTE, 6.1M KOH (pH =14.8); WORKING ELECTRODE, PLATINIZED Pt (a) 889 cm^2 AND (b) 810 cm^2; SCAN RATE, 5 mV/s; TEMPERATURE (a) 23°C AND (b) 68°C.

Table 5. ANODIC PEAK POTENTIALS AND CURRENT DENSITIES FROM THE CYCLIC VOLTAMMOGRAMS FOR THE ELECTROOXIDATION OF GLUCOSE ON PLATINIZED PLATINUM AT AMBIENT TEMPERATURE (23°C) AND VARIABLE pH

Peak Designation	Electrode Region	Scan Direction	$E_{p,a}$, mV vs MSE*	$i_{p,a}$, μA/cm²**
		pH = 0.0 (Figure 6a)		
A	H	F	−514 (4)	4.2 (0.2)
B	DL	F	+31 (3)	5.4 (0.3)
C	DL	F	+99 (3)	5.4 (0.3)
D	PtO	F	+501 (3)	17.6 (0.8)
E	DL	R	−226 (3)	5.6 (0.4)
		pH = 0.3 (Figure 7a)		
A	H	F	−490 (3)	5.5 (0.6)
B	DL	F	+23 (6)	7.2 (0.7)
C	PtO	F	+503 (3)	21.1 (0.9)
D	DL	R	−261 (5)	4.7 (0.3)
		pH = 1.8 (Figure 8a)		
A	H	F	−513 (3)	9.5 (0.4)
B	H	F	−377 (3)	6.0 (0.2)
C	DL	F	−41 (1)	8.1 (0.3)
D	PtO	F	+502 (3)	17.5 (0.6)
E	DL	R	−280 (5)	2.5 (0.4)
		pH = 2.4 (Figure 9a)		
A	H	F	−533 (19)	5.2 (1.1)
B	DL	F	−54 (10)	5.9 (0.3)
C	PtO	F	+481 (21)	13.7 (0.5)
D	DL	R	−257 (12)	3.3 (0.1)
		pH = 6.6 (Figure 10a)		
A	H	F	−801 (5)	5.1 (0.4)
B	DL	F	−336 (9)	9.8 (0.3)
C	PtO	F	+196 (4)	11.8 (0.2)
D	PtO	F	+409 (11)	13.6 (0.4)
E	DL	R	−408 (18)	8.0 (0.3)
		pH = 11.7 (Figure 11a)		
A	H	F	−1107 (6)	10.6 (0.2)
B	DL	F	−622 (11)	9.4 (0.3)
C	PtO	F	−408 (6)	10.4 (0.1)
D	PtO	F	+212 (4)	19.3 (0.2)
E	PtO	R	−459 (2)	8.2 (0.1)
F	PtO	R	−582 (6)	8.2 (0.2)
		pH = 14.8 (Figure 12a)†		
A	H	F	−1415	23.2
B	DL	F	−910	29.1
C	DL	F	−812	29.5
D	PtO	F	−555	37.1
E	DL	R	−905	26.3

* Parentheses indicate standard deviations calculated from at least three measurements.

** Current densities not corrected for blank electrolyte currents.

† Because of visual reaction with time only the values of the first scan are given.

Table 6. ANODIC PEAK POTENTIALS AND CURRENT DENSITIES FROM THE CYCLIC VOLTAMMOGRAMS FOR THE ELECTROOXIDATION OF GLUCOSE ON PLATINIZED PLATINUM AT ELEVATED TEMPERATURE (66° ±3°C) AND VARIABLE pH

Peak Designation	Electrode Region	Scan Direction	$E_{p,a}$ vs. MSE, mV*	$i_{p,a}$, μA/cm²**
		pH = 0.0 (Figure 66)		
A	H	F	−488 (11)	2.0 (0.4)
B	DL	F	−35 (0)	37 (6)
C	DL	F	+45 (0)	34 (6)
D	PtO	F	+500 (7)	86 (18)
E	DL	R	−152 (11)	41 (5)
F	DL	R	+78 (12)	29 (5)
		pH = 0.3 (Figure 76)		
A	H	F	−495 (7)	1.8 (0.2)
B	DL	F	−36 (1)	37 (2)
C	DL	F	+38 (11)	33 (2)
D	PtO	F	+494 (9)	103 (4)
E	DL	R	−164 (2)	40 (0)
F	DL	R	+61 (6)	26 (1)
		pH = 1.8 (Figure 8b)		
A	H	F	−398 (4)	6.8 (0.4)
B	DL	F	−65 (7)	41.4 (0.4)
C	PtO	F	+500 (0)	77 (3)
D	DL	R	−192 (8)	20.6 (0)
E	DL	R	+21 (13)	21.7 (0)
		pH = 2.4 (Figure 9b)		
A	DL	F	−78 (11)	36 (2)
B	DL	F	0 (7)	31 (2)
C	PtO	R	+480 (0)	59 (1)
D	DL	R	−201 (8)	21 (0)
E	DL	R	−94 (16)	24 (1)
		pH = 6.6 (Figure 10b)		
A	DL	F	−456 (37)	20 (1)
B	DL	F	−250 (50)	33 (3)
C	PtO	R	+450 (0)	64 (10)
D	PtO	R	−185 (78)	26 (2)
		pH = 11.7 (Figure 11b)		
A	DL	F	−735 (35)	24 (1)
B	PtO	F	−435 (14)	32 (2)
C	PtO	F	−171 (34)	37 (2)
D	PtO	F	+178 (62)	57 (1)
E	PtO	R	−395 (50)	39 (1)
F	PtO	R	−164 (65)	57 (11)
		pH = 14.8 (Figure 12b)		
A	H	F	−858 (4)	20 (1)
B	DL	F	−510 (2)	53 (3)
C	PtO	F	+276 (11)	94 (2)
D	DL	R	−446 (4)	77 (3)

* Parentheses indicate standard deviations calculated from at least three measurements.

** Current densities not corrected for blank electrolyte currents.

electrooxidations in the H region, as well as the other two potential regions, are plotted as a function of pH in Figure 13. Except for deviations at pH extremes, pH dependence is linear following Nernstian behavior for one H^+ per electron. Figure 14 gives the current density as a function of pH for this peak and shows that it is roughly constant at about 5 $\mu A/cm^2$ from acidic to neutral electrolyte. Further pH increases result in substantial current density increases, particularly for the most alkaline pH.

An exception to this regular pattern was found at pH = 1.8 (HSO_4^-/SO_4^{2-} buffer). As Figures 8a and 14 show, the H region peak at this pH has a larger current density than fits the pattern and is accompanied by a second peak at the boundary of the H and DL regions. This extra peak does not result from impurities as evidenced by the fact that the electrolyte alone and the same glucose in other electrolytes do not exhibit this peak. In addition, repeated cyclic voltammograms confirmed that the peak was a real feature of these particular experimental conditions. This being the case, a specific interaction between glucose and the pH = 1.8 electrolyte to yield an additional electroactive species must be postulated.

The cyclic voltammograms with glucose present at the elevated temperature (Figures 6 through 12) show that the currents in the H region are depressed, in most cases to virtually nothing, from those associated with the hydrogen desorption peaks in the electrolyte alone. Thus, not only is little, if any, glucose electrooxidation occurring at this higher temperature, but its presence inhibits the hydrogen adsorption, presumably by competitive adsorption of the glucose.

At ambient temperature the glucose electrooxidation in the DL region is in many ways similar to that found in the H region. A single anodic peak was detected in the DL region over the majority of the pH range except for doubling at the pH extrema. (See Figure 13.) The doubling took the form of a shoulder structure, as shown in Figures 6 and 12. The appearance of the doubling at pH extrema may be the result of greater peak resolution at these pH's as the intermediate pH's exhibit much broader features that could mask such doubling. Again like the H region, a series of DL peaks as a function of pH can be seen to follow Nernstian behavior, Figure 13, for one H^+ per electron in the reaction mechanism. The peak current densities for the DL region peaks (chosen from those which best fit a straight line in the pH plot,

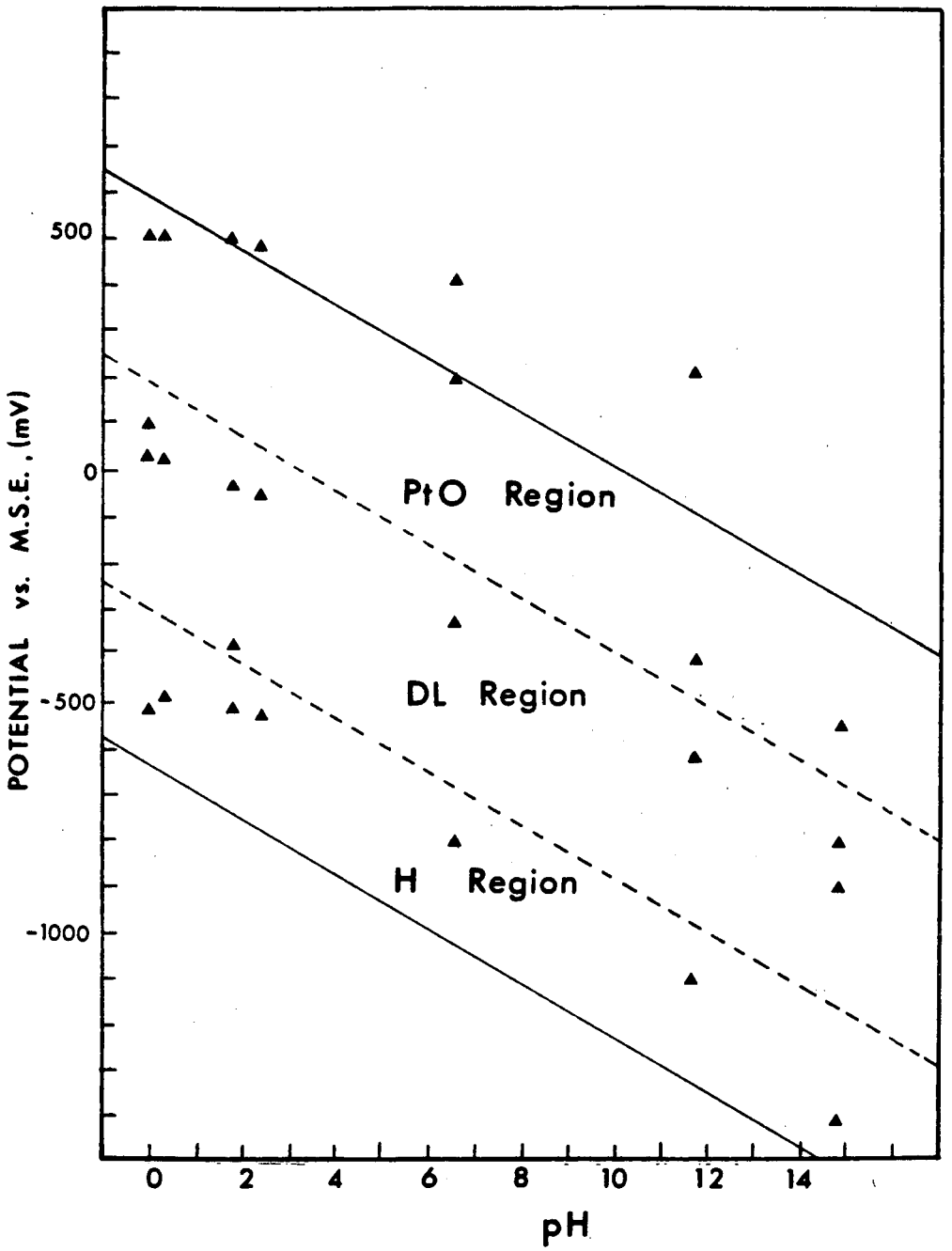

Figure 13. PEAK POTENTIALS VERSUS pH FOR GLUCOSE ELECTROOXIDATION ON PLATINIZED Pt IN THE FORWARD SCAN AT 23°C. BOTTOM SOLID LINE: $E(H_2)$ VERSUS MSE = 2.303 RT/F (pH) -640 V; TOP SOLID LINE: $E(O_2)$ VERSUS MSE = 0.59 - 2.303 RT/F (pH). DASHED LINES ARE BOUNDARIES BETWEEN ELECTRODE REGION.

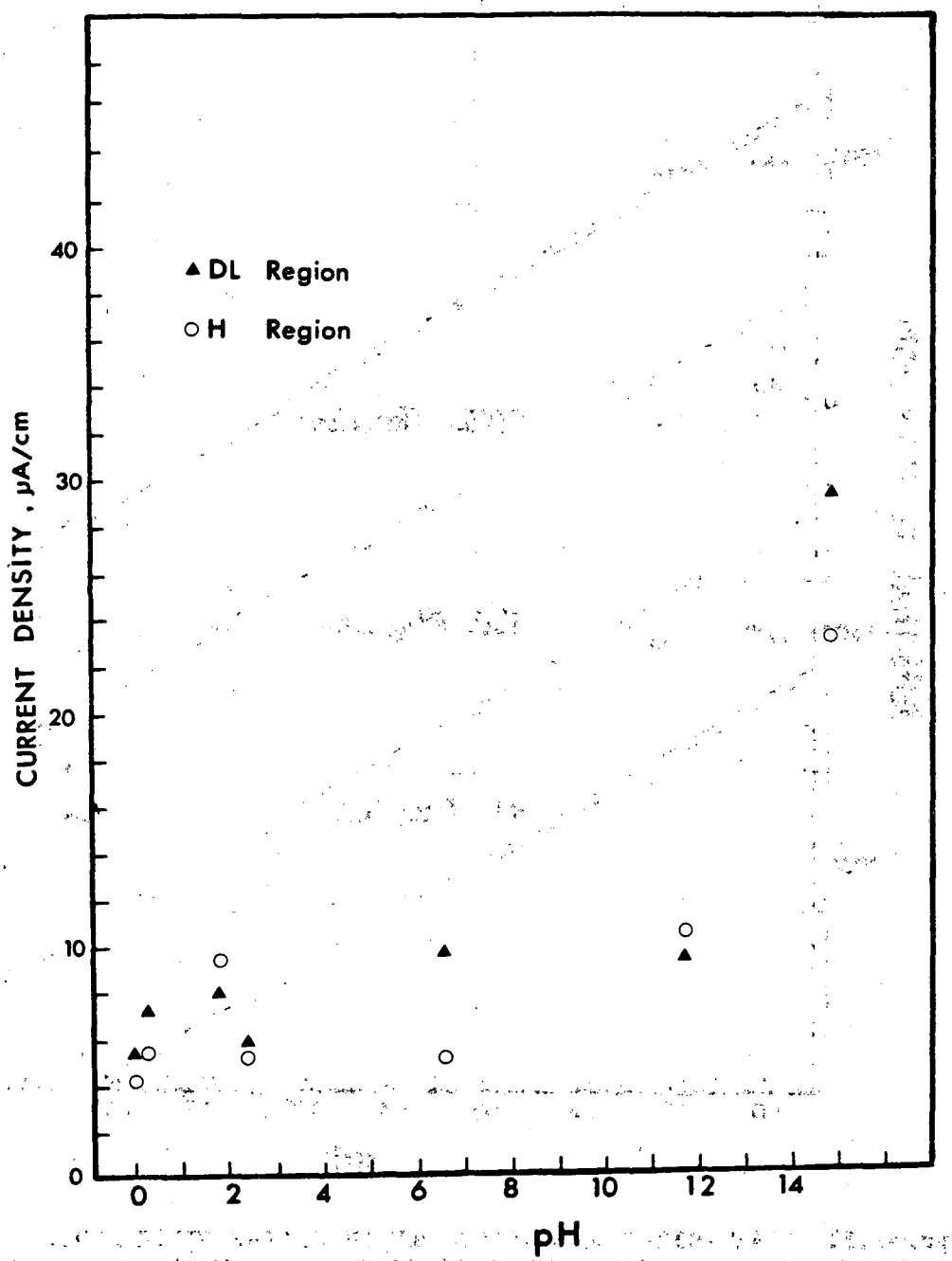

Figure 14. PEAK CURRENT DENSITIES VERSUS pH FOR GLUCOSE ELECTROOXIDATION ON PLATINIZED Pt's H AND DL REGIONS FOR THE FORWARD SCAN AT 23°C

Figure 13) exhibit a slow increase from pH = 0.0 to 11.7 going from ~5 to 10 $\mu A/cm^2$ (Figure 14.). A sharp increase then occurs at the most alkaline pH.

As Figure 14 shows, a sharp increase in current density is detected for glucose electrooxidation in both the H and DL regions at the most alkaline pH. Glucose chemical reactivity is greatest in the alkaline electrolyte,[41,67,68] and the presence of additional, more electroactive species may account for this. In particular, the pK_a of the hydroxyl hydrogen on the 1 carbon of the glucopyranose ring, Figure 4, is 12.3, indicating that above pH = 12.3 the ionized form would predominate.[69,70] The results of the current density as a function of pH, Figure 14, coincide favorably with some sort of change occurring in the vicinity of pH = 12.3 and may, therefore, indicate that the ionized glucopyranose ring is more electrochemically active than the unionized ring.

Considerable changes in the glucose electrooxidation are evident in the cyclic voltammograms when the temperature is increased to 66°C (Figures 6 through 12b). Unlike the results in the H region where currents decreased when the temperature increased, large current increases occurred for the glucose electrooxidation in the DL region. The magnitude of the increase was in the range of 5 to 10 times the ambient temperature value. (Compare DL currents in Table 6 with those in Table 5.) In addition to this reaction rate increase, qualitative changes in the peak structures were evident. In the acid electrolytes (pH < 4), Figures 6 through 9b, a broad anodic structure with a relatively distinct initial peak followed by a less distinct shoulder is observed in the forward scan. Thus the initial sharp peak and shoulder peak behavior which was seen at ambient temperature was accentuated by the temperature increase. The anodic oxidation in the reverse scan exhibited a structure close to that found in the forward scan, but shifted to more negative potentials. As the pH is increased to 11.7 (Figures 10b and 11b), the glucose electrooxidation structure in the DL region becomes less and less distinctive, resulting in a plateau at pH = 11.7. In the most alkaline pH (14.8), Figure 12, a large broad peak centered on the DL region becomes the cyclic voltammogram's dominant feature. In addition, the intensity of the peak is about the same as that found for the DL electrooxidation at ambient temperature, indicating little effect of increased temperature on glucose electrooxidation rate in this region.

The dependence of peak potentials in the DL region on pH at 66°C is shown in Figure 15. Although no clear continuous set of peaks can be distinguished, the overall trend of the peak potentials is again to follow roughly Nernstian behavior for one H^+ per electron.

The qualitative changes in the cyclic voltammograms were more dramatic in the alkaline electrolytes, which is consistent with the fact that glucose is chemically less stable in alkaline. Support for increased glucose reactivity at the higher tempreature in alkaline over the course of an experiment was given by the color change of the electrolyte, which was only minor in acid but substantial in alkaline. At pH = 14.7 and 66°C the glucose-containing electrolyte was an opaque dark brown and, as mentioned earlier, a complete absence of glucose was found in this electrolyte by HPLC, which indicates complete reaction of the glucose to another species, possibly gluconic acid.

Glucose electrooxidation in the Pt-O region showed the most complex behavior as a function of pH. Considering first the ambient-temperature cyclic voltammograms in acidic electrolytes (pH < 4), only a single broad anodic peak (almost a plateau in many cases) is detected. These peak potentials are essentially independent of pH, as Figure 14 shows, indicating the absence of H^+ (or OH^-) participation in the glucose electrooxidation. As the pH is increased to neutral and beyond a second anodic peak appears that does exhibit a potential shift with pH, again roughly with a Nernstian behavior for one H^+ per electron. At the maximum pH, there is only a single peak in keeping with the lack of pH dependence of the other peak which would now occur at potentials positive of oxygen evolution. This description of the peak potential's behavior in the Pt-O region must be considered only tentative, however. Because of the scarcity of data points in the alkaline region, other interpretations are undoubtedly possible.

Raising the temperature to 66°C causes a substantial increase in current (approximately 5 times above the ambient temperature values), and these are the largest values observed on platinized Pt, 60 $\mu A/cm^2$ (real) or more. For pH's < 7, the anodic oxidation appears more as a shoulder on the rapid current increase near the electrolyte limit, which occurs at a much more rapid rate with glucose present.

Unique findings were obtained at pH's 11.7 and 14.8. At 11.7 (Figure 11b) an overall current increase was found over the entire Pt-O

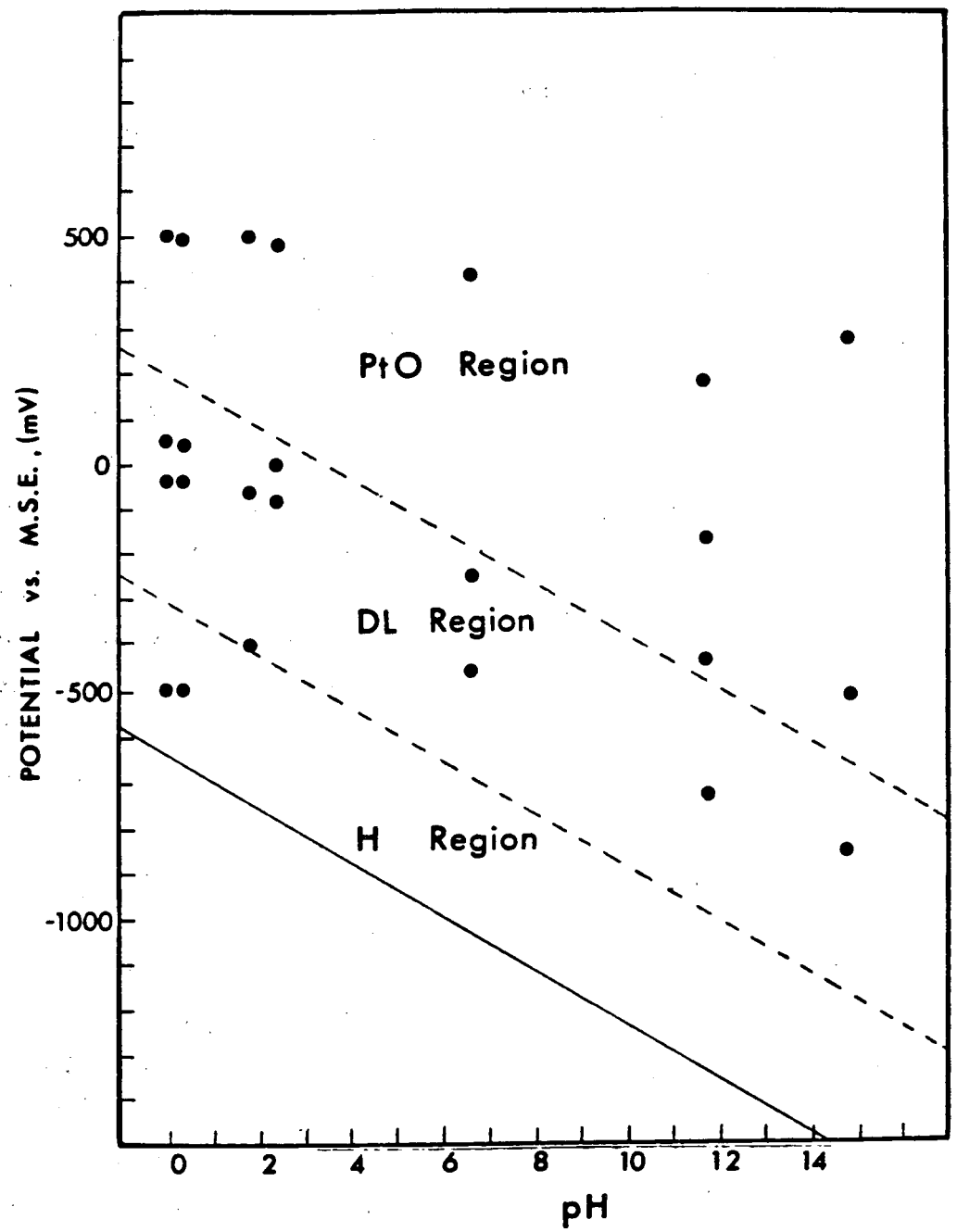

Figure 15. PEAK POTENTIALS VERSUS pH FOR GLUCOSE ELECTROOXIDATION ON PLATINIZED Pt IN THE FORWARD SCAN AT 66°C. SOLID LINE: $E(H_2)$ VERSUS MSE = 2,303 RT/F (pH) -640 V. DASHED LINES ARE BOUNDARIES BETWEEN ELECTRODE REGIONS.

potential region, but three local maxima were identifiable with the most positive being the most distinct. The results obtained at pH = 14.8 showed a lack of any glucose electrooxidations except for the trailing edge of the oxidation in the DL region and the more rapid electrolyte breakdown at the positive potential extreme. Again, the greater difference observed in these alkaline pH's is most likely the result of the enhanced chemical activity of glucose in these electrolytes.

Important observations were made during the recording of the cyclic voltammograms in regards to the evolution of gas. At ambient temperature and acidic electrolytes, gas evolution was often observed to occur in the DL and Pt-O potential regions. The gas evolution in the DL region appeared as gas blisters on the electrode that disappeared by dissolution when the currents declined. In the Pt-O region enough gas was formed to result in the bubbles leaving the electrode surface. The appearance of gas in the DL region was somewhat dependent on electrode pretreatment. The only alternatives for the gas composition would seem to be CO_2 and O_2, and on the basis of the electrode potential at which gas appears, CO_2 would be the most likely candidate — especially in the DL region. Bulk electrolysis results (to be presented later) confirmed that CO_2 was evolved in both potential regions. Although CO_2 formation would be expected for the alkaline electrolytes as well, formation of carbonate would disguise its appearance.

The evolution of gas at 66°C was greatly accelerated, and generous amounts were evolved off of the electrode even in the DL region. In fact, the rate was so great that gas could be observed even in the alkaline electrolyte at pH = 11.7; none was observed at pH = 14.8, however.

The importance of this observation lies in the fact that the majority of the limited past work on glucose electrooxidation in the literature suggests that the only or major oxidation product is gluconic acid,[28,29,32] and clearly the appearance of CO_2 requires substantial electrooxidation beyond that stage. These results are more in keeping with those reported by Giner, et al. in which a so called "reduced CO_2" species[71,72] is formed from the electrosorption of the glucose molecule.[34,36,37]

One of the features common to all the cyclic voltammograms is the electrooxidation observed in the reverse scan. Its appearance coincides with the stripping of the "Pt-oxide" layer to Pt metal and, therefore, strongly

suggests that an oxidation inhibited by the "Pt-oxide" coating is allowed to proceed on the Pt metal surface found in the DL region. As this electro-oxidation occurs after the substantial oxidations associated with the forward scan, its origin could arise not only from glucose but from the myriad of possible reaction products formed during the forward scan. Consequently, litle meaning can be assigned to this electrooxidation.

Effects of Electrode Pretreatment. Because the cyclic voltammograms were found to be dependent on the electrode pretreatment history prior to the start of a scan, which led to irreproducibility, and because a substantial effort was made to overcome this problem, presentation and discussion of these results is in order. During the earlier portion of the program when Pretreatment I and related pretreatments were used, difficulties in reproducibility were encountered in all three potential regions of the Pt electrode. The severity of the irreproducibility varied with potential region and pH, with greatest irreproducibility appearing at intermediate pH's. At all pH's the largest discrepancies occurred in the H region. Under the worst circumstances the number of peaks in this region would vary from scan to scan, and large deviations in peak potentials and currents were common. As the electro-oxidation of glucose in the H region is believed to be a surface reaction,[31] the state of the electrode surface and consequently the experimental conditions employed is expected to influence this oxidation greatly.

More subtle discrepancies were detected in the cyclic voltammograms for the glucose electrooxidation in the DL region. A distinctive peak was always obtained in this potential region, but the variations in peak potentials and current densities were larger than experimental errors would warrant. Peak potentials could vary as much as 100 mV between scans, and current densities could vary by 25%. In addition, the presence of a shoulder peak indicating a second oxidation in this region was found to come and go.

The glucose electrooxidation in the Pt-O region was the least troublesome, and only exhibited major problems at intermediate pH ranges of 6.6 and 11.7. At these pH's the relative magnitudes of a double peak feature could be highly variable. The procedural factors which are believed to influence this behavior and were modified are enumerated below:

1. The presence of the strongly adsorbing anion, Cl^-, associated with the use of a SCE reference

2. The positioning of the start potential

3. The time spent at the start potential prior to scanning

4. The transfer of the electrode from an external cleaning cell to the reaction cell

5. The method with which the electrode is exposed to the glucose.

6. The time associated with glucose exposure prior to scanning.

The presence of Cl^- ion is known to interfere with the electrooxidation of organic materials on Pt.[30,73,74] Its influence on glucose electrooxdiation has even been reported.[30] In that work, the only effect of the Cl^- was to decrease the peak current magnitudes, and relatively high values of Cl^- concentration were required, on the order of 10^{-3}M.

In the experiments performed with a SCE reference electrode, a 0.50M KCl salt bridge was separated from the electrolyte by a vycor tip. Because the rate of seepage through the vycor tip was expected to be slow and the electrolyte volume in the experiments was large (>500 mL), the small amount of Cl^- entering the electrolyte from the bridge was initially believed to have a negligible effect. However, qualitative effects were identified in this work and they were similar to those observed with methanol.[73] In particular, it affected the shoulder peak in the DL region and depressed currents in the H region. The amount of Cl^- in the electrolyte under the experimental conditions used may be expected to vary greatly and may account for at least some of the problems of irreproducibility encountered both in the hydrogen and double-layer regions. Amounts of Cl^- in the electrolyte capable of easily giving a positive test with $AgNO_3$ were observed. In order to eliminate any uncertainty surrounding the presence of Cl^-, MSE was substituted for SCE as the reference electrode in the final voltammetry performed.

The choice of start potential also influences the cyclic voltammogram. This influence is expected for at least three reasons. First, since some glucose oxidation occurs over the entire DL region, a scan must necessarily begin in the midst of this oxidation. Clearly, such a circumstance will influence the appearance of this initial oxidation as well as any consecutive oxidations which may follow. Secondly, the amount of hydrogen present on the electrode has been reported to play a part in the glucose electrooxidation,

and this amount will vary depending on the start potential. Thirdly, the glucose electrosorption is potential dependent,[31] and the amount of initially adsorbed glucose will also be a function of start potential. A clearly defined start potential is thus required for the precise glucose cyclic voltammetry.

Upon placing the electrode at the start potential, as was done in Pretreatment I and those preceding it, a transient current was detected which decayed away at a variable rate. Periods up to 10 minutes were sometimes required for the current to decay away to a negligible value, although 5 minutes would usually suffice. Prior to Pretreatment I cyclic voltammetry scans were recorded without adequate regard to these transient currents, which is believed to have contributed to the irreproducibility of these scans. The transient currents are most likely attributable to electrosorption of the glucose, and if so, the recording of cyclic voltammograms before equilibrium was reached would be expected to yield variable results, particularly in the H region.

The transfer of the electrode after pretreatment in an external cell, as in all pretreatments except Pretreatment III, is also a potential source of uncertainty. Experiments were initially performed with the electrode transfer because of the reduced time and materials required and because a previous report suggested that such a transfer would not effect the result voltammetric results.[75] In addition, results obtained here showed that a clean, platinized Pt electrode scan resulted when a cyclic voltammogram was recorded in the electrolyte alone after transfer to the reaction cell. A cyclic voltammogram of Pt that exhibited good resolution of the three Pt potential regions, particularly in the H region, was taken to indicate a true or clean Pt electrode. A clean Pt scan could not be obtained after the transfer with a shiny Pt electrode, however. Thus, contamination of the Pt presumably occurs during transfer, but the area contaminated is a small fraction of the total area for a platinized electrode while the opposite is true for a shiny Pt electrode.

Although the considerations in the previous paragraph initially suggested that the platinized Pt electrode transfer would not greatly influence the cyclic voltammograms through the changes in the surface conditions, the introduction of glucose into the situation adds a complicating factor which could

generate problems in the transfer process. Pt forms a "Pt-oxygen" adduct when it is exposed to oxygen. This adduct has actually been used to oxidize glucose and gluconic acid chemically by bubbling oxygen through suspended Pt (Adams catalyst).[76-80] Potentiometric measurements of a Pt electrode prepared with a "Pt-oxide" coating exhibit a potential change when glucose is added and attain a value representative of a potential obtained when a Pt electrode is prepared with a Pt metal surface and exposed to glucose. This potentiometric measurement also indicates reaction of the glucose with the "Pt-oxide" coating. In light of this information, a Pt electrode transferred from one cell to another will pick up oxygen, and this oxygen can very well react with the glucose. Consequently, the resultant initial electrode state will not only have the presence of glucose but its oxidation products as well, and cyclic voltammograms would vary according to how much oxygen adduct was formed. No problem would be identified in the absence of glucose because the Pt-oxide formation is electrochemically reversible, and placing the electrode at a fixed potential in electrolyte alone will fix the surface composition. To eliminate any possible problems related to the transfer, Pretreatment III, which requires no transfer or exposure to oxygen, was finally adopted.

In Pretreatment III, glucose in the form of concentrated solution was added to the electrolyte in the reaction cell from a separatory funnel with the electrode maintained at all times at the start potential. This is in contrast to the prior pretreatments in which the cleaned electrode was introduced to the glucose containing electrolyte under open-circuit conditions before placement at the start potential. Figure 16 compares the cyclic voltammograms of glucose in the well behaved H_2SO_4 electrolyte recorded with the glucose added to the electrolyte at a fixed potential (Pretreatment III) with the electrode introduced to the glucose containing electrolyte under open-circuit conditions followed by placement at the start potential (Pretreatment I). Reducing the time that the electrode was exposed to glucose at the open-circuit potential to value as short as possible, i.e. placement of the electrode at the start potential immediately after immersion in the electrolyte, did not change the result from that shown in Figure 16. Differences are found in both the H and DL regions. In the H region, the open-circuit exposure reduces the anodic current to suggest a reduction in adsorption sites. In the DL region, an increase in the more negative peak is detected. This observation, and others like it, support the contention that the plateau

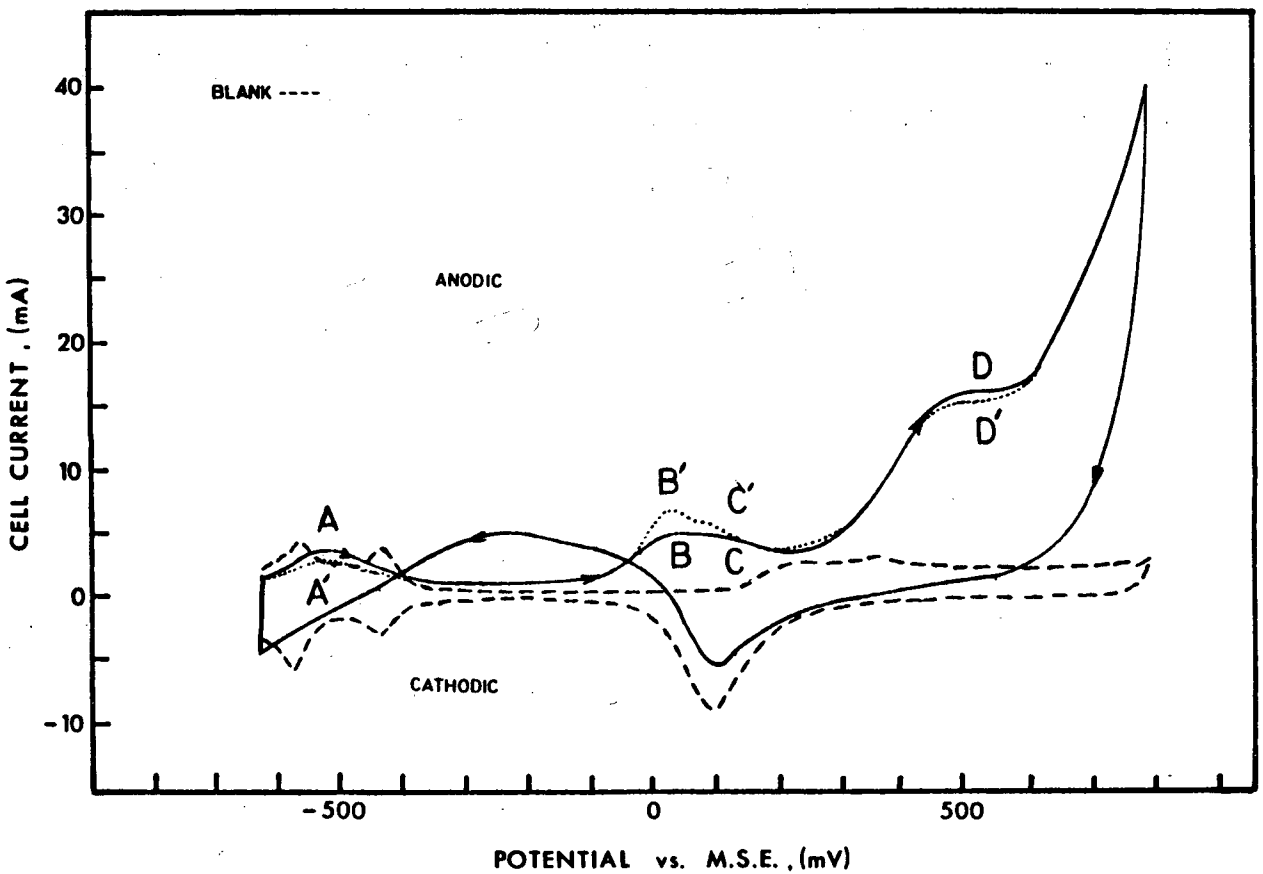

Figure 16. COMPARISON OF CYCLIC VOLTAMMOGRAMS OF 0.50M GLUCOSE RECORDED USING PRETREATMENT I (Dotted Line) AND PRETREATMENT III (Solid Line). DASHED LINE IS ELECTROLYTE ALONE. EXPERIMENTAL CONDITIONS: ELECTROLYTE, 1.00M H_2SO_4 (pH = 0.0); WORKING ELECTRODE, PLATINIZED Pt (898 cm^2); SCAN RATE, 5 mV/s; TEMPERATURE, 22°C.

structure in the DL region observed when Pretreatment III is used is really two independent peaks. Also, the use of Pretreatment I having an electrode open-circuit exposure time resulted in gas blister formation in this potential region which did not occur with Pretreatment III without this exposure.

Thus, these experimental results indicate that the method of Pt electrode exposure to the glucose is an important experimental aspect to control. The most likely cause of this effect is believed to be different, irreversible adsorption behavior of the glucose.

For reproducible results, sufficient exposure time of the glucose to the electrode must be allowed prior to recording a scan, even when the glucose is added to the electrolyte at fixed potential (Pretreatment III). The time between glucose addition and recording the cyclic voltammogram was varied, and a period of 10 minutes was found to be satisfactory. This time is believed to be associated with the establishment of the glucose adsorption equilibrium, since glucose adsorption measurements indicate that the equilibrium is closely approached in this time period.[31]

Differences in the cyclic voltammograms resulting from the pretreatment procedures are exemplified by comparing the set of cyclic voltammograms reported in the Biannual report (Figures 2 through 6, therein) recorded using a Pretreatment I procedure with those reported here (Figures 6, 9 through 12) using Pretreatment III. Comparison of these data, as well as others, showed that the cylic voltammograms obtained in the strong alkaline electrolyte (pH = 14.8) were negligibly affected by the electrode pretreatment used. However, this was not the case for such comparisons made at any other pH. For all the pH's except pH = 14.8, the electrooxidation in the H-region was virtually absent when variations of Pretreatment I were used, while oxidative currents larger than those found for the Pt hydrogen desorption peaks were observed when Pretreatment III was used. Thus, earlier pretreatments appear to yield a Pt surface that inhibits all reaction in the H region, even hydrogen desorption, while Pretreatment III gave a surface on which glucose electrooxidation takes place.

In the acid electrolytes (pH < 5.0), the DL region of the cyclic voltammogram exhibited subtle changes and the Pt-O region exhibited essentially no change with the differing electrode pretreatments. The electrooxidation with the DL region could appear as a single peak (Figure 2 of the Biannual report),

an initial sharp peak with a trailing shoulder, and a plateau-type structure, the latter two being illustrated in Figure 16. The actual peak form was found to vary among these except when Pretreatment III was employed.

The cyclic voltammograms of glucose recorded in electrolytes of pH = 6.6 and 11.7 showed the largest differences with electrode pretreatment. Although electrooxidations of some sort were always detected in the DL and Pt-O regions at these pH's, the peak structures were found to differ substantially depending on the electrode pretreatment used. (Compare Figures 4 and 5 of the Biannual report with Figures 10 and 11 here for example.) Only Pretreatment III gave consistently reproducible results, however.

Influence of O_2. All data presented up to this point were obtained under an inert N_2 atmosphere. Because glucose as well as other carbohydrates can be catalytically oxidized on Pt in the presence of oxygen,[76,80] cyclic voltammograms were recorded in its presence in order to detect any perturbation on the glucose oxidation which it might cause. Data were collected in electrolytes of 1.00M H_2SO_4 and 6.1M KOH containing 0.50M glucose at ambient temperature and 62°C. Pretreatment I was used in these experiments. The electrolytes were purged either with N_2 or O_2. No significant differences were observed between the cyclic voltammograms obtained from electrolytes purged with the two gases. Consequently, the presence of O_2 does not seem to interfere with the electrochemical processes taking place.

Conclusions. The cyclic voltammetry results obtained for glucose on platinized Pt exhibited considerable variation dependent on electrolyte and electrode pretreatment. Variation in electrolyte, primarily pH, affected the glucose results by influencing the electrochemical reaction through their rates and potentials and by determining the molecular entities present through chemical reaction of the glucose in the electrolyte. Both phenomena were believed to have occurred. Based upon literature evidence[81-83] and that given here, the variations associated with electrode pretreatment arise from complex adsorption and reaction behavior of glucose on the various surfaces of the Pt electrode. As a result of this, a precise statement of the electrode surface conditions, i.e. the pretreatment, must be specified for any cyclic voltammetry to be meaningful. In addition, because the cyclic voltammograms of glucose electrooxidation appear to be influenced so heavily by the adsorption phenomena, their information content relates more heavily to this

transient adsorption behavior than to bulk electrolysis of the glucose, which is the aspect of interest here. Nonetheless, the electrooxidations observed in the DL and Pt-O regions under all conditions examined are more than transient electrosorption reactions, although they may involve adsorption in the oxidative pathway and can be considered as possible candidates as depolarizing reactions.

The peak current densities reported for the electrooxidations of glucose (Tables 5 and 6) are only in the tens of microamperes per cm^2 of real area. However, such small values are not unreasonable when viewed in the light of available Pt-supported fuel cell electrodes. Carbon-supported platinum electrodes commonly have 500 to 1000 cm^2 of real Pt area per cm^2 of electrode area with a Pt loading of 1 mg/cm^2 electrode area.[84] Therefore, the real current densities given in Tables 5 and 6 should be multiplied by 500 to 1000 if an operating current density per square centimeter of fuel cell electrode area is desired. If this is done, acceptable rates of electrooxidation may be contemplated. Electrooxidation in the DL region is the most negative and would be the most beneficial for purposes of depolarization. Based upon the potential difference between the glucose peak potentials and the reversible hydrogen potential, electrolysis cell voltages in the range from 600 to 800 mV might be expected. These potentiodynamic experiments yield only limited information on whether the oxidations can be sustained for times greater than in these experiments or about the reaction products formed. Further work addressing these issues is considered in Task 3.

Platinum Anode — Shiny

To identify any possible consequences of platinizing, a comparison was made between the cyclic voltammograms of glucose in 1.00M H_2SO_4 recorded with shiny and with platinized Pt electrodes. Pretreatment I was employed. The results are in Table 7. For the oxidation occurring in the DL region, the current densities were about equal, indicating that it scales well with the increased area afforded by platinization. The peak potentials obtained with the shiny Pt were shifted significantly to more positive values. In the Pt-O region the situation was reversed. The peak potentials were the same within experimental error, but the current density obtained with the shiny Pt electrode was significantly larger than that recorded with the platinized electrode. It is not clear why these differences occur. The differences

Table 7. COMPARISON OF PEAK POTENTIALS AND CURRENT DENSITIES IN THE CYCLIC VOLTAMMOGRAMS FOR THE OXIDATION OF GLUCOSE ON PLATINIZED PLATINUM AND SHINY PLATINUM*

Pt Electrode Type	DL Region		PtO Region	
	$E_{p,a}$ vs. SCE, mV	$i_{p,a}$, $\mu A/cm^2$	$E_{p,a}$ vs. SCE, mV	$i_{p,a}$, $\mu A/cm^2$
Shiny	+542	9.9	+915	35.6
Platinized	+406	6.7	+895	12.9

detected are believed to be of a quantitative nature with no differences in the actual types of processes occurring.

Platinum Anode — Shiny With Underpotentially Deposited Metals

Rates of glucose electrooxidation on Pt are far below the diffusional limit dictated by the concentration of the glucose used. In addition, even though the initial currents per geometric area may be made large by increasing the anode's roughness (platinization), undesirable declines in the current density occur during the course of glucose electrooxidation, as will be shown in Task 3. This situation is also encountered during the electrooxidation of other organic materials as well. One approach currently being explored to remedy these problems during the electrooxidation of organic substrates is the underpotential deposition of foreign adatoms on the Pt electrode surface.[85-90] The deposition of foreign metal adatoms on to the surface of Pt not only has the effect of increasing the reaction rate appreciably, in some instances, but also of shifting the oxidation to more negative anode potentials. Because the literature has reported beneficial catalytic effects for the electrooxidation of simple alcohols and aldehydes using this method, its applicability to the functionally related glucose molecule seemed appropriate. Metals that have exhibited the greatest catalytic effects are Pb, Bi, and Tl; consequently, they were chosen in the present study.

Experimental. Experimentally, cyclic voltammetry was used to identify any catalytic effect of metal adatoms. Shiny Pt was used as the anode, and 0.50M $HClO_4$ was the electrolyte with and without 0.50M glucose. The metals were introduced as nitrates, normally at the 1.0×10^{-3}M level. Data were recorded at a 50 mV/s scan after preparation of the anode by Pretreatment III. All other methods were identical to those previously described in the platinized Pt section.

Results and Discussion. To identify any catalytic effect, four voltammograms are required for comparison: 1) blank electrolyte, 2) blank electrolyte plus glucose, 3) blank electrolyte plus metal nitrate, and 4) blank electrolyte plus glucose and metal nitrate. Figure 17 compares the blank electrolyte scan on Pt in 0.50M $HClO_4$ with and without 0.50M glucose; these scans are given for comparison to those to be presented which contain the metalions in the electrolyte. As has been presented earlier the glucose exhibits electrooxidation in all three potential regions of the Pt electrode. The cyclic voltammograms shown in Figure 17 were recorded at a 50 mV/s scan rate. At the 5 mV/s scan rate, which has been used in the past, the peak in the hydrogen region (A) is reduced and that in the double-layer region (B) is increased.

Figure 18 gives the cyclic voltammograms obtained in the presence of 1.0 X 10^{-3}M $Pb(NO_3)_2$ with and without 0.50M glucose along with the blank electrolyte as a reference. Clearly the presence of Pb^{2+} has an enormous catalytic effect on the glucose electrooxidation. Peaks A and B in Figure 18 are attributed to catalytic glucose oxidation, Peak C is attributed to the stripping of the under potential deposited Pb^{2+}, and Peak D is attributed to the normal glucose oxidation in this potential region. Peak I of Figure 18 shows the stripping of the Pb^{2+} in the absence of glucose. The current density for the glucose oxidation in the double-layer region under these conditions increased by about an order of magnitude from 30 $\mu A/cm^2$ without Pb^{2+} to 350 $\mu A/cm^2$ with Pb^{2+}. The doubling of the glucose oxidation (Peaks A and B) is interesting in light of prior results that have exhibited this behavior. What each peak represents is unknown at this time, however. Increasing the Pb^{2+} concentration to 0.99 X 10^{-2}M gave additional increases in the peak current density up to a value of about 425 $\mu A/cm^2$ for the oxidation in the double-layer region. One experiment with platinized Pt (976 cm^2 area) was performed using a Pb^{2+} concentration of 1.0 X 10^{-3}M. A 16% increase in current density was observed for the glucose oxidation in the double-layer region. This less dramatic increase presumably arises because the amount of Pb^{2+} available per unit area is a thousand times less.

Figure 19 shows the electrocatalytic effect of Tl^+ on glucose electrooxdiation. Like Pb^{2+}, there is an order of magnitude increase in glucose electrooxidation in the double-layer region. Current densities of the order

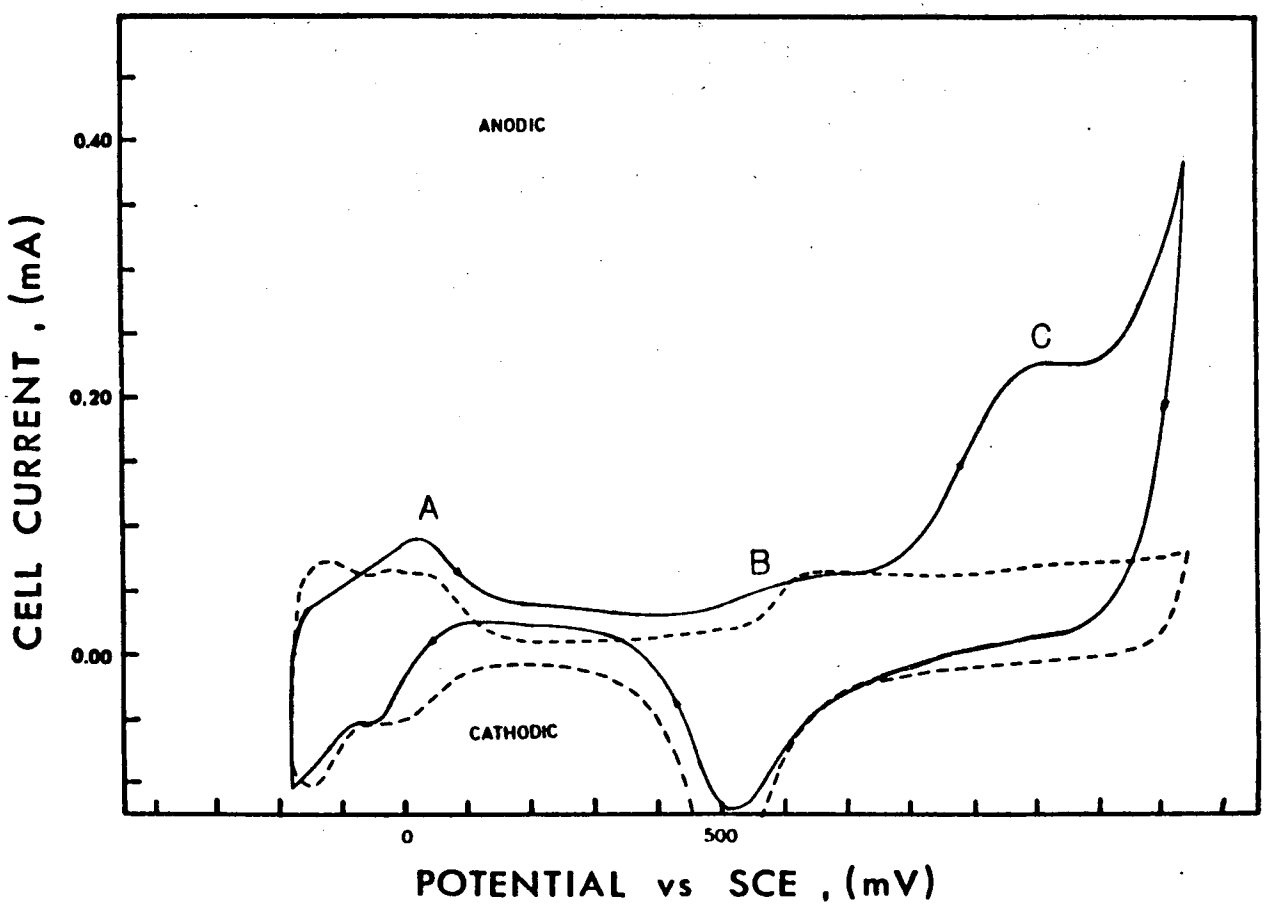

Figure 17. COMPARISON OF CYCLIC VOLTAMMOGRAMS ON SHINY Pt (1 cm^2) IN a) 0.50M $HClO_4$ (Dashed Line) AND b) 0.50M $HClO_4$/0.50M GLUCOSE (Solid Line); SCAN RATE, 50 mV/s; TEMPERATURE, 23°C.

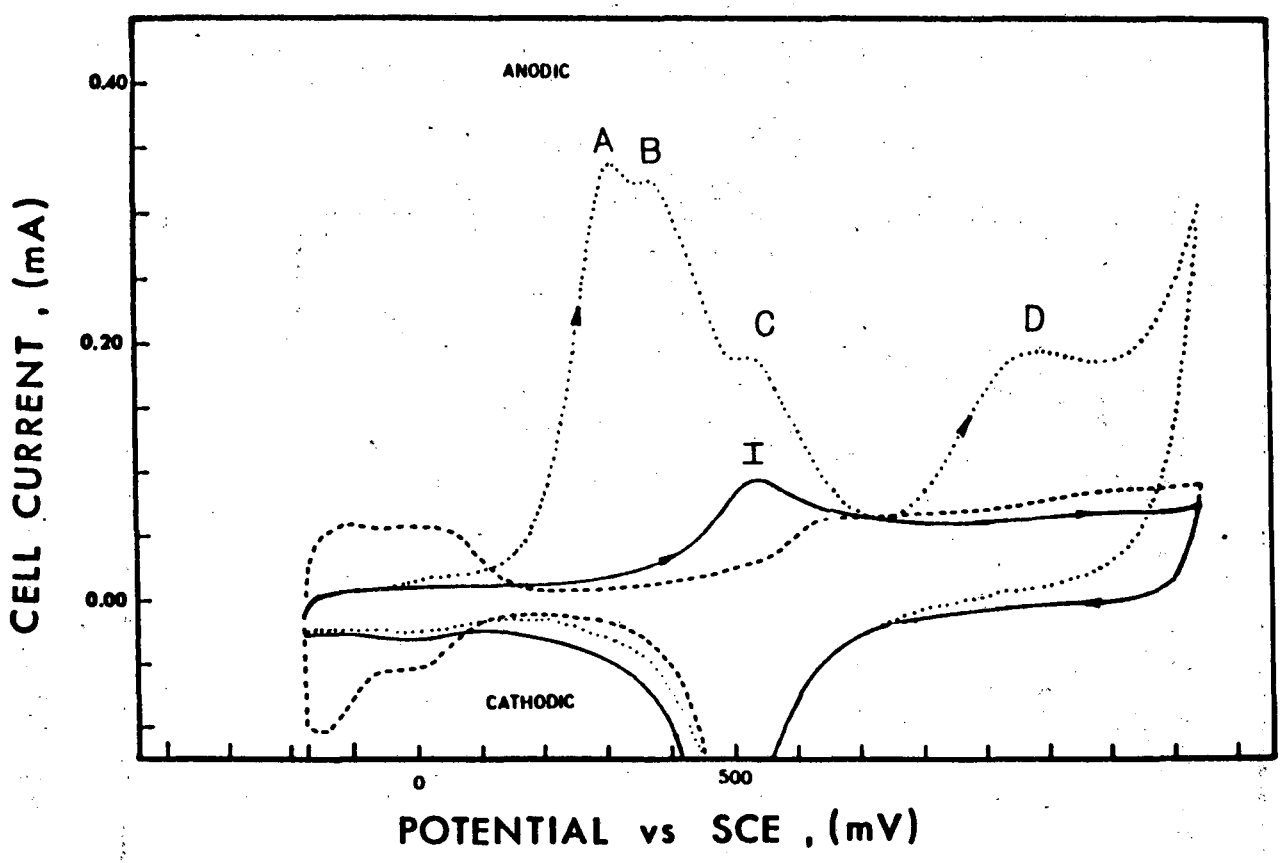

Figure 18. COMPARISON OF CYCLIC VOLTAMMOGRAMS ON SHINY Pt (1 cm^2) IN a) 0.50M $HClO_4$ (Dashed Line), b) 0.50M $HClO_4$/1.0 X 10^3M $Pb(NO_3)_2$ (Solid Line), AND c) 0.50M $HClO_4$/1.0 X 10^3M $Pb(NO_3)_2$/0.50M GLUCOSE (Dotted Line); SCAN RATE, 50 mV/s; TEMPERATURE, 23°C.

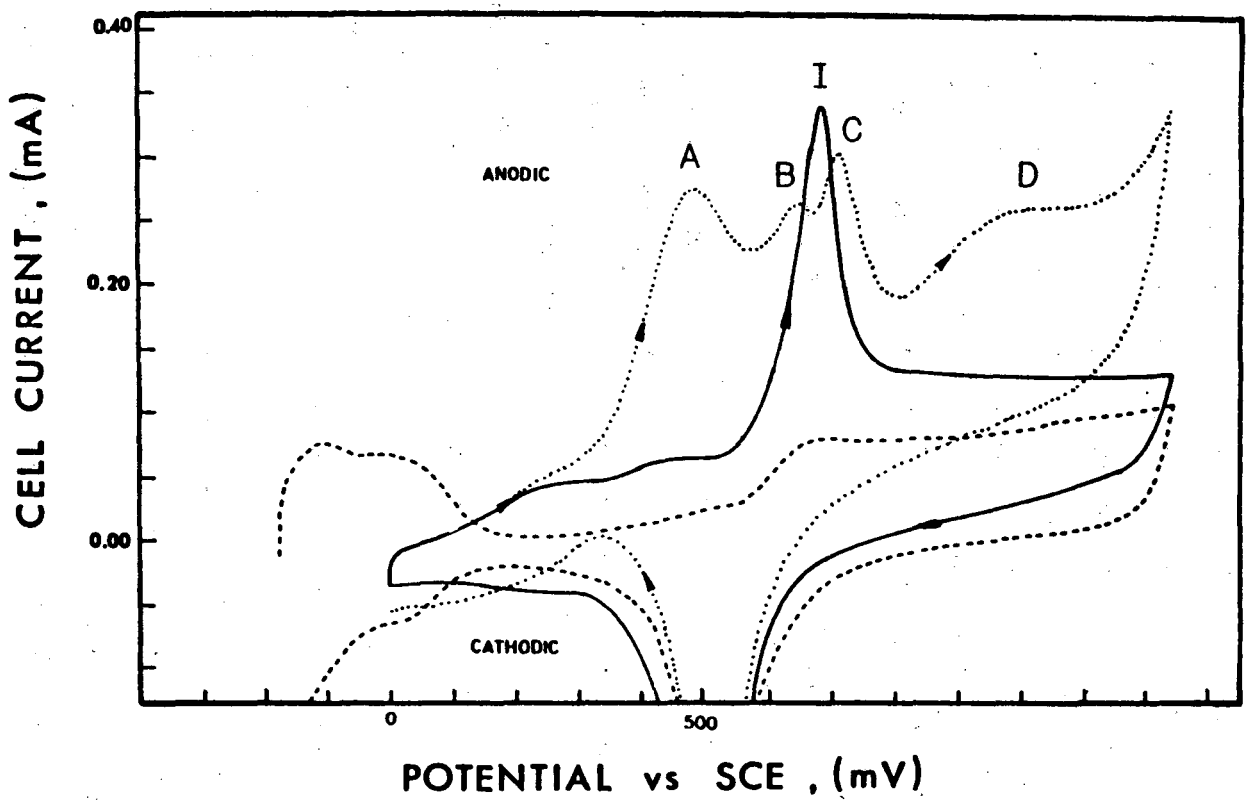

Figure 19. COMPARISON OF CYCLIC VOLTAMMOGRAMS ON SHINY Pt (1 cm^2) IN a) 0.50M $HClO_4$ (Dashed Line), b) 0.50M $HClO_4$/1.0 X 10^{-3}M $Bi(NO_3)_3$ (Solid Line), AND c) 0.50M $HClO_4$/1.0 X 10^{-3}M $Bi(NO_3)_3$/0.50M GLUCOSE (Dotted Line); SCAN RATE, 50 mV/s; TEMPERATURE, 21°C

350 μA/cm^2 (Peak A, Figure 19). Only a single broad peak is found with Tl^+, as opposed to the double peak exhibited in the presence of Pb^{2+}.

At more positive potentials (Peak C or II) the $Tl^+ \rightarrow Tl^{3+}$ couple comes into play. Increased current is found with the glucose present at these potentials although it may result only from the additivity of the Tl couple and the glucose oxidation currents in this region. Peaks I and B are believed to arise from the stripping of the underpotential deposited Tl.

Bi was also observed to exhibit an electrocatalytic effect (Figure 20), but it was less than those detected when Pb^{2+} or Tl^+ was used. The Bi^{3+} background was also substantially larger than the other metals. Glucose oxidation (Peak A, Figure 20) was still on the order of 275 μA/cm^2, which is considerably larger than the 30 μA/cm^2 seen in the absence of the Bi^{3+}. The origin of Peaks B and C of Figure 20 are unknown, but at least one of them arises from Bi stripping. The normal oxidation of glucose (Peak D, Figure 20) appears in the "Pt-O" region.

Conclusions. The presence of the heavy metal adatoms on the Pt clearly has a substantial beneficial effect on the rate of glucose electrooxidation in the DL region, at least over short periods of time. Increases in peak currents for the glucose DL-region oxidation were increased tenfold by the presence of the adatoms. Peak potentials were also beneficially shifted to slightly more negative values. Although the voltammetric results obtained using underpotential deposited heavy metals appears very promising, they do not necessarly accurately describe steady-state electrooxidation of the glucose, and further work would be required to identify their effect in the steady-state case. An expanded version of this adatom work was recently published,[91] the results of which were identical to those found here.

Palladium Anode

Pd, like Pt, is an electrode material often capable of electrocatalyzing organic oxidations. In addition, because oxygen evolves at positive potentials before metal corrosion begins, Pd is useful as an anode material. Lack of opportunity allowed only a very limited study of glucose electrooxidation of glucose on Pd, and only a single electrolyte at a single temperature was investigated.

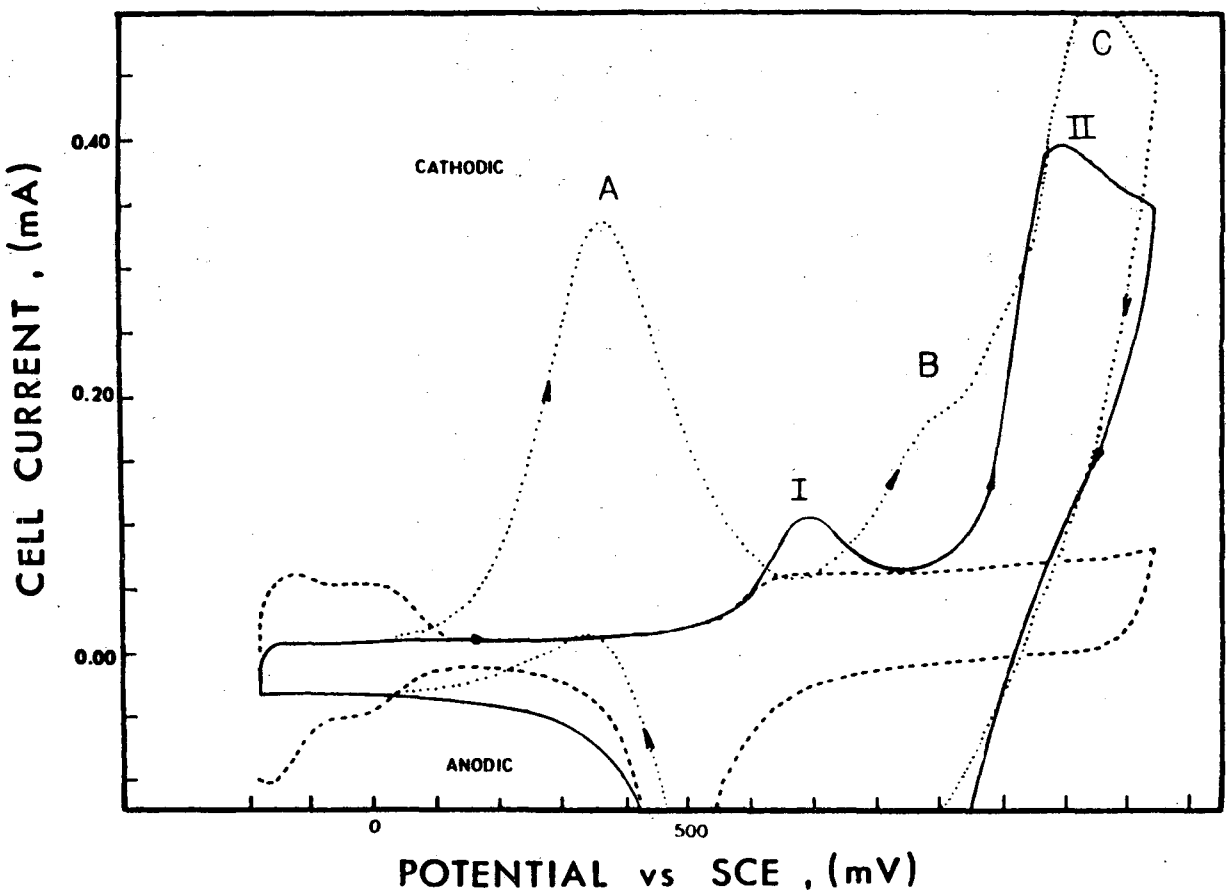

Figure 20. COMPARISON OF CYCLIC VOLTAMMOGRAMS ON SHINY Pt (1 cm^2) IN a) 0.50M $HClO_4$ (Dashed Line), b) 0.50M $HClO_4$/1.3 X 10^{-3}M $TlNO_3$ (Solid Line), AND c) 0.50M $HClO_4$/1.3 X 10^{-3}M $TlNO_3$/0.50M GLUCOSE (Dotted Line); SCAN RATE, 50 mV/s; TEMPERATURE, 21°C

Experimental. Cyclic voltammograms were recorded in the 6.1M KOH (No. 7, Table 4) electrolyte with and without glucose at 23°C. The anode was a shiny Pd disc; 1.00 cm^2 was exposed to the electrolyte. Before each scan, an anodizing pretreatment of the electrode was performed at 250 mA constant current in 1.00M H_2SO_4 for 2 minutes. After thorough rinsing, the anode was transferred to the reaction cell and maintained at the start potential (—700 mV versus Hg/HgO) for 2 minutes prior to beginning the scan. The pretreatment gave qualitatively reproducible scans, but the peak current densities varied by as much as 25%.

Results and Discussion. The cyclic voltammogram of glucose on Pd in the strong alkaline electrolyte is shown in Figure 21. Substantial anodic peak current densities (20 to 40 mA/cm^2) are detected in the presence of glucose in an attractive potential range, —400 to 0 mV versus Hg/HgO (add +926 mV for RHE). The voltammogram without glucose is not shown in Figure 21 because at the gain used no current would be detectable; Figure 22 gives the electrolyte scan alone on an expanded scale, indicating that the maximum background currents are on the order of 50 μA or less at potentials where the glucose electrooxidation occurs. As Figure 21 illustrates, Pd exhibited the same potential regions associated with Pt. Comparison of Figures 21 and 22 indicates that glucose electrooxidations occur in the Pd DL region and that the current drops precipitously as Pd oxide begins to form near a potential of 0 mV versus Hg/HgO. Two glucose electrooxdiations appear to occur in the Pd DL region and, as with Pt, an anodic peak is found in the reverse scan after the Pd oxide has been stripped.

Even though the similarities of Pt and Pd are great, the oxidation of glucose on them under the same conditions is almost totally unrelated. (Compare Figure 21 with Figure 12a.) Whereas glucose electrooxidation occurs in all three electrode potential regimes for Pt, it only occurs in the DL region on Pd. In addition, the peak currrent densities on Pd are three orders of magnitude larger in this region than on Pt. The results also indicate that the Pd oxide surface is inactive toward glucose while the Pt oxide is active.

Conclusions. The electrooxidation of glucose on the Pd anode looks very promising for this single set of experimental conditions. The peak current densities observed were large and could possibly be made larger by heating and

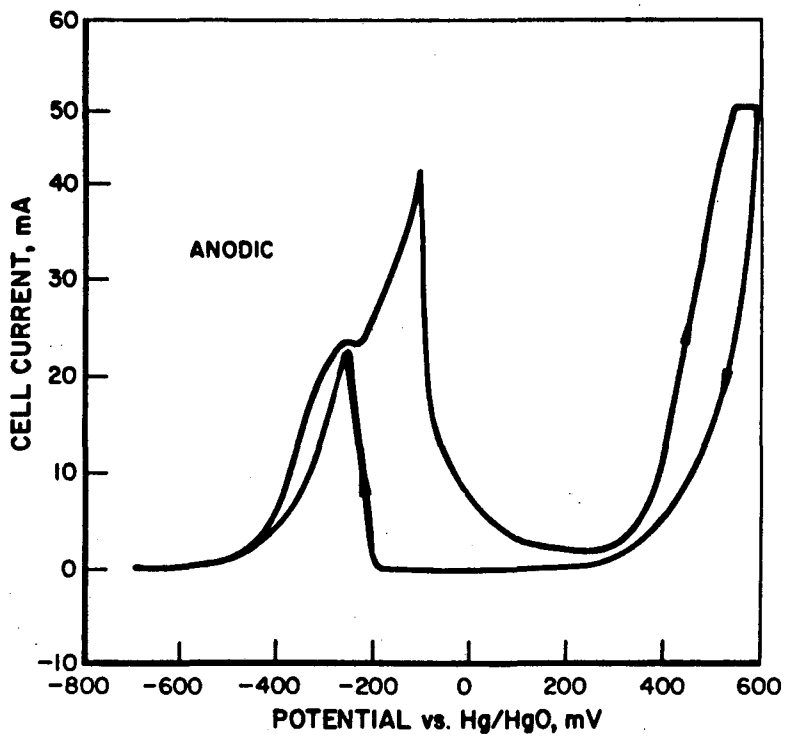

Figure 21. CYCLIC VOLTAMMOGRAM OF 0.50M GLUCOSE IN 6.1M KOH ON A SHINY Pd (1 cm^2) ANODE AT A 5 mV/s SCAN RATE AND 28°C

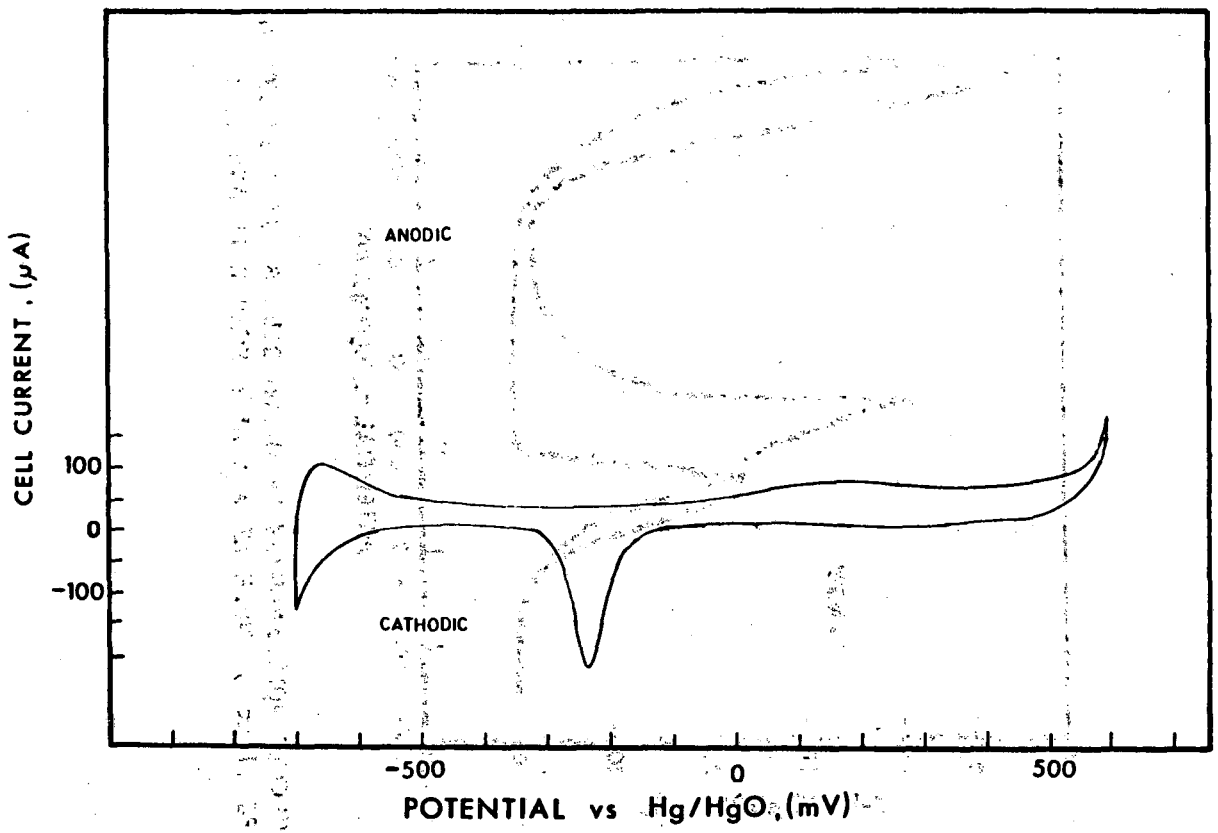

Figure 22. CYCLIC VOLTAMMOGRAM OF SHINY Pd (1 cm^2) IN 6.1M KOH ALONE AT A 5 mV/s SCAN RATE AND 23°C. SURFACE REACTIONS ARE SIMILAR TO THOSE OF Pt.

INSTITUTE OF GAS TECHNOLOGY

61060

by increasing the active area per electrode geometric area. In addition, the oxidations occur at desirable electrode potentials versus the RHE.

Nickel Anode

Nickel as anode material was of interest from a number of viewpoints. It is one of the few non-noble metals which has a history of use as an anode and is the material presently used as the anode in most commercial water electrolyzers.[92] The literature also describes the use of Ni as an anode material for electrooxidation of organic compounds, in particular alcohols.[93-98] As the glucose molecular structure is dominated by alcohol groups, Ni was considered to be a likely candidate for application here. A report in which the electrooxidation of glucose on Ni appeared only as an entry in a table[93] also suggested that Ni might be a desirable anode.

Experimental. Cyclic voltammograms were recorded on a 1-cm^2, shiny anode in Electrolyte Nos. 5 through 7 of Table 4 with and without 0.50M glucose present. These electrolytes covered the pH range from neutral to strongly basic. Acidic electrolytes were, of course, avoided because of Ni corrosion. Data were obtained in all the electrolytes at ambient temperature and at 67°C for the pH = 14.8 electrolyte (No. 7, Table 4) only. The 6.1M KOH electrolyte at 67°C closely mimics the conditions found in a commercial Stuart Electrolyzer, which contains a Ni anode.

Little electrode pretreatment was required to obtain good voltammetry results with the Ni anode. After degreasing, the electrode was placed in the reaction cell containing electrolyte only and a blank scan was recorded. Then, as in Pretreatment III previously discussed, concentrated glucose was added to the electrolyte with the anode maintained at the start potential. Unlike Pt, the Ni anode did exhibit sensitivity to the pretreatment used.

Results and Discussion. The most dramatic results were found in the strongly basic electrolyte (pH = 14.8), and Figure 23 shows the cyclic voltammograms under these conditions. As can be seen from Figure 23, very large current densities were obtained in the presence of glucose which were not seen in its absence. At 22°C (Figure 23A) a single well-defined anodic peak was detected at +525 mV versus Hg/HgO with a peak current density of 92 mA/cm^2 at a 5 mV/s scan rate. Increasing the temperature to 67°C converted the well-defined peak observed at 22°C into a plateau structure (Figure 23B) with a

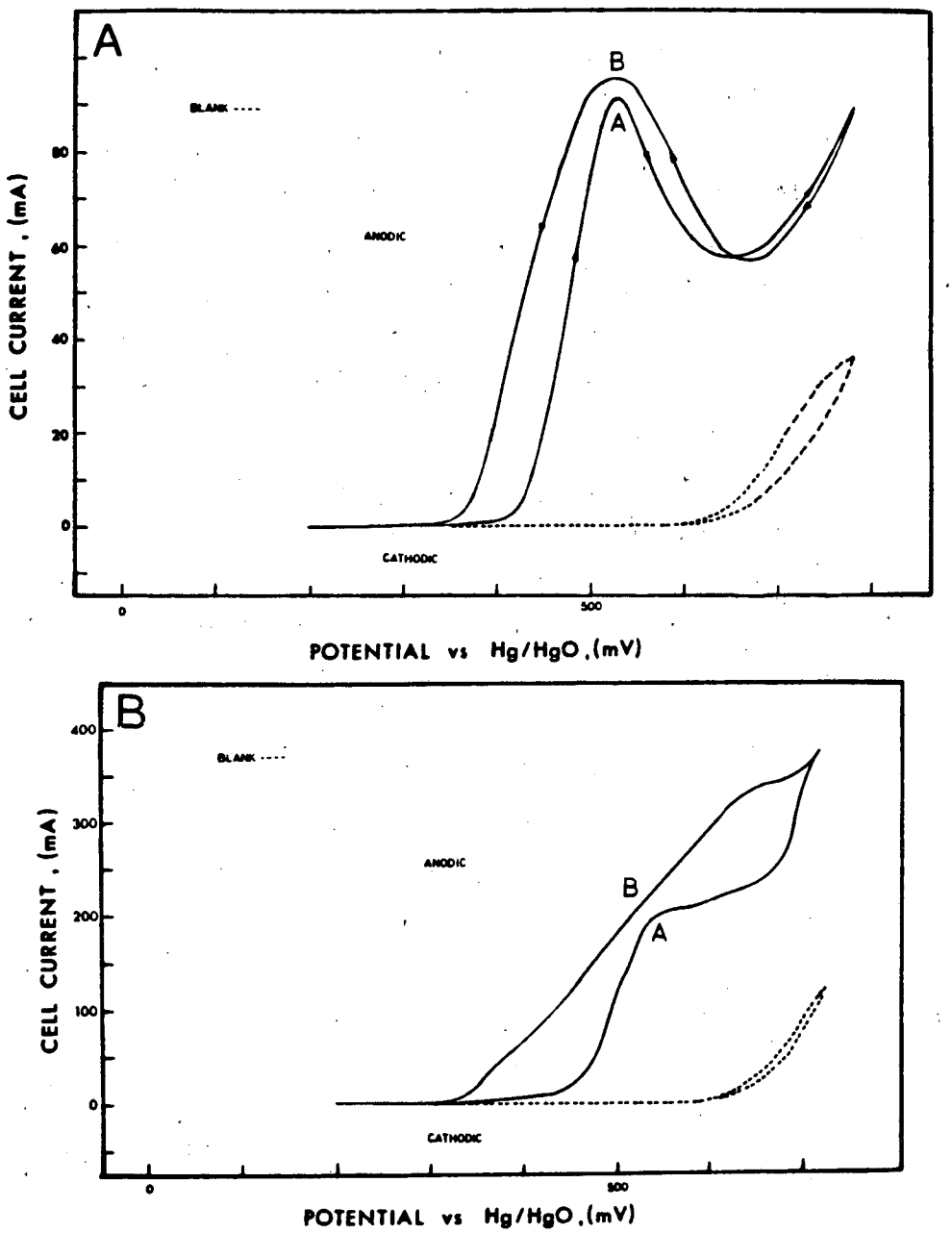

Figure 23. COMPARISON OF CYCLIC VOLTAMMOGRAMS WITH (Solid Line) AND WITHOUT (Dashed Line) 0.50M GLUCOSE PRESENT. EXPERIMENTAL CONDITIONS: ELECTROLYTE, 6.1M KOH (pH = 14.8); WORKING ELECTRODE, NICKEL (1 cm^2); SCAN RATE, 5 mV/s; TEMPERATURE, (a) 22°C AND (b) 67°C.

current density of 205 mA/cm^2 at a potential of 550 mV versus Hg/HgO (Point A). This magnitude of current density is more in keeping with direct oxidation of bulk glucose. Note that the currents measured on the return scan are even larger than those in the forward positive scan.

The cyclic voltammogram of Ni in the KOH electrolyte alone is shown in Figure 24 at greater current gain than to the voltammograms of Figure 23. The surface reaction of the Ni anode can be seen here by comparing Figures 23 and 24. The onset of glucose oxidation can be seen to coincide with the Ni surface reaction, an "oxide" formation.

At the lower pH's of 11.7 and 6.6 (Electrolyte Nos. 5 and 6, Table 4) little glucose electrooxidation was detected. This observation can be correlated with the behavior of the Ni "oxide" formation. In the pH = 11.7 electrolyte at 23°C, "oxide" does not form until very positive potentials are reached. When it does form, the anode potential is only 100 mV away from the anodic breakdown of the electrolyte, and what glucose elctrooxidation can be detected is quickly masked by the large anodic breakdown currrents. On the basis of data at pH's 14.8 and 11.7, the potential of the oxide formation moves more positive as a function of pH at a rate approximately twice as large as the anodic breakdown potential. This trend is, of course, the opposite of that desired.

Only a very slight negative shift in the anodic breakdown potential is observed with the Ni anode at pH = 6.6 and 23°C in the presence of glucose. No Ni "oxide" formation is detected in the scan of the electrolyte alone, which is consistent with the observed trend of the "oxide" formation potential as function of pH mentioned above.

Conclusions. The Ni anode exhibits the ability to electrooxidize glucose at current densities as high as 100 mA/cm^2 in the pH = 14.8 electrolyte. The evidence suggests that the Ni "oxide" surface is required to catalyze the reaction. Although large current densities are found, the potentials at which they occur are larger than desired; that is, there is only a small depolarizing effect. The peak potential (Peak A in Figure 23A) versus the RHE is 1450 mV, for example.

Because of the unfortunate pH dependence of the potential for Ni "oxide" formation, no advantage can be gained by lowering the pH.

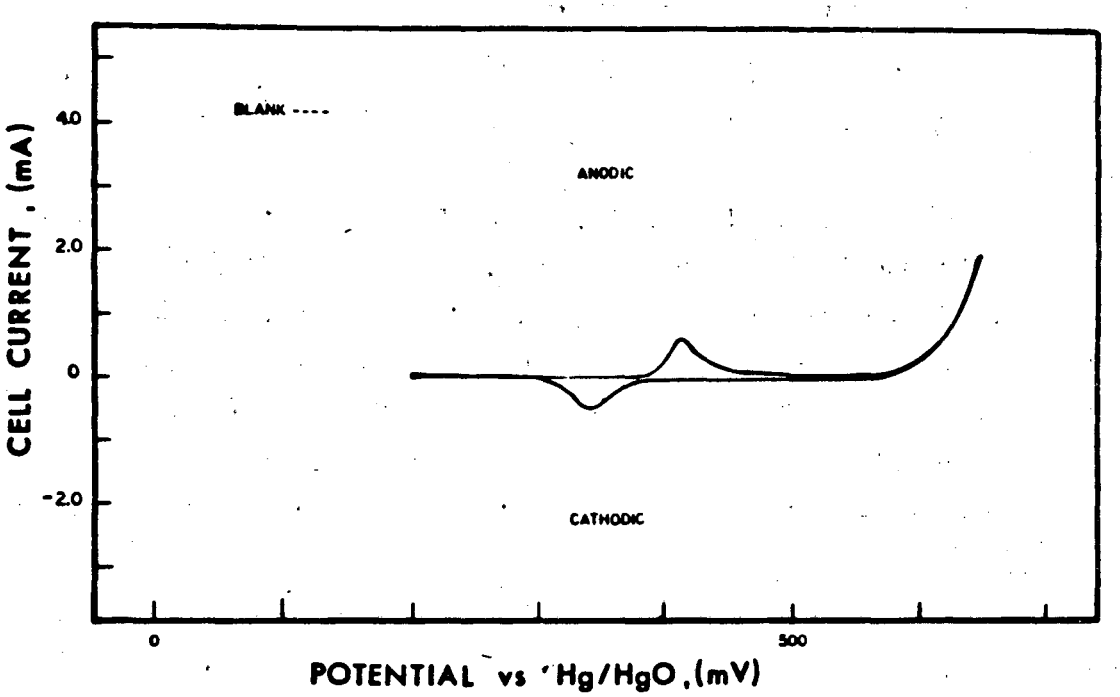

Figure 24. CYCLIC VOLTAMMOGRAM OF Ni (1 cm^2) IN 6.1M KOH AT 24°C WITH 5 mV/s SCAN RATE

Rhodium Anode

A prior literature report suggested that glucose may be more readily electrooxidized on Rh than on Pt.[25] In addition, Rh is a generally known electrocatalytic material, and for this reason it was selected for investigation.

Experimental. The possible oxidation of glucose on a shiny 1-cm^2 Rh electrode was investigated in Electrolytes 1, 5, and 7 in Table 4 and at temperatures of 25° and 65°C. These electrolytes were selected to cover acid, neutral, and base. The cyclic voltammograms in electrolyte alone exhibited similar features to those found with Pt. Hydrogen, double-layer, and "Rh-oxide" regions were observable with the DL being much smaller than that found with Pt. Although a pretreatment of the Rh electrode similar to that described for the Pt electrode was initially explored, it was not found to be required in order to obtain reproducible surfaces on the Rh electrode as evidenced by cyclic voltammetry. Therefore, simple rinsing in conductivity water was the only electrode pretreatment prior to recording voltammograms.

Results and Discussion. In the H_2SO_4 and phosphate buffer, differences between cyclic voltammograms recorded with and without glucose present were insignificant. Only a slightly earlier increase in current occurred near the anodic breakdown potential of the electrolyte.

In the KOH electrolyte, electrooxidations appeared in the cyclic voltammograms when glucose was present. At 25°C and a scan rate of 5 mV/s, a peak was observed at —375 mV versus Hg/HgO with a peak current density of 0.10 mA/cm^2. In addition, the increase at the positive end of the scan occurred 250 mV more negative than with the electrolyte alone. When the electrolyte temperature was raised to 65°C, oxidation of the glucose solution occurred over a wide range of potential beginning at —450 mV versus Hg/Hgo as shown in Figure 25. Three local maxima were discernible as the current rose with increasing potential. Table 8 lists the peak potentials and peak current densities, which show how the current increases with potential.

Conclusions. Significant electrochemical reaction of glucose only occurs with the Rh electrode in strong alkaline electrolyte. The peak current densities at pH = 14.8 of about 1 mA/cm^2 (real), although not extremely large, could presumably be increased per electrode geometric area by appropriate

Table 8. PEAK POTENTIALS ($E_{p,a}$) AND PEAK CURRENT DENSITIES ($i_{p,a}$) FOR THE CYCLIC VOLTAMMETRY OF GLUCOSE IN 6.1M KOH ON A Rh ELECTRODE AT 65°C

Peak Designation Figure 25	$E_p^*{}_{,a}$, mV vs. Hg/HgO	$i_p^*{}_{,a}$, mA/cm^2
A	−445	0.55
B	−275	0.80
C	−68	1.35

* Average of three scans.

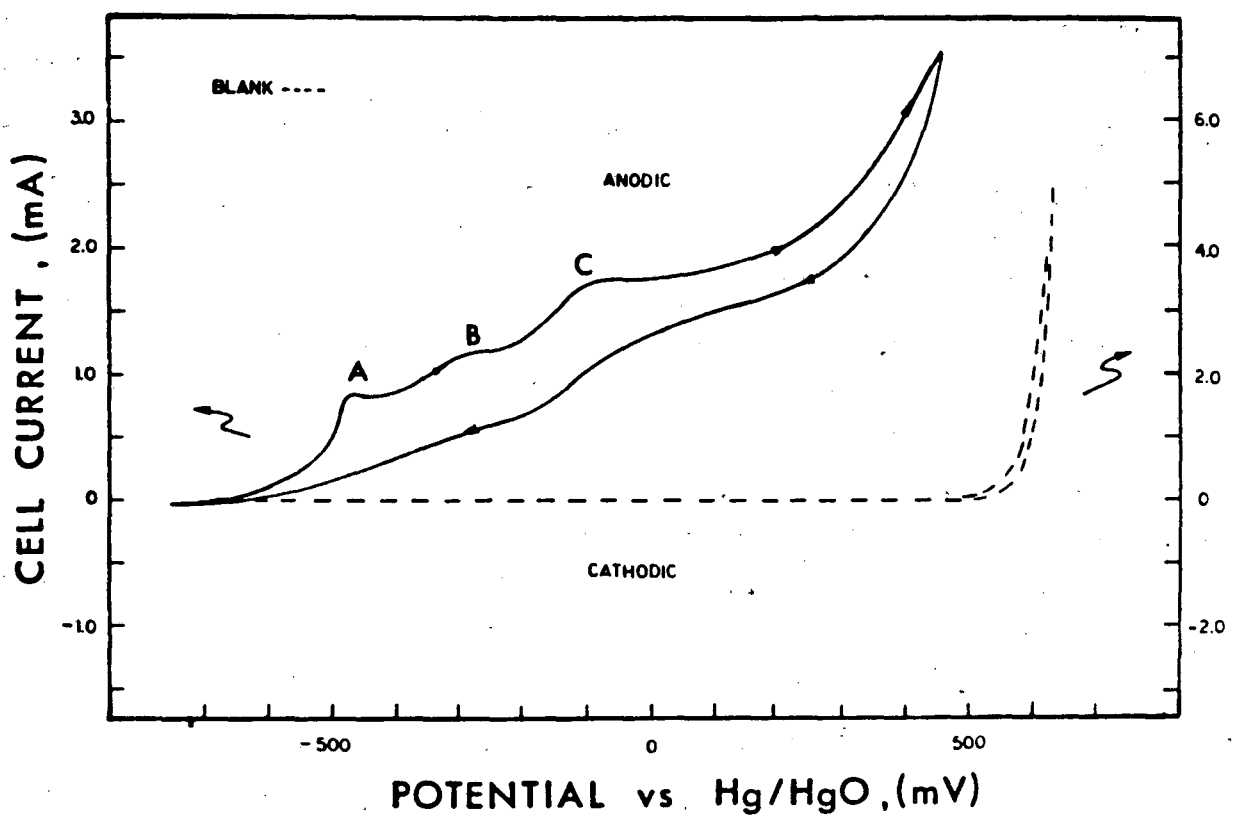

Figure 25. COMPARISON OF CYCLIC VOLTAMMOGRAMS WITH (Solid Line) AND WITHOUT (Dashed Line) 0.50M GLUCOSE PRESENT. EXPERIMENTAL CONDITIONS: ELECTROLYTE, 6.1M KOH (pH = 14.8); WORKING ELECTRODE, SHINY Rh (1 cm^2); SCAN RATE, 5mV/s; TEMPERATURE, 66°C.

dispersion of the Rh. The potential at which glucose electrooxidation occurs is satisfactory beginning approximately at +500 mV versus RHE (—445 mV versus Hg/HgO). The fact that appreciable glucose electrooxidation on Rh occurs only in strong alkaline at elevated temperature may suggest, on the basis of the HPLC data, that it is not glucose directly which is active on Rh but another chemically derived species formed under these conditions.

Lead Anode

Pb is a common and inexpensive anode material, and cyclic voltammetry in glucose-containing electrolytes was also performed with it.

Experimental. The 1-cm^2 Pb (Alfa Products) electrode was pretreated by rinsing it in conductivity water prior to each voltammogram. The electrolytes investigated were H_2SO_4 and KOH, Nos. 1 and 7 in Table 4, at ambient and 65°C. The cyclic voltammograms of Pb in these electrolytes contained some unusual features, presumably attributable to Pb surface reactions. This behavior is exemplified in Figure 26. A reversible surface reaction, designated A in Figure 26, is found at negative potentials. Then nothing occurs in the forward scan until the anodic breakdown of the electrolyte begins, near 2000 mV versus SCE. In the return scan the unusual feature designated B in Figure 26 is observed in which a sharp anodic spike is followed by a cathodic peak. An identical pattern occurs in the 6.1M KOH electrolyte except that it is shifted in potential.

Results and Discussion. Qualitatively, the cyclic voltammograms recorded in 1.00M H_2SO_4 with glucose at 23° and 66°C were identical. The currents detected at 66°C were 5 times greater than at 23°C, and the voltammogram at the higher temperature is shown in Figure 27. The currents detected between 1300 and 1700 mV versus SCE appear in the reverse scan only, after the potential had made a small excursion into the electrolyte breakdown range. Thus, it appears necessary to provide a sufficient positive potential to break down some surface structure before glucose electrooxidation can commence. The electrooxidation observed appears at a very positive potential, however.

Rather complicated cyclic voltammograms were found in the alkaline electrolyte. Figure 28 illustrates the behavior at 23°C. The scans with and without glucose are qualitatively similar. Glucose causes distortions at the Pb surface reaction peaks and also produces an overall increase in anodic cur-

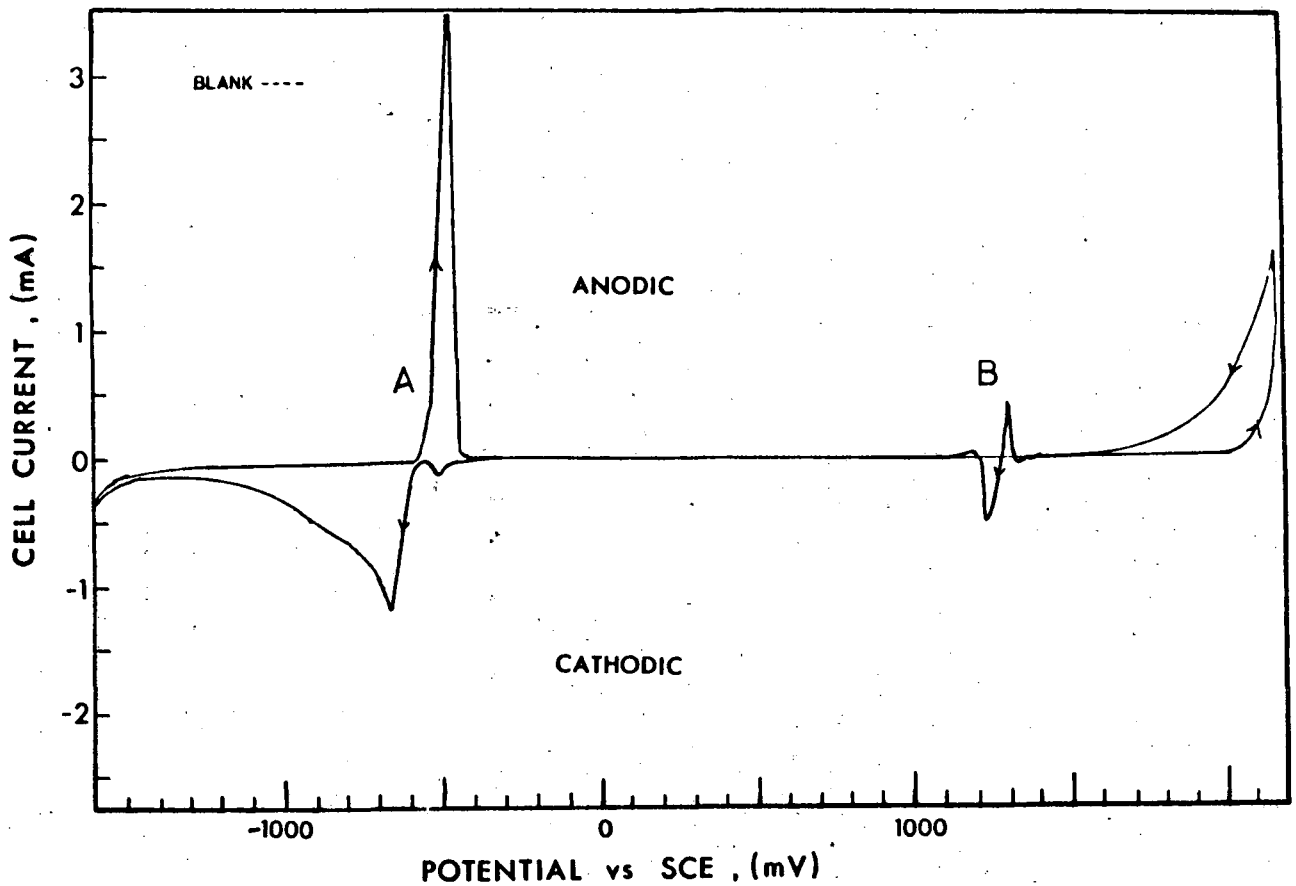

Figure 26. CYCLIC VOLTAMMOGRAM OF Pb ($1cm^2$) IN 1.00M H_2SO_4 ALONE AT A 5mV/s SCAN RATE AND 23°C

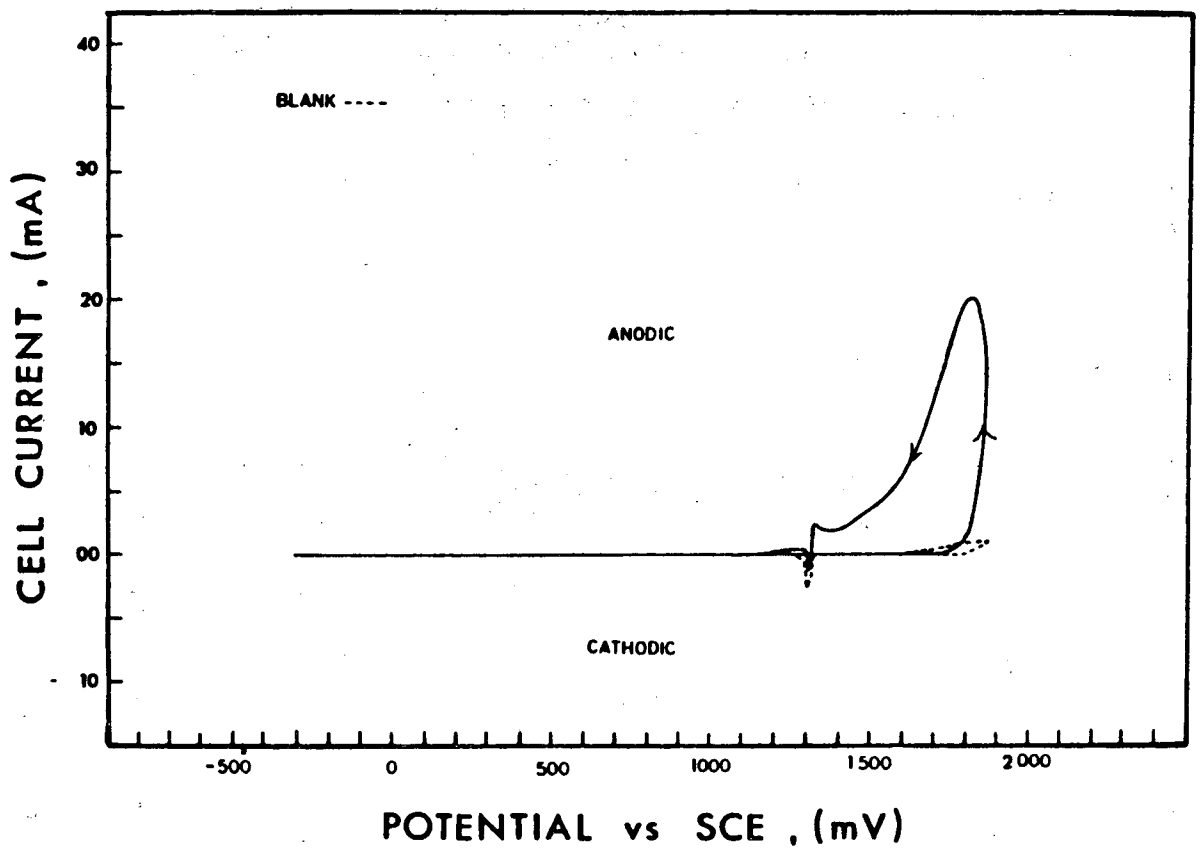

Figure 27. COMPARISON OF CYCLIC VOLTAMMOGRAMS WITH (Solid Line) AND WITHOUT (Dashed Line) 0.50M GLUCOSE PRESENT. EXPERIMENTAL CONDITIONS: ELECTROLYTE, 1.00M H_2SO_4 (pH = 0.0); WORKING ELECTRODE, Pb (1 cm^2); SCAN RATE, 5 mV/s; TEMPERATURE, 66°C.

INSTITUTE OF GAS TECHNOLOGY

61060

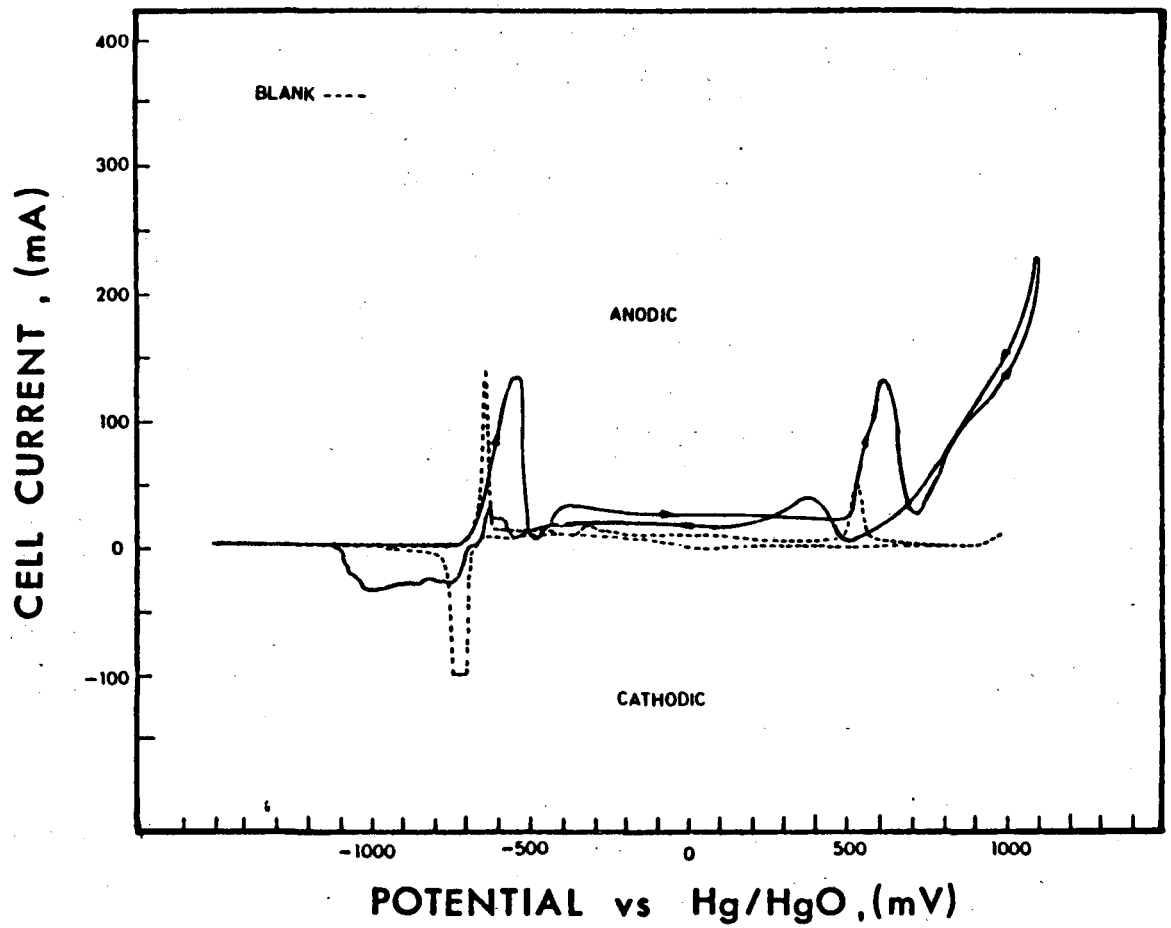

Figure 28. COMPARISON OF CYCLIC VOLTAMMOGRAMS WITH (Solid Line) AND WITHOUT (Dashed Line) 0.5M GLUCOSE PRESENT. EXPERIMENTAL CONDITIONS: ELECTROLYTE, 6.1M KOH (pH = 14.8); WORKING ELECTRODE, Pb (1 cm^2); SCAN RATE, 5 mV/s; TEMPERATURE, 23°C.

rents following the first Pb surface reaction near —500 mV versus Hg/HgO. In the region between the Pb surface reactions the current densities are about 20 mA/cm^2 greater in the presence of glucose. At 66°C the cyclic voltammograms were qualitatively similar to those at 23°C; the current densities above the blank did not increase significantly, however.

Conclusions. The electrochemical oxidation of glucose on Pb appears to show feasibility as a depolarizing agent in the alkaline electrolyte. Electrooxidation from 0 to —500 mV versus Hg/HgO and a rate of 20 mA/cm^2 could be satisfactory. Further work would be required to ascertain these results.

Vitreous Carbon Anode

Anodes constructed from carbon are common and generally economical. Because of this, some exploration of carbon-based anode materials was deemed desirable.

Experimental. Vitreous (or glassy) carbon Type V25 from Atomergic Chemetals Inc. was chosen for the initial study of carbon-based anodes because of its inertness. The form of the electrode was as a disk 15 mm in diameter and 2.0 to 2.5 mm thick of which 1-cm^2 was exposed to the electrolyte. Because of the high overpotentials for H_2 and O_2 evolution shown by the vitreous carbon electrode, a large potential range was available for investigation in aqueous electrolytes. A reversible surface reaction occurred with this electrode, but it appeared at a sufficiently negative potential that it could be avoided. Cyclic voltammograms were always recorded at potentials more positive than the electrode reaction in a potential region where residual currents were negligible. Electrolytes explored were again Nos. 1, 5, and 7 of Table 4.

Results and Discussion. In the H_2SO_4 electrolyte little difference was observed between cyclic voltammograms recorded with and without glucose. Only a slightly more rapid current increase was detected at the anodic breakdown potential.

The cyclic voltammograms obtained in the near-neutral phosphate buffer also showed no structure. However, the anodic breakdown potential occurred at significantly more negative potentials in the presence of glucose, which suggests its oxidation. Table 9 lists the potentials required to obtain 2 mA/cm^2

in the electrolyte alone and with glucose present at ambient temperature and at 65°C. In the presence of glucose, 2 mA/cm^2 can be reached at potentials 300 to 400 mV more negative than in its absence. The higher temperature apparently lowers the rather large overpotential significantly for the phosphate buffer alone as well as with glucose.

Table 9. POTENTIAL REQUIRED TO ATTAIN 2 mA/cm^2 IN THE CYCLIC VOLTAMMETRY OF GLUCOSE IN PHOSPHATE BUFFER (pH = 6.6) AT 5 mV/s ON VITREOUS CARBON

Electrolyte	Temperature, °C	Potential vs. SCE, mV
Blank*	21	+1800
Blank*	65	+1420
Blank* + 0.50M Glucose	21	+1470
Blank* + 0.50M Glucose	65	+1140

* Blank = 0.5M NaH_2PO_4/0.50M Na_2HPO_4.

As has been the case using other electrode materials, the glucose showed the greatest acitivity in alkaline electrolyte. Figure 29 displays the cyclic voltammograms recorded with the vitreous carbon electrode at the two temperaures comparing scans with and without glucose. Figure 29a shows an example of the early breakdown in the presence of glucose for the ambient temperature scan. At 3 mA/cm^2 a shift of 640 mV is encountered. Upon increasing the temperature, Figure 29b, structure develops in the cyclic voltammogram when glucose is present showing shoulder peaks at —50 (A) and +400 (B) mV versus Hg/HgO and current densities of a few milliamperes per square centimeter.

Conclusions. Although the evidence here suggests that glucose can be electrochemically oxidized on vitreous carbon, the potentials at which oxidation occurs are very positive relative to a RHE. Only Peak A in Figure 29b is sufficiently negative to be of any real interest for depolarizing, and it has only a modest current density, 1.2 mA/cm^2.

Lead Ruthenate Anode

Metal oxides are a potentially attractive group of new anode materials[99] for organic oxidations. Recently, the use of the metal oxide lead ruthenate,

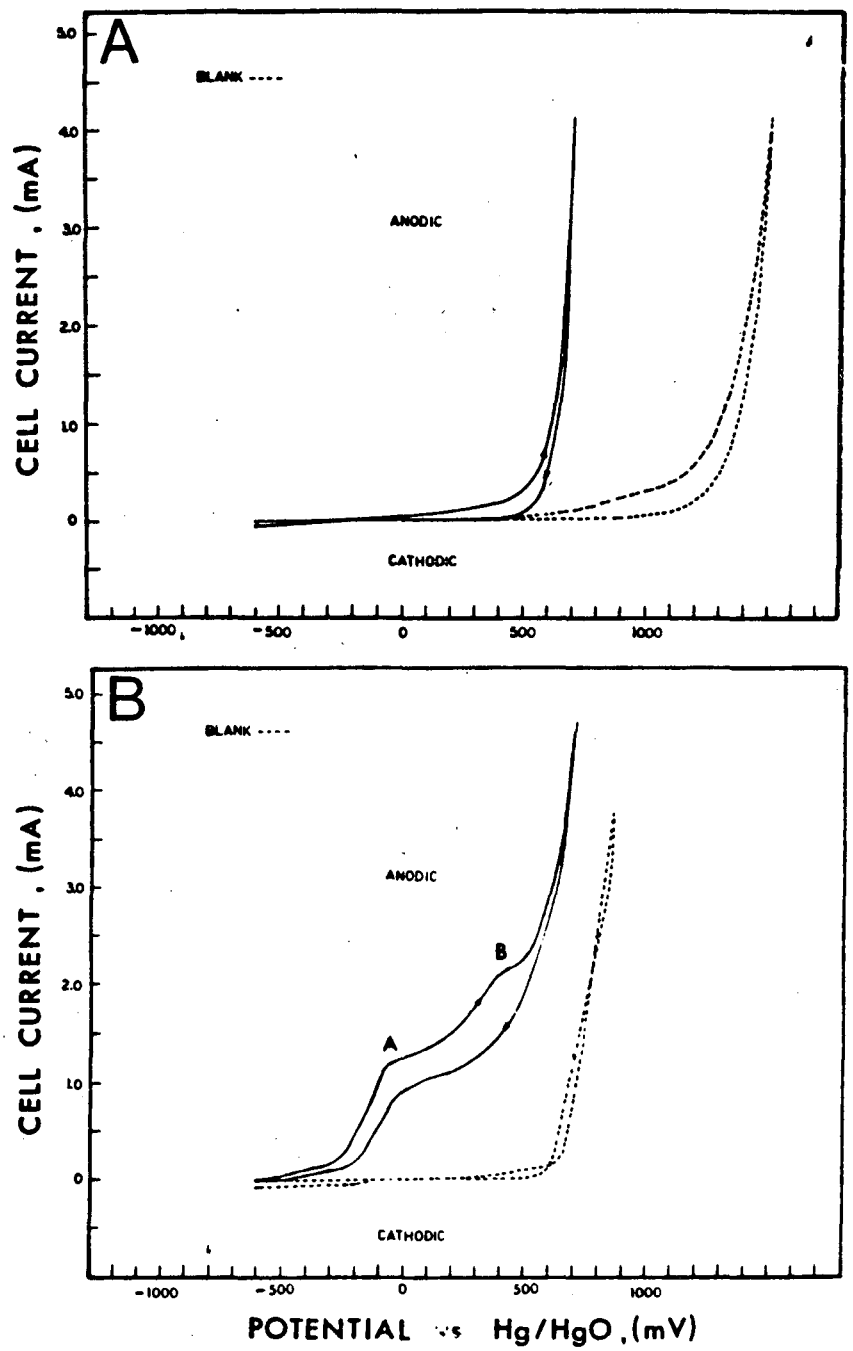

Figure 29. COMPARISON OF CYCLIC VOLTAMMOGRAMS WITH (Solid Line) AND WITHOUT (Dashed Line) 0.50M GLUCOSE PRESENT. EXPERIMENTAL CONDITIONS: ELECTROLYTE, 6.1M KOH (pH = 14.8); WORKING ELECTRODE, VITREOUS CARBON (1 cm^2); SCAN RATE 5 mV/s; TEMPERATURE, (a) 23°C AND (b) 63°C.

Pb_2 $[Ru_{2-x}$ $Pb_x]$ O_{7-y}, for the oxidation of alcohols and the oxidative cleavage of diols was reported.[100] These functionalities are just those of which carbohydrates are composed (Figure 1), and consequently this electrode material was considered to be potentially useful in the present context.

Experimental. Lead ruthenate ($Pb_2[Ru_{2-x}$ $Pb_x]O_{7-y}$) was synthesized by solid-state reaction of excess $Pb(NO_3)_2$ and RuO_2 at 600°C.[101] Excess PbO_2 formed was leached out of the mixture with acetic acid. The powder material was fabricated into an electrode by Teflon bonding it to a Pt screen. The geometrical area was approximately 3-cm^2 with a lead ruthenate loading of about 300 mg. This type of electrode was tested for glucose oxidation activity in Electrolyte Nos. 1, 5, and 7 listed in Table 4. Again, these three electrolytes provided a survey of acid, neutral, and basic conditions. No electrode pretreatment was required beyond thorough rinsing in water.

Cyclic voltammograms recorded with a 5 mV/s scan rate were not very informative because of the large background currents, typically 20 to 30 mA. At a fixed potential these currents would disappear in 15 to 45 seconds, and consequently information was obtained by recording steady-state current-potential (I-V) curves and log I potential curves. This was done by stepping the working electrode potential at an appropriate rate through the desired potential range and recording either I or log I.

Results and Discussion. I-V curves recorded in H_2SO_4 showed increased currents in the presence of glucose at more negative potentials than in the acid alone. At 61°C the effect was accentuated, and the comparison of I-V curves at this temperature is shown in Figure 30. Steady-state currents as large as 100 mA were easily attainable in the presence of glucose at potentials ~250 mV more negative than the potential required to attain this current in the electrolyte alone. The anode potential versus RHE at this current is a little less than 1100 mV. The gas evolution was observed at anode potentials between 800 and 850 mV versus SCE. CO_2 was detected in the gas evolved. (See Task 3.)

In the near-neutral phosphate buffer, the presence of glucose had very little effect. At ambient temperature, glucose was observed to actually inhibit the onset of electrolyte breakdown.

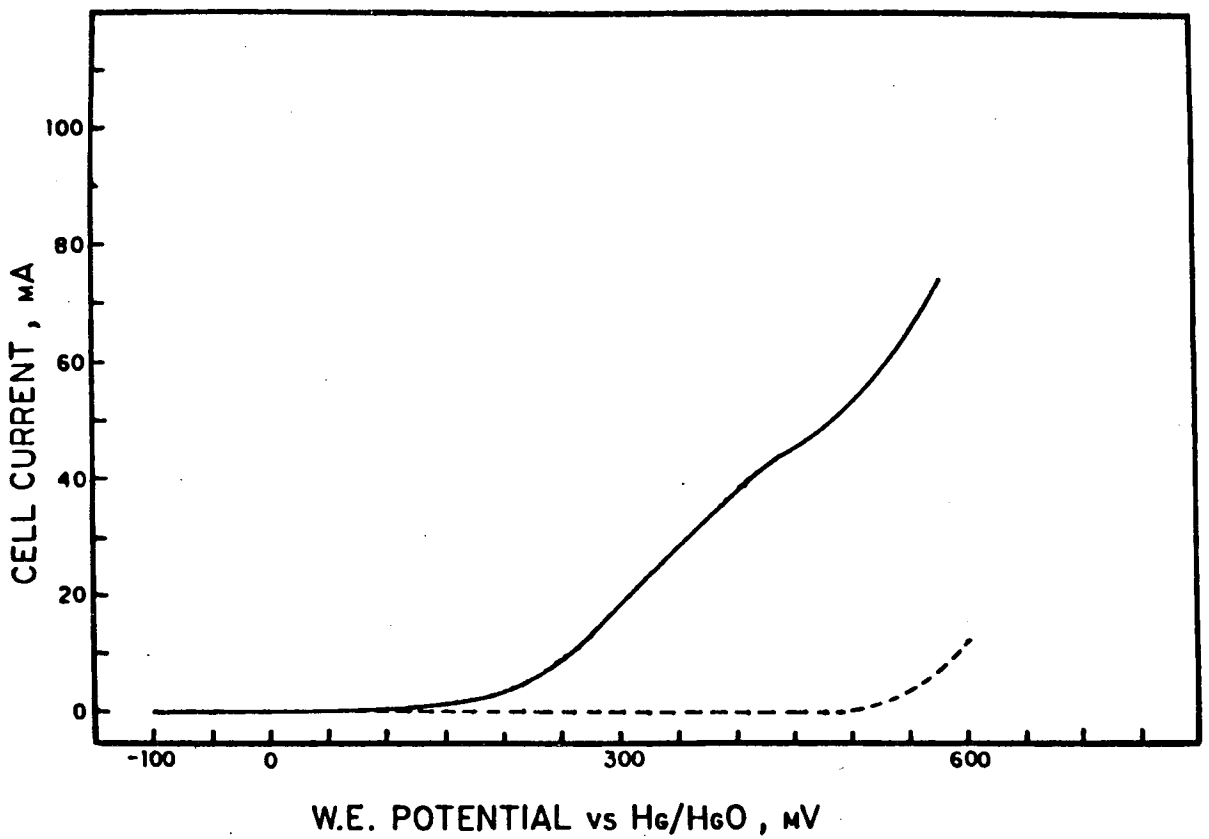

Figure 30. STEADY-STATE CURRENT-POTENTIAL CURVES FOR A TEFLON-BONDED LEAD RUTHENATE ELECTRODE (~3 cm^2 Geometrical Area) IN 1.00M H_2SO_4 WITH (Solid Line) AND WITHOUT (Dashed Line) 0.50M GLUCOSE AT 61°C. POTENTIAL STEPPED 6 steps/min WITH 10 mV/step.

61060

Only a room temperature (25°C) I-V curve was recorded in the KOH electrolyte (Figure 31). As can be seen from Figure 31, even at this low temperature currents of hundreds of milliamperes were attainable at potentials ~400 mV more negative than potentials required to generate the same current without glucose. Similar to the acid electrolyte, the potential versus RHE at which significant currents occurred was in the range from 1000 to 1100mV. No gas evolution was detected in this case because CO_2 would be captured by the electrolyte. Two distinct regions are evident in the I-V curve (Figure 31), suggesting that two differenct reactions or processes are occurring.

Conclusions. These current-potential data show that the steady-state electrooxdiation of glucose can be accomplished with lead ruthenate electrodes at substantial rates, hundreds of milliamperes per square centimeter of electrode area, in both acidic and basic electrolytes. The anode potential versus RHE of about 1000 mV is adequate for depolarization at these high reaction rates.

Ruthenized Titanium Anode

A well-known metal oxide electrode used widely as an anode for oxygen and chlorine evolution is ruthenized titanium (RuO_x/Ti),[102-104] and its ability to electrooxdiize glucose was investigated.

Experimental. The RuO_x/Ti electrode was made by repeated immersions of a Ti disk into a 0.5M $RuCl_3$ solution followed by baking at 350°C as described in Yeo *et al.*[105] A geometrical area of 1 cm^2 was exposed to the electrolyte.

Electrolyte Nos. 1, 5, and 7 in Table 4 with and without glucose were investigated at ambient temperature (~25°C) and 65°C. Like the lead ruthenate electrode, substantial background current prohibited the use of cyclic voltammetry for electrode evaluation, and steady-state I-V curves were again recorded. Also, no pretreatment was required for this electrode.

Results and Discussion. In acid electrolyte, only a slight depolarizing effect was observed, which increased at the higher temperature. At 65°C and a reaction rate of 1 mA/cm^2 (geometric) only a 90 mV shift in potential between curves with and without glucose was detected. I-V curves recorded in the phosphate buffer were similar to those obtained in the acid electrolyte, showing only a slight depolarizing effect.

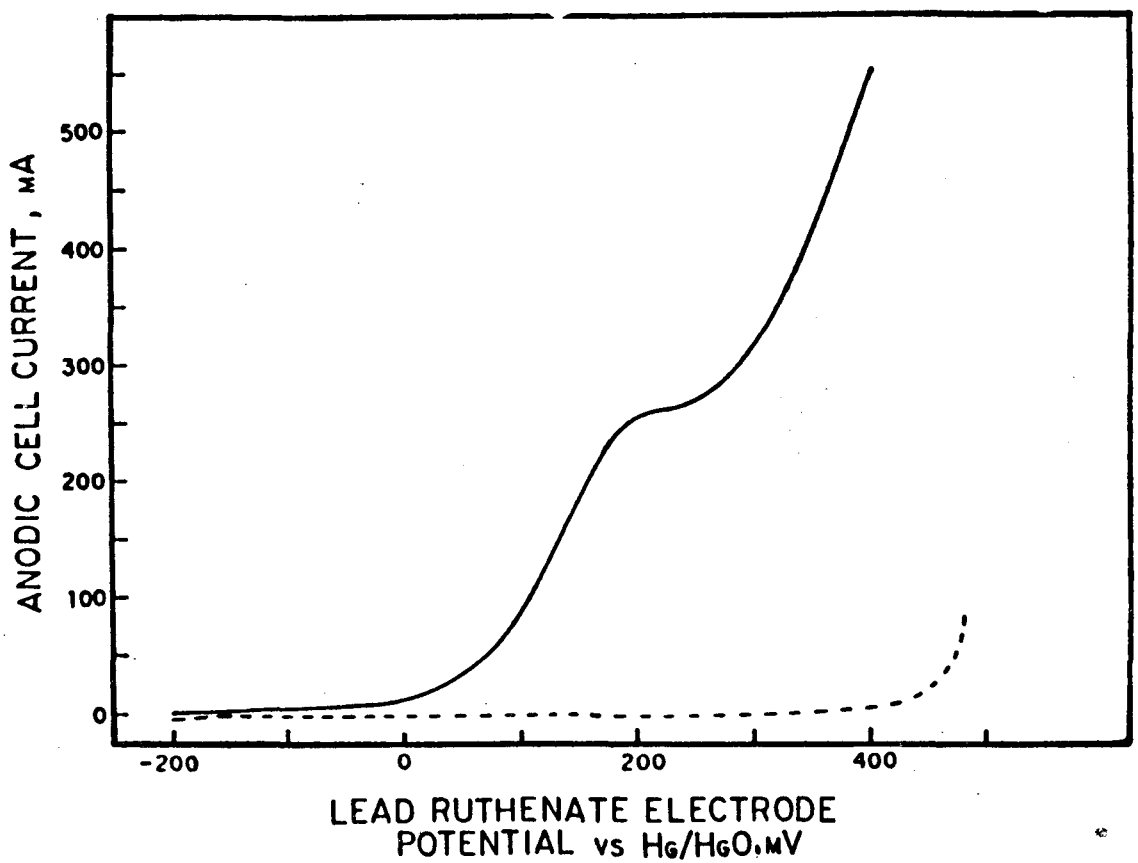

Figure 31. STEADY-STATE CURRENT-POTENTIAL CURVES FOR A TEFLON-BONDED LEAD RUTHENATE ELECTRODE (~3 cm^2 Geometrical Area) IN 6.1M KOH WITH (Solid Line) AND WITHOUT (Dashed Line) 0.50M GLUCOSE AT 25°C. POTENTIAL STEPPED 6 step/min WITH 10 mV/step.

In the alkaline electrolyte, a depolarizing effect was observed as illustrated in Figure 32. Current densities of tens of milliamperes per square centimeter were found, and at currents of 10 mA a negative shift of 325 mV from the potential necessary to attain 10 mA without glucose was obtained. Increasing the temperature seemed to have little effect, and what effect was detectable was in the direction of smaller currents for a fixed potential.

Conclusions. The results obtained with RuO_x/Ti were, in general, not very promising. As has been found with other anode materials, significant activity was found only in strong alkaline electrolytes and at rather positive potentials (>1200 mV versus RHE).

Electrooxidation of Glucose Derivatives

A number of glucose derivatives were investigated for electrooxidative activity. Oxidative glucose derivatives included gluconic acid, glucaric (saccharic) acid, and glucuronic acid. (See Figure 2.) The lone reductive derivative was glucitol (sorbitol). (See Figure 2.) In addition, α-methylglucoside, in which the anomeric carbon (Carbon 1, Figure 1) is sterically blocked by substitution of its hydroxyl hydrogen by a methyl group, was a special derivative selected. Because these derivatives differ from glucose by modification of a limited number of functionalities (usually only one), comparison of the results among the derivatives and glucose was expected to yield information about the mode of glucose electrooxidation. Most also appear as natural constituents in limited amounts.[44] The glucose-derived acids more frequently appear as degradation products in carbohydrate waste streams[13,106] and are potential intermediates through which glucose must pass in its electrochemical oxidation. For these reasons information on these derivatives was thought to be desirable.

All data consisted of cyclic voltammograms obtained using a platinized Pt anode and techniques previously described for the glucose study. As with glucose, variables were electrolyte (pH) and temperature with some derivatives receiving greater attention than others.

Gluconic Acid Results

Gluconic acid is the simplest oxidation product derivable from glucose by oxidation of the terminal, number 1 carbon (Figures 2 and 4) to the carboxylic acid. This simple, two-electron electrooxidation of glucose to gluconic acid

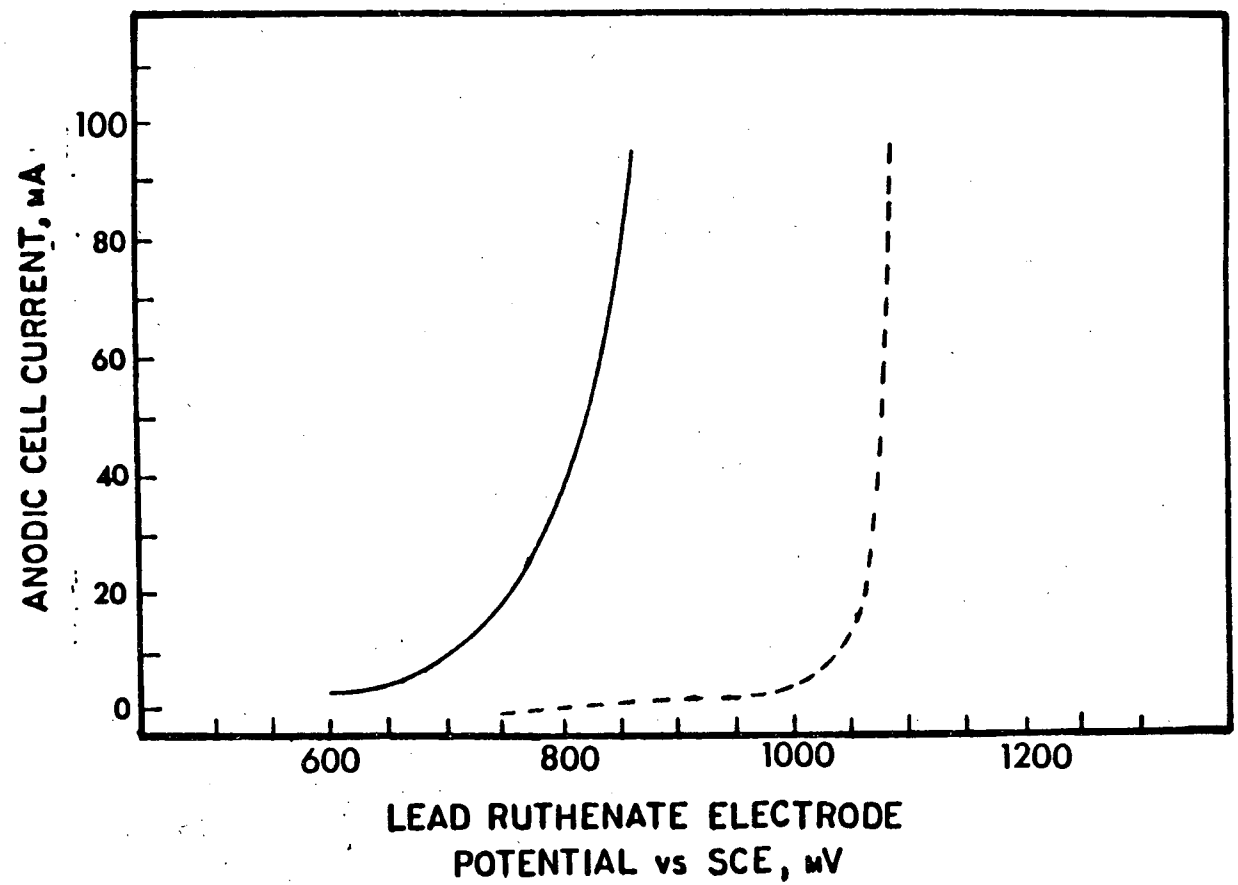

Figure 32. STEADY-STATE CURRENT-POTENTIAL CURVES FOR A RUTHENIZED TITANIUM WORKING ELECTRODE (1 cm^2 Geometrical Area) IN 6.1M KOH WITH (Solid Line) AND WITHOUT (Dashed Line) 0.50M GLUCOSE AT 25°C. POTENTIAL STEPPED 3 steps/min WITH 10 mV/step.

is well known, primarily via an indirect oxidation using Br^-/BrO^- couple. The half-reaction may be written as—

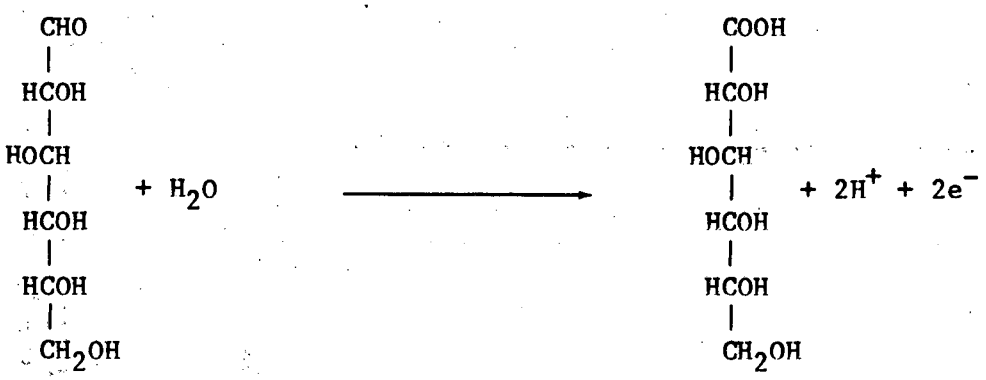

This glucose electrooxidation has been widely postulated as the reaction occurring on the Pt anode.[28,29,32]

Cyclic voltammetry of gluconic acid/gluconate was performed in strongly acidic and basic electrolytes at ambient and elevated temperatures, as was done with glucose. Pretreatment III with a MSE reference and Pretreatment I with a SCE reference were used to record data in 1.33M H_2SO_4 containing 0.50M potassium gluconate, the results using Pretreatment III are given in Figure 33 and Table 10, and those from Pretreatment I are in the Biannual Report. The pretreatments were found to cause differences in the cyclic voltammograms. At ambient temperature a distinct peak in the H region was found using Pretreatment III with MSE, which was absent with Pretreatment I with SCE, and the anodic peak in the DL region was much less intense and shifted positively in going from I to III. At elevated temperature only minor differences in currents were detected. Generous evolution of gas was detected between Points B and C (Figure 33b), which terminated near the current minimum at +300 mV versus MSE and began again at +475 mV versus MSE.

More important is the comparison between gluconic acid (Figure 33) and glucose (Figure 6). The most striking difference between gluconic acid and glucose results in acid is the loss of a distinct anodic peak in the Pt-O region at ambient temperature in the gluconic acid case. Although an anodic peak occurs in the DL region for gluconic acid, it appears as if it is only one of the two electrooxidations found with glucose. At the higher temperature the cyclic voltammograms of the two compounds (Figures 6b and 33b) are strikingly similar, with the broadening and gas evolution found for glucose in the DL region being duplicated by gluconic acid. As at the lower temperature,

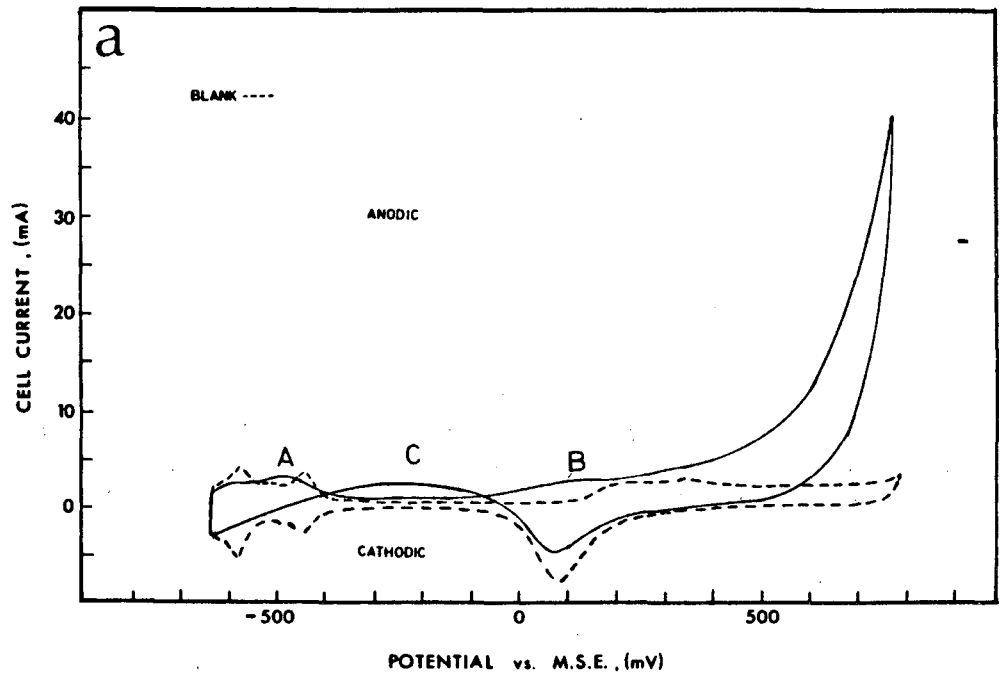

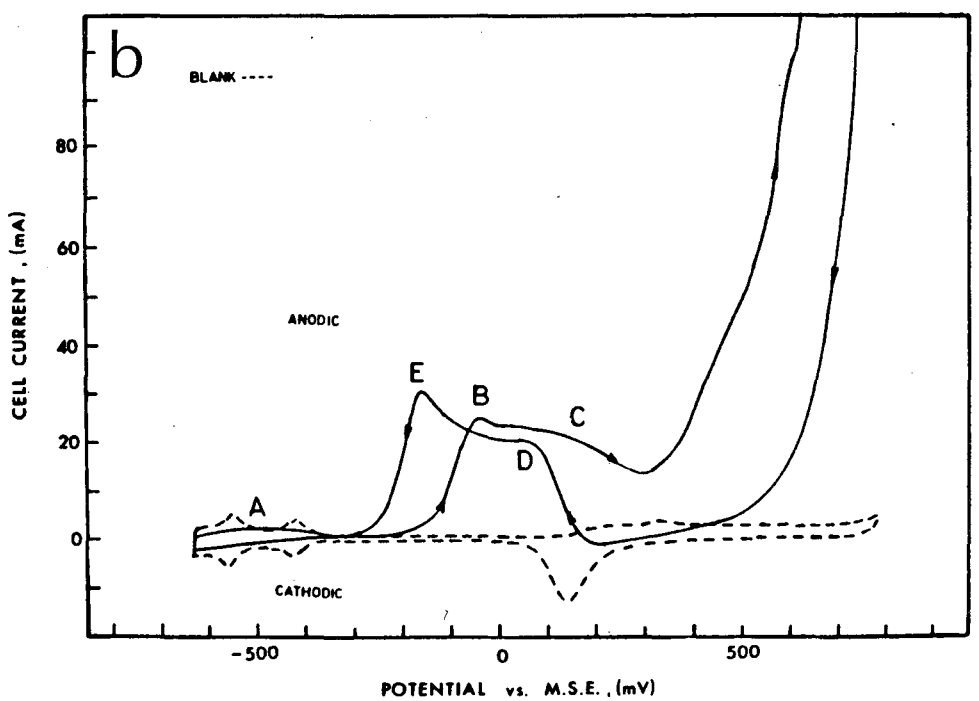

Figure 33. COMPARISON OF CYCLIC VOLTAMMOGRAMS WITH (Solid Line) AND WITHOUT (Dashed Line) 0.50M POTASSIUM GLUCONATE PRESENT. EXPERIMENTAL CONDITIONS: ELECTROLYTE, 1.33M H_2SO_4; WORKING ELECTRODE, PLATINIZED Pt (788 cm^2); SCAN RATE, 5 mV/s; TEMPERATURE, (a) 23°C AND (b) 67°C.

Table 10. ANODIC PEAK POTENTIALS AND CURRENT DENSITIES IN THE CYCLIC VOLTAMMOGRAMS FOR THE ELECTROOXIDATION OF 0.50M POTASSIUM GLUCONATE IN 1.33M H_2SO_4 (pH ~ 0.0)AT VARIABLE TEMPERATURE

Peak Designation	$E_{p,a}$ vs. MSE, mV	$i_{p,a}$, μA/cm^2
	23°C (Figure 33a)	
A	−470	3.5
B	+130	3.2
C	−250	3.0
	67°C (Figure 33b)	
A	−495	2.8
B	−40	27.6
C	+152	23.1
D	+60	22.5
E	−160	33.8

there seems to be loss of a peak in the Pt-O region for gluconic acid, but this feature is less clear at the higher temperature than at the lower.

The cyclic voltammetry results of gluconate in 6.1M KOH are in Figure 34 and Table 11. Although these data were obtained using Pretreatment I and an SCE reference, it is believed to be acceptable because the glucose results indicated that in strongly alkaline electrolyte these factors had negligible effect. The gluconate voltammograms have much in common with those recorded with glucose under the same conditions (Figures 12 and 34) but differences do exist. The most significant difference found for the gluconate cyclic voltammetry occurred in the Pt-O region of the electrode. Unlike results obtained in acid electrolyte, where no distinctive features appeared in the Pt-O region, the alkaline electrolyte results shown in Figure 34 exhibited well-developed anodic peaks, D in Figure 34a and C in Figure 34b. At elevated temperatures and alkaline electrolytes, glucose actually lost the anodic peak in the Pt-O region, while the gluconic acid retained a very definite oxidation there. Current densities were of comparable magnitude for the glucose and gluconate under these conditions.

Glucaric Acid Results

If continued oxidative attack occurs at the terminal carbons, the next simplest oxidation of glucose beyond gluconic acid converts the No. 6 carbon alcohol to a carboxylic acid. The dicarboxylic acid formed from this four-electron oxidation of gluconic acid results in the formation of glucaric acid, as shown below:

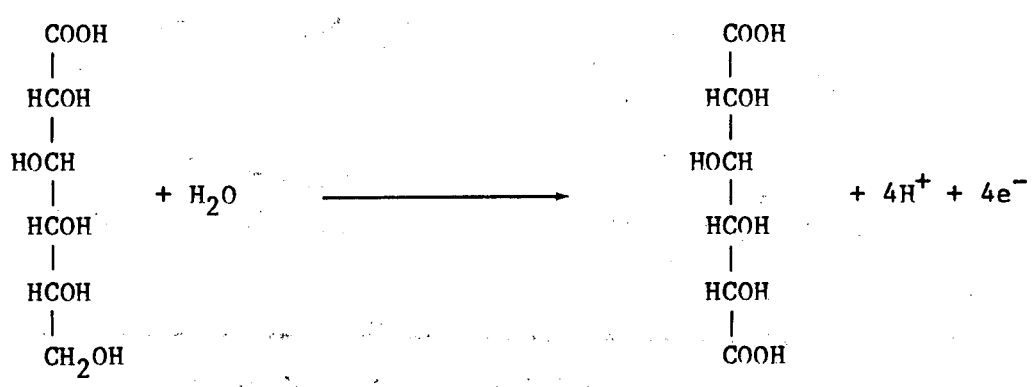

As with the gluconic acid, glucaric acid was surveyed for electooxidative activity on platinized Pt in acidic (1.26M H_2SO_4) and basic (6.1M KOH) electrolytes containing 0.50M monopotassium glucarate.

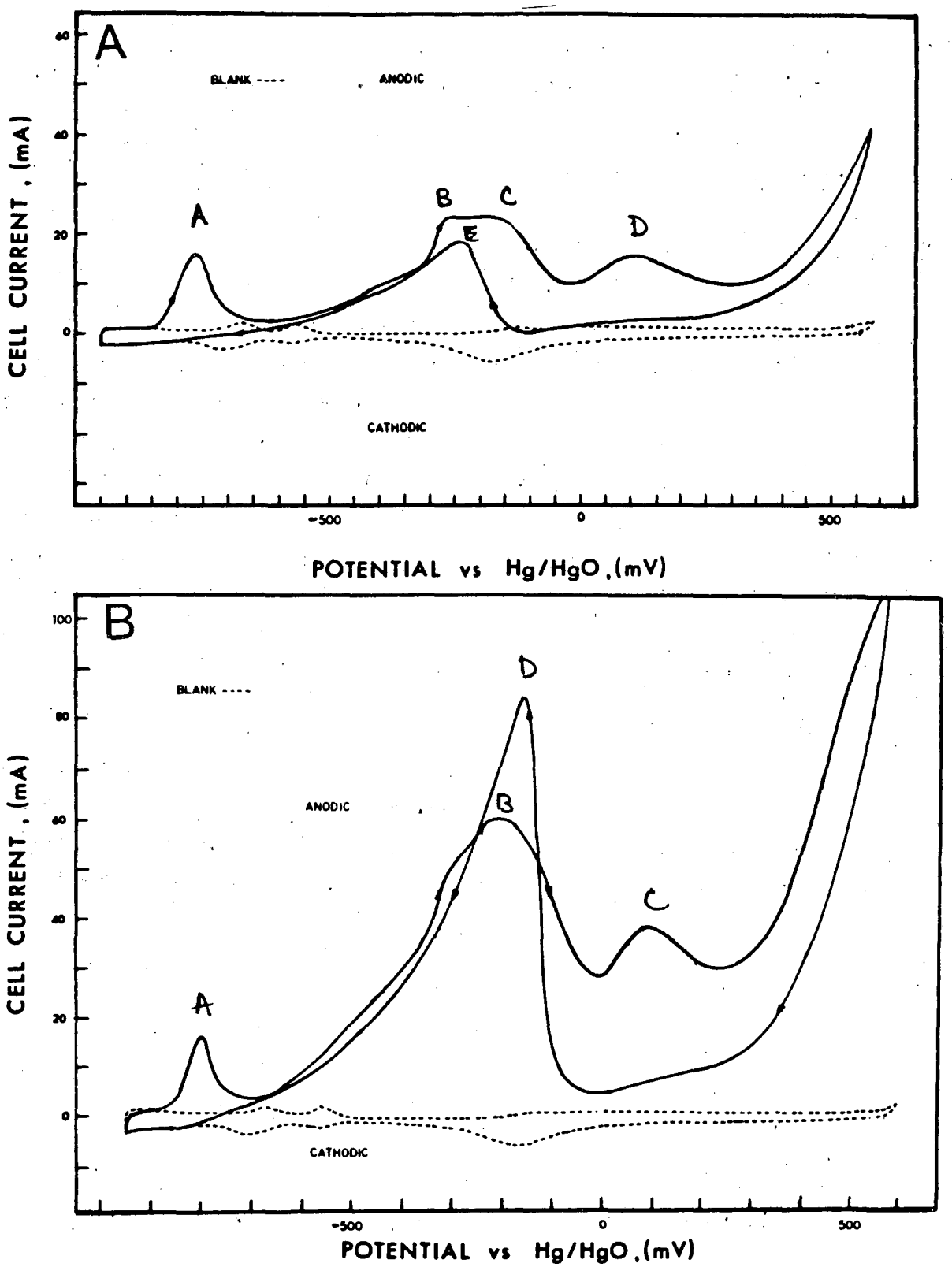

Figure 34. COMPARISON OF CYCLIC VOLTAMMOGRAMS WITH (Solid Line) AND WITHOUT (Dashed Line) 0.43 POTASSIUM GLUCONATE PRESENT. EXPERIMENTAL CONDITIONS: ELECTROLYTE, 6.1M KOH; WORKING ELECTRODE, PLATINIZED Pt (484 cm^2); SCAN RATE, 5 mV/s; TEMPERATURE, (a) 23°C AND (b) 60°C.

Table 11. ANODIC PEAK POTENTIALS AND CURRENT DENSITIES IN THE CYCLIC VOLTAMMOGRAMS FOR THE ELECTROOXIDATION OF 0.43 POTASSIUM GLUCONATE IN 6.1M KOH(pH = 14.8) AT VARIABLE TEMPERATURE

Peak Designation	$E_{p,a}$ vs. Hg/HgO, mV	$i_{p,a}$, $\mu A/cm^2$
	23°C (Figure 34a)	
A	−762	33.1
B	−252	49.2
C	−157	47.5
D	+120	33.1
E	−227	39.3
	60°C (Figure 34b)	
A	−800	34.1
B	−205	125.0
C	+92	79.6
D	−155	174.6

As with gluconic acid, cyclic voltammograms were recorded in the acidic electrolyte using both Pretreatment I with SCE reference and Pretreatment III with MSE reference. However, unlike the gluconic acid case, the pretreatment was found to have no effect on the cyclic voltammograms of glucaric acid.

The results obtained in acidic solution at 23° and 61°C are given in Figure 35. At the lower temperature (Figure 35a), no significant activity was observed for glucaric acid in the DL region or H region and only a more rapid anodic breakdown limit was detected in the Pt-O region. The increased temperature (Figure 35b) resulted in the appearance of a small oxidative peak (A) in the DL region at +425 mV versus SCE with real current density of 2.5 $\mu A/cm^2$. Clearly, a substantial decline in electrooxidative activity occurs for glucaric acid in strongly acidic electrolyte when compared with either glucose or gluconic acid.

The use of alkaline electrolyte resulted in dramatic changes in the cyclic voltammograms (Figure 36). Table 12 lists the peak potentials and peak current densities for the cyclic voltammograms of Figure 36. Numerous anodic peaks at significant reaction rates were observed over the entire potential range of the electrolyte, several at quite negative potentials. No other carbohydrate-derived material exhibited such large current densities on platinized Pt in any electrolyte. The large reaction rates are particularly unusual when contrasted with the almost complete inactivity of the glucaric acidic in the acid electrolyte. The unusual results were verified by repeating the experiment and obtaining identical results.

Glucuronic Acid Results

Oxidation of glucose at the 6 carbon leaving the anomeric (#1) carbon intact leads to glucuronic acid (Figure 2). Electrochemically this would be accomplished as given below.

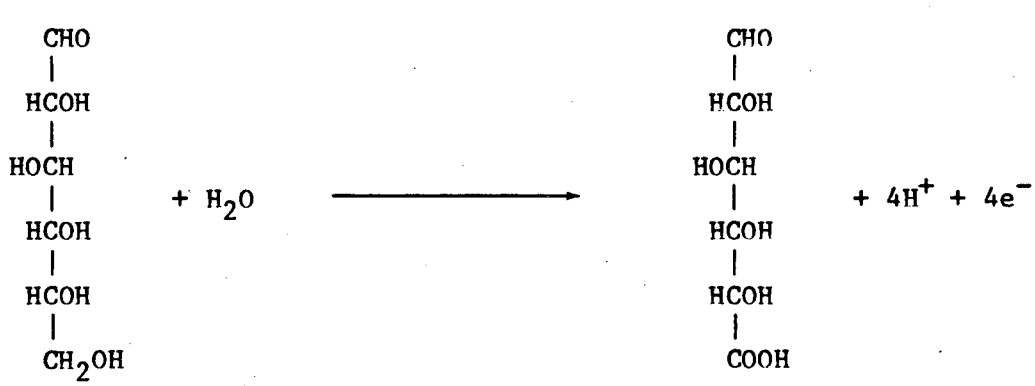

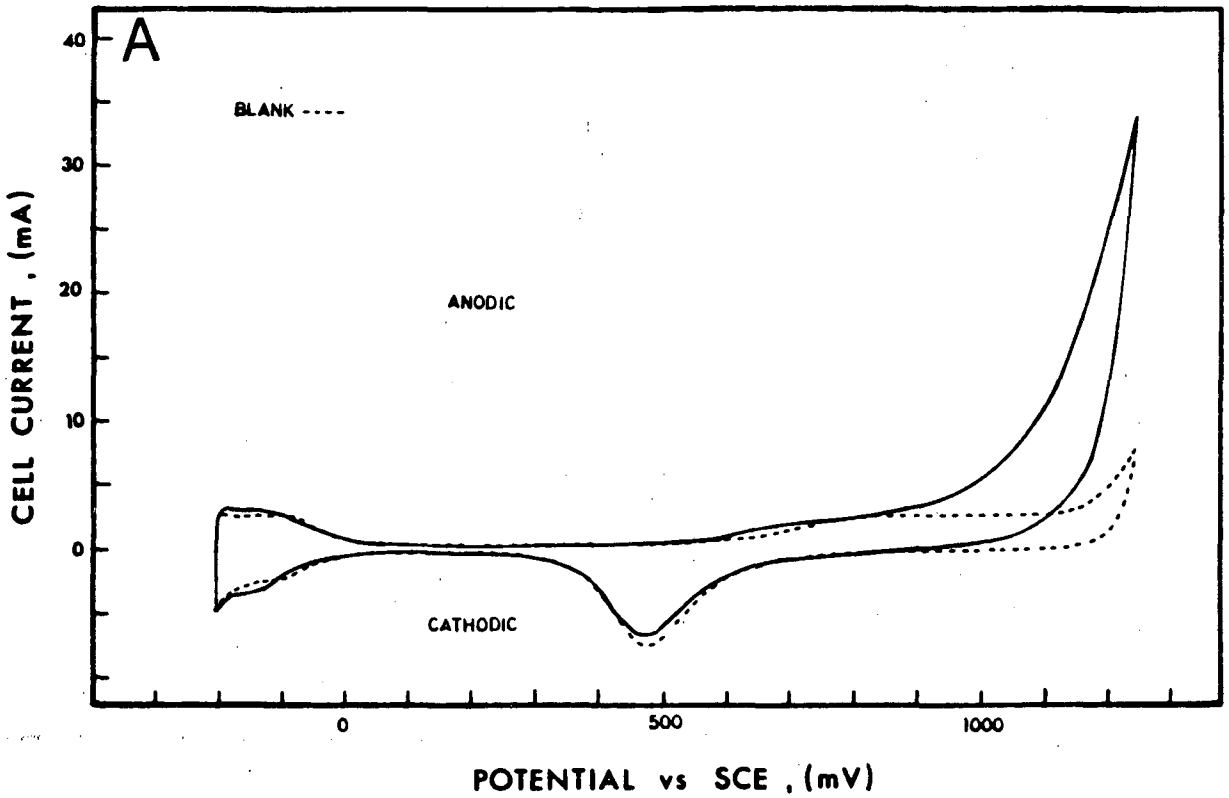

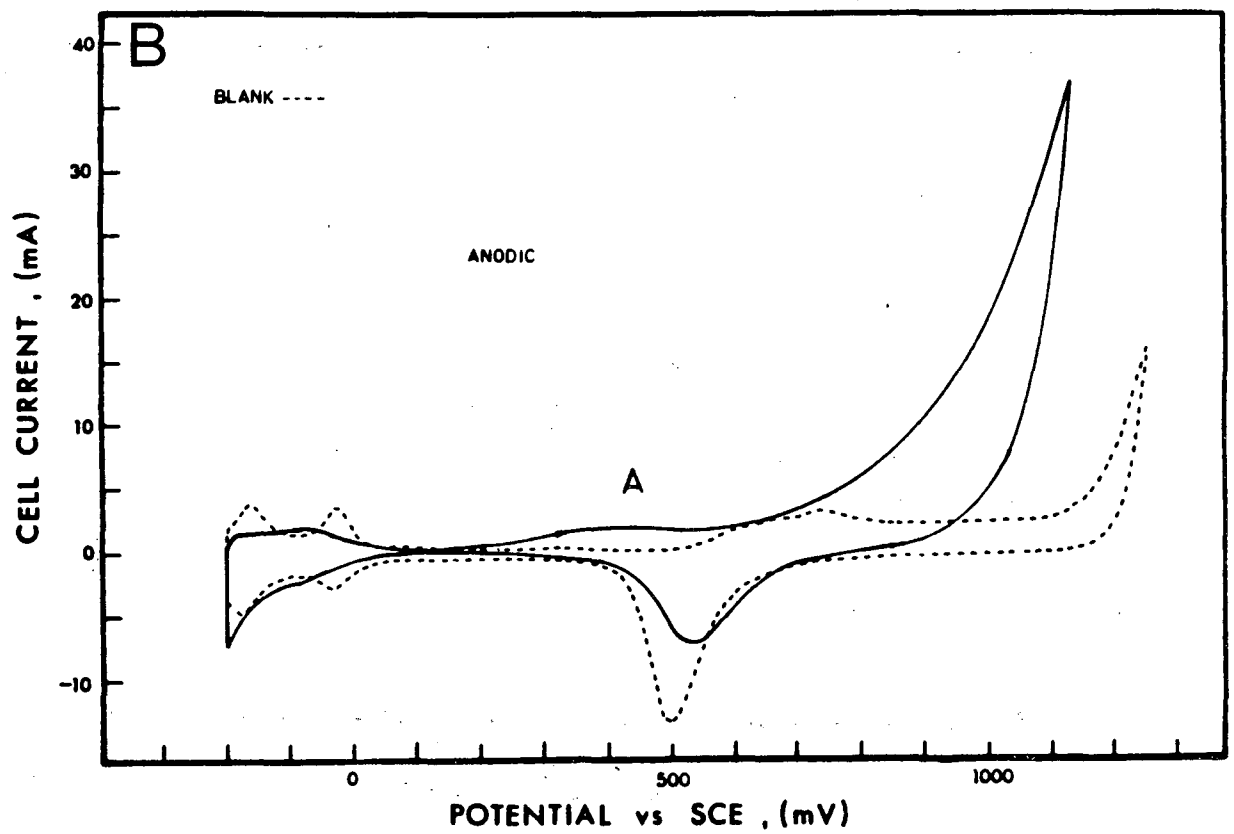

Figure 35. COMPARISON OF CYCLIC VOLTAMMOGRAMS WITH (Solid Line) AND WITHOUT (Dashed Line) 0.50M MONOPOTASSIUM GLUCARATE PRESENT. EXPERIMENTAL CONDITIONS: ELECTROLYTE 1.26M H_2SO_4; WORKING ELECTRODE, PLATINIZED Pt (801 cm^2); SCAN RATE, 5 mV/s; TEMPERATURE, (a) 28°C AND (b) 61°C.

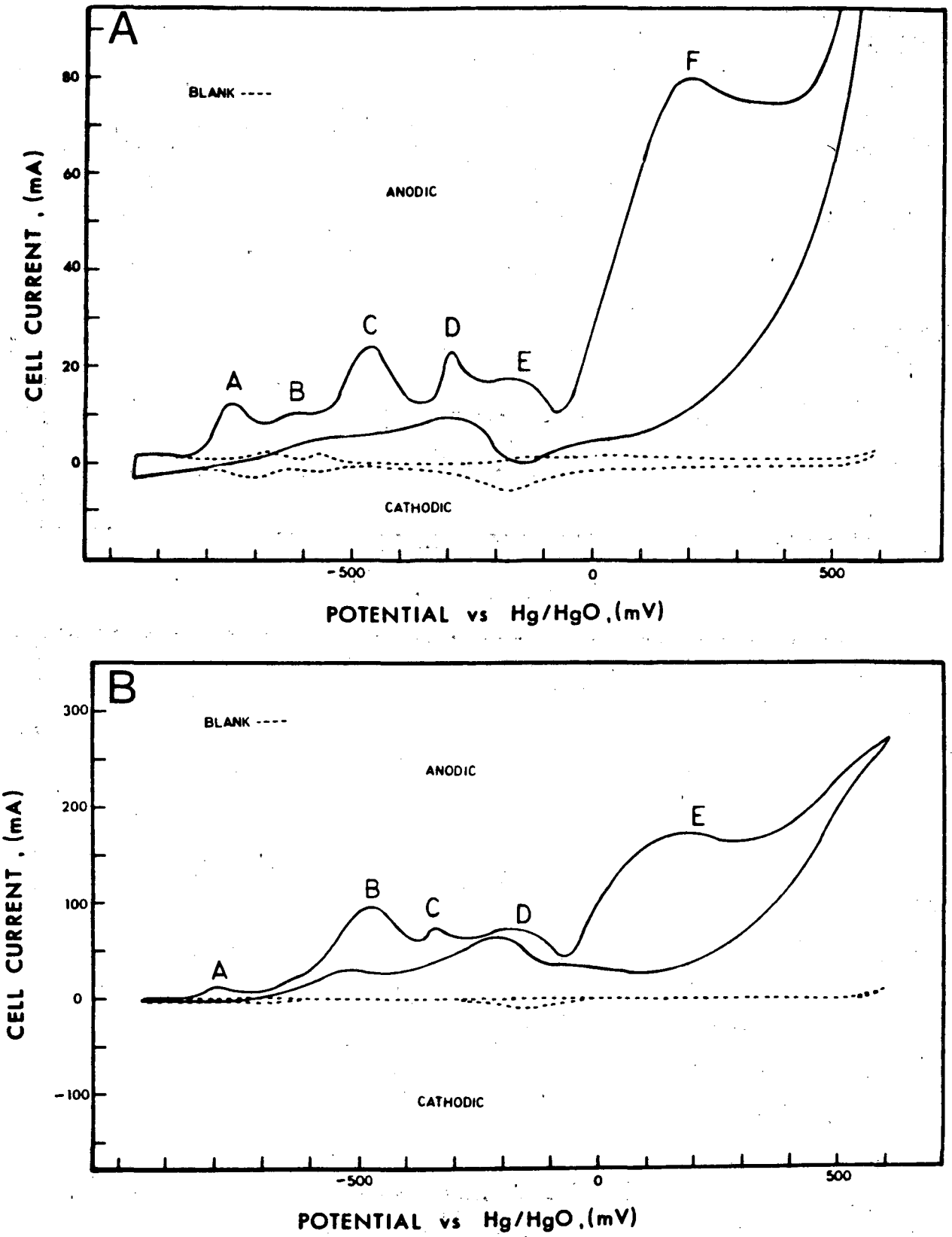

Figure 36. COMPARISON OF CYCLIC VOLTAMMOGRAMS WITH (Solid Line) AND WITHOUT (Dashed Line) 0.50M MONOPOTASSIUM GLUCARATE PRESENT. EXPERIMENTAL CONDITIONS: ELECTROLYTE, 6.1M KOH; WORKING ELECTRODE, PLATINIZED Pt (746 cm^2); SCAN RATE, 5 mV/s; TEMPERATURE, (a) 26°C AND (b) 62°C.

Table 12. PEAK POTENTIALS ($E_{p,a}$) AND CURRENT DENSITIES ($i_{p,a}$) IN THE CYCLIC VOLTAMMOGRAMS FOR THE ELECTROOXIDATION OF GLUCARIC ACID ON PLATINIZED Pt IN 6.1M KOH*

Peak Designation	$E_{p,a}$ vs. Hg/HgO, mV	$i_{p,a}$, μ/cm^2 real)
	26°C (Figure 36a)	
A	—745	15.4
B	—615	12.1
C	—465	32.2
D	—295	30.8
E	—150	22.1
F	+200	105.2
	62°C (Figure 36b)	
A	—790	34
B	—470	127
C	—340	100
D	—160	94
E	+190	224

* Experimental Conditions: electrode, platinized Pt (746 cm^2); electrolyte, 6.1M KOH/0.50M monopotassium glucarate; scan rate, 5 mV/s.

This oxidation is usually difficult to accomplish without attack at the anomeric (No. 1) carbon, but the possibility of selective or parallel electro-oxidation of glucose to glucuronic acid exists.

Data were obtained with 0.50M 6,4-lactone of glucuronic acid in 1.26M H_2SO_4 at 23°C only. The 6,4-lactone is the internal ester formed by the carboxylic acid on the 6 carbon and the alcohol on the 4 carbon, and it is expected to hydrolyze to the free acid in the strong acid used. The cyclic voltammogram under the conditions stated is given in Figure 37. The features observed are 1) inhibited currents in the H region, 2) an electrooxidation in the DL region reminiscent of glucose and gluconic acid, and 3) a more rapid increase in anodic breakdown currents in the Pt-O region.

Glucitol Results

If the simplest reduction of glucose is made at the anomeric (#1) carbon, the aldehyde is converted to an alcohol and glucitol (common name, sorbitol) results. (See Figure 2). Glucitol is a structurally uniform molecule having a hydroxyl functional group on every carbon.

Cyclic voltammograms of 0.50M glucitol on a platinized Pt anode were recorded in acidic and near-neutral (Nos. 1 and 5, Table 4) electrolytes at 23° and 65°C. Like gluconic acid, scans in the H_2SO_4 electrolyte were obtained using both Pretreatment I with a SCE reference and Pretreatment III with a MSE reference. Differences arising from changes in pretreatment occurred only in the H-region. As has been frequently the case in earlier results, a distinct glucitol electrooxidation is found in the H-region when Pretreatment III was used, whereas inhibition was observed in this region with Pretreatment I. These cyclic voltammetry results of glucitol in H_2SO_4 are given in Figure 38 and Table 13. At ambient temperature the cyclic voltammograms of glucitol (Figure 38a) exhibit 1) a peak in the H-region similar to glucose, 2) a peak in the DL region which is both much broader and more intense (approximately 5 times) than that found for glucose, and 3) no distinct feature in the Pt-O region other than a more rapid current increase to the anodic breakdown limit. Thus significant differences exist between the results for glucose and glucitol. The elevated temperature cyclic voltammogram of glucitol (Figure 38b) was, nonetheless, quite similar to that of glucose and gluconic acid, showing little change in the H-region and double

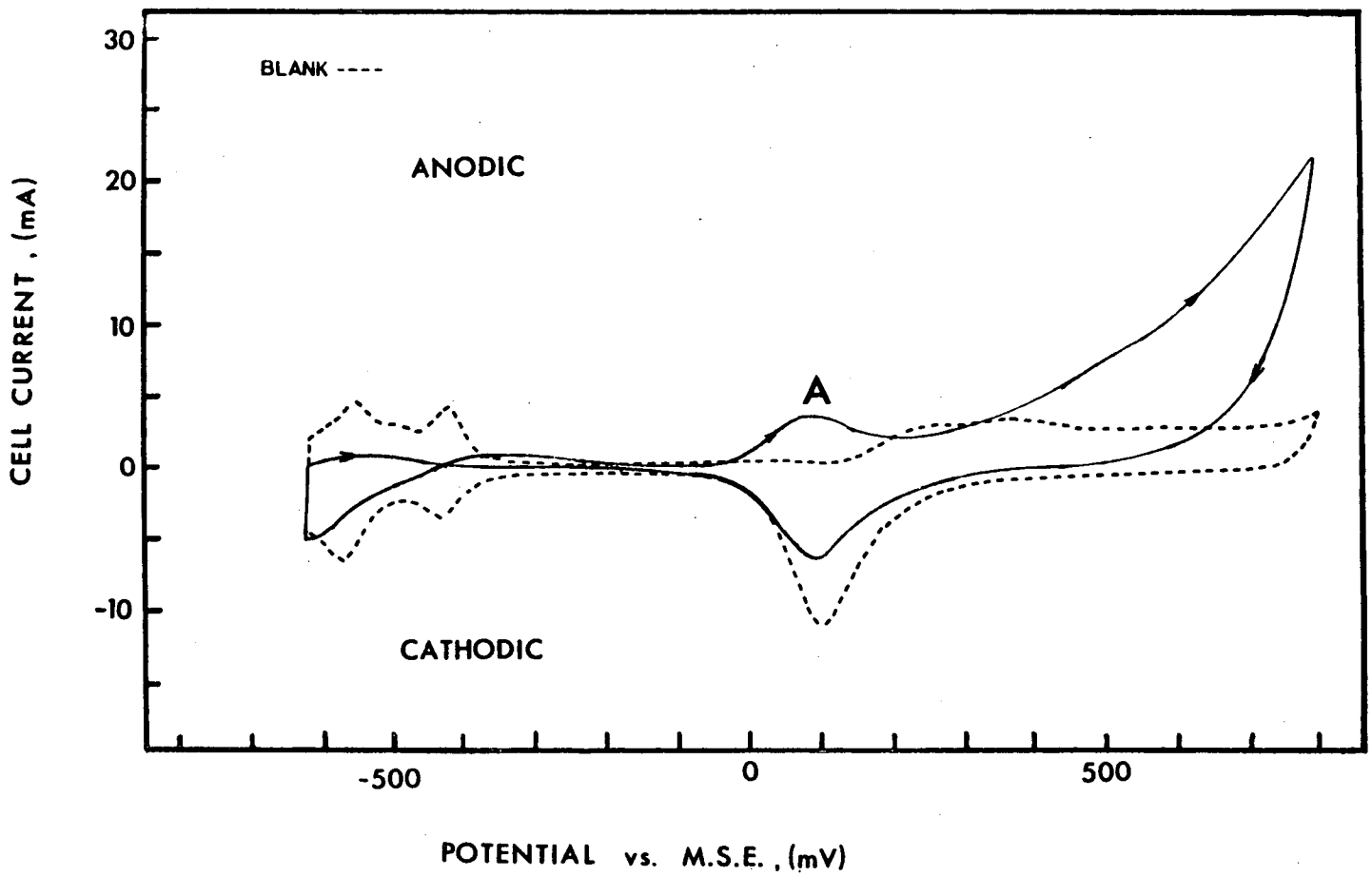

Figure 37. COMPARISON OF CYCLIC VOLTAMMOGRAMS WITH (Solid Line) AND WITHOUT (Dashed Line) 0.50M GLUCURONIC ACID, 6,4 LACTONE PRESENT. EXPERIMENTAL CONDITIONS: ELECTROLYTE, 1.00M H_2SO_4; WORKING ELECTRODE, PLATINIZED Pt (728 cm^2); SCAN RATE, 5 mV/s; TEMPERATURE, 23°C.

61060

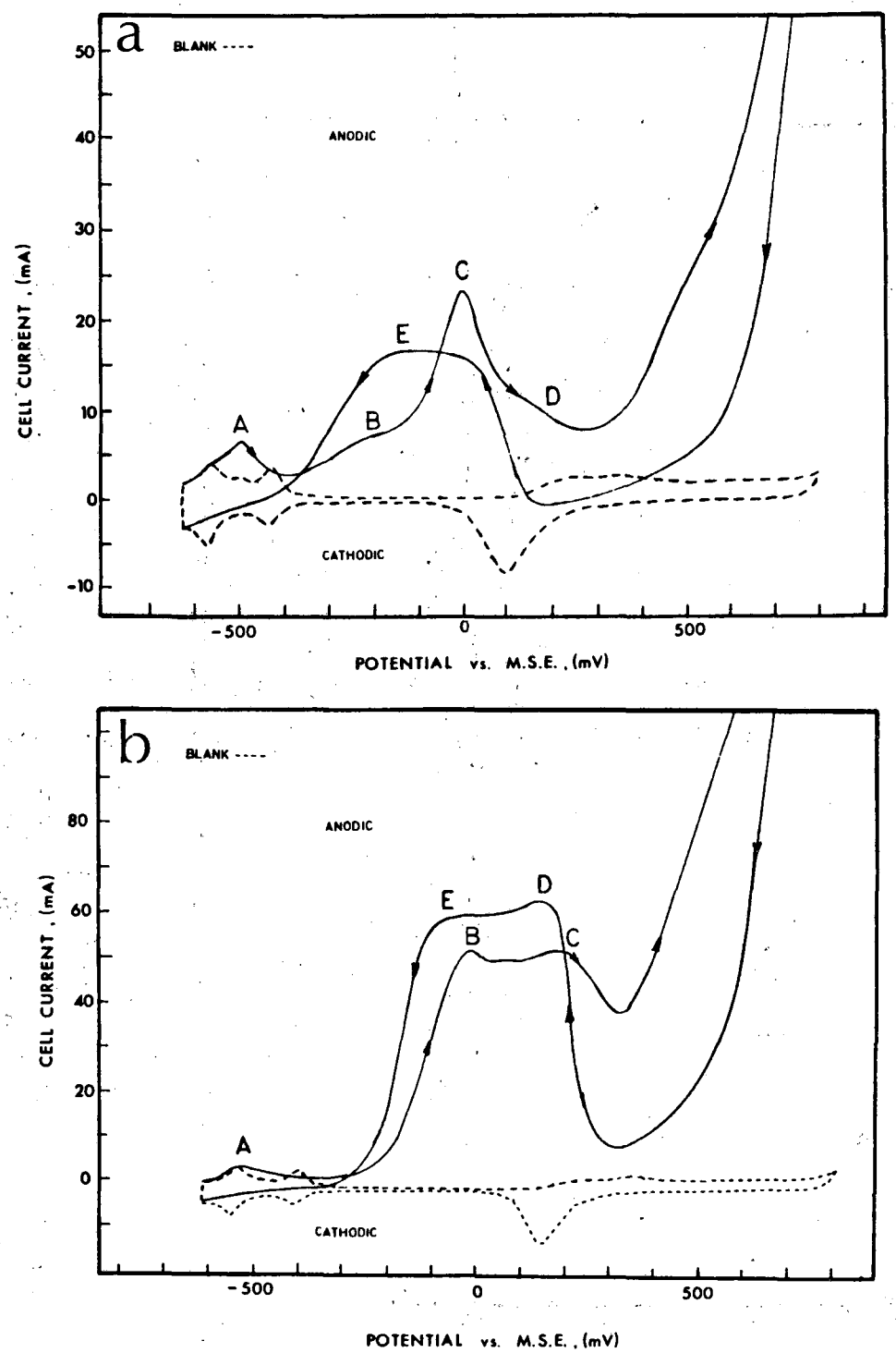

Figure 38. COMPARISON OF CYCLIC VOLTAMMOGRAMS WITH (Solid Line) AND WITHOUT (Dashed Line) 0.50M GLUCITOL PRESENT. EXPERIMENTAL CONDITIONS: ELECTROLYTE, 1.00M H_2SO_4; WORKING ELECTRODE, PLATINIZED Pt (825 cm^2); SCAN RATE, 5 mV/s; TEMPERATURE, (a) 23°C AND (b) 64°C.

Table 13. ANODIC PEAK POTENTIALS AND CURRENT DENSITIES IN THE CYCLIC VOLTAMMOGRAMS FOR THE ELECTROOXIDATION OF 0.50M GLUCITOL IN 1.00M H_2SO_4 (pH = 0.0) AT VARIABLE TEMPERATURE

Peak Designation	$E_{p,a}$ vs. MSE, mV	$i_{p,a}$, $\mu A/cm^2$
	23°C (Figure 38a)	
A	—490	7.3
B	—205	7.7
C	+2	25.9
D	+175	11.3
E	—115	18.6
	64°C (Figure 38b)	
A	—542	5.6
B	—30	59.7
C	+175	59.9
D	+165	72.6
E	—62	68.7

peak structure in the DL region of comparable magnitude. Again, as observed with glucose and gluconic acid at elevated temperature, gas evolution was detected during the electrooxidation in the DL region. It stopped as the Pt-O region began, about + 150 mV versus MSE, and was seen to begin again at +475 mV versus MSE.

Further results for glucitol in the near-neutral phosphate buffer are given in Figure 39 and Table 14. Scans were recorded with Pretreatment III. The features of the glucitol cyclic voltammogram at ambient temperature in this buffer (Figure 39a) are as follows: 1) a single distinct peak in the H-region, again similar to glucose; 2) a broad anodic structure in the DL region containing two peaks, one whose peak potential occurs at the same position as that found with glucose and the other whose peak potenial is at the boundary of the DL and Pt-O regions (Peak C) which is totally absent from the glucose (compare Figures 10a and 39a); and 3) only a more rapid increase in anodic breakdown current in the Pt-O, unlike glucose which exhibits a peak structure here. The magnitude of the current densities detected for glucose and glucitol are comparable in the phosphate buffer at ambient temperature, unlike what was observed in the H_2SO_4 electrolyte. Slight gas evolution was detected around Peak C of Figure 39a.

At the elevated temperature (Figure 39b) the dominate glucitol feature becomes the anodic peak appearing at a potential value corresponding to the boundary between the DL and Pt-O region (Peak B, Figure 39b) with relatively large current density, ~80 $\mu A/cm^2$. As at the lower temperature, this feature is absent in glucose data (Figure 10b). The peak occurring in the early portion of the DL region (Peak A, Figure 39b) is found in both glucitol and glucose scans. At this temperature and pH gas evolution was detected beginning at —325, ending near the minimum at +237, and beginning again shortly thereafter at +375 (all potentials versus MSE).

α-Methyl-D-Glucoside Results

The available literature on the electrochemical oxidation of glucose on Pt electrodes claims that the oxidative attack occurs at the anomeric carbon. Formation of the methylglucoside should have the effect of blocking oxidation at the anomeric carbon position. Mutarotation is also eliminated. Cyclic voltammograms of 0.50M α-methyl-D-glucoside in 1.00M H_2SO_4 were obtained on platinized Pt. Hydrolysis of the glucoside bond should not occur

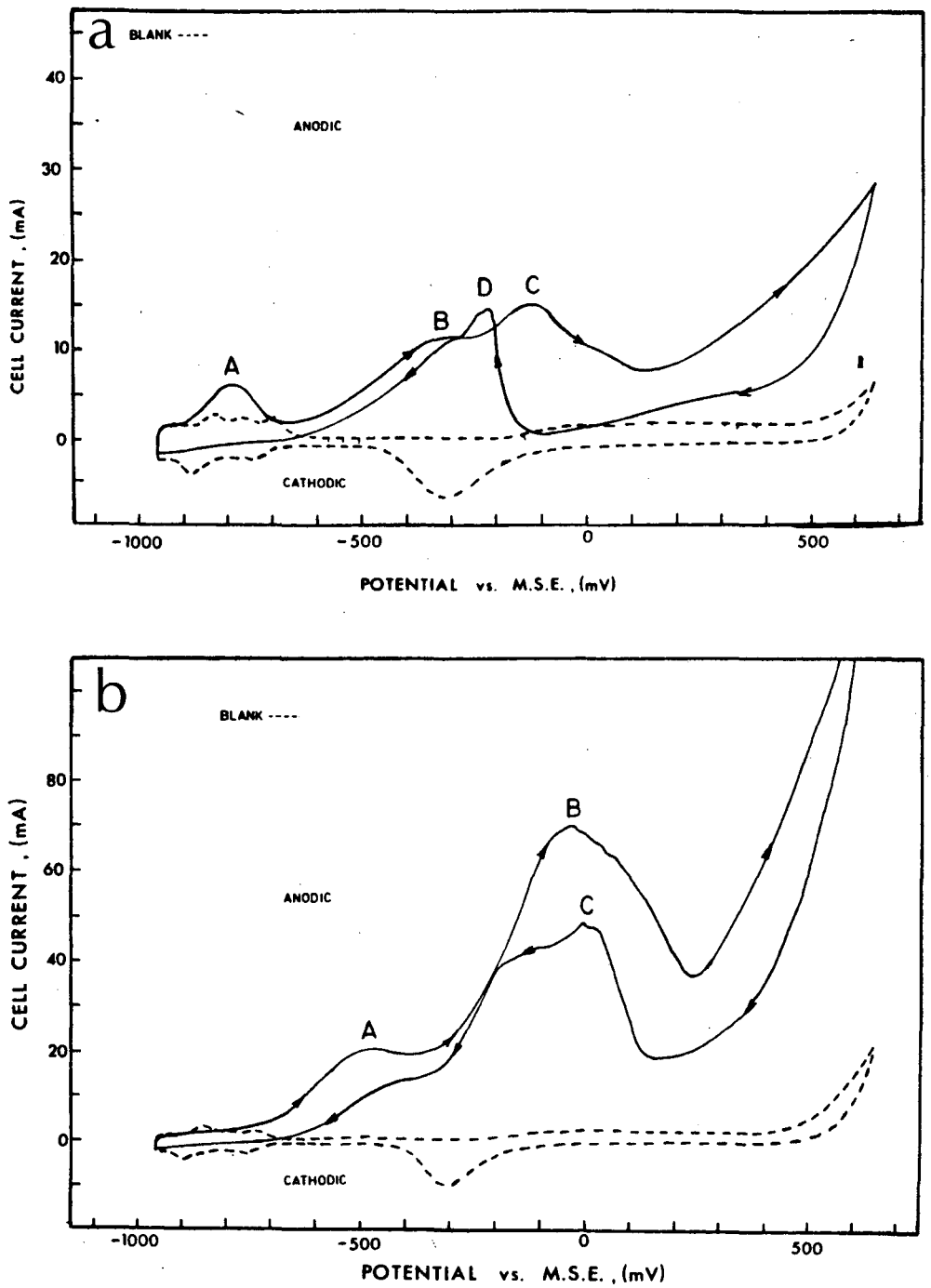

Figure 39. COMPARISON OF CYCLIC VOLTAMMOGRAMS WITH (Solid Line) AND WITHOUT (Dashed Line) 0.50M GLUCITOL PRESENT. EXPERIMENTAL CONDITIONS: ELECTROLYTE, 0.50M NaH_2PO_4/0.50M Na_2HPO_4 (pH =6.6); WORKING ELECTRODE, PLATINIZED Pt (825 cm^2); SCAN RATE, 5 mV/s; TEMPERATURE, (a) 24°C AND (b) 65°C.

Table 14. ANODIC PEAK POTENTIALS AND CURRENT DENSITIES FROM THE CYCLIC VOLTAMMOGRAMS FOR THE ELECTROOXIDATION OF 0.50M GLUCITOL IN 0.50M, NaH_2PO_4/0.50M Na_2HP_4O (pH = 6.6) AT VARIABLE TEMPERATURE

Peak Designation	$E_{p,a}$ vs. MSE, mV	$i_{p,a}$, $\mu A/cm^2$
	24°C (Figure 39a)	
A	—790	8.2
B	—305	13.0
C	—120	17.2
D	—220	16.5
	65°C (Figure 39b)	
A	—465	23.1
B	—35	78.8
C	—5	54.6

at room temperature to an appreciable extent, but may be a potential problem. Oualitative features at 27° and 63°C were identical to those found for glucose under the same conditions. But quantitatively, differences in the current densities occurred between cyclic voltammograms of glucose and methylglucoside. The oxidative current densities in the "Pt-O" region were significantly reduced for the methylglucoside data. However, the anodic peak in the "Pt-O" region was about twice as large as that in double-layer region for glucose electrooxdiation. The current densities in these two regions were essentially the same for methylglucoside. Because no appreciable difference was detected between the cyclic voltammograms of glucose and α-methylglucoside, partial hydrolysis of the glucoside is believed to have occurred, and the data are not considered to be reliable.

Discussion and Conclusions

Figure 40 shows the molecular structures of glucose and the derivatives studied with the differences the terminal carbons concisely illustrated. The No. 1 carbon can be a primary alcohol, aldehyde, or carboxylic acid. All the structures contain the four secondary alcohols represented by R.

Cyclic voltammetry data on platinized Pt at ambient temperature were obtained for all the structures 1 through 5 in 1.00M H_2SO_4, and they provide some interesting comparisons. As a caveat, mention is made of the fact that comparison of the straight-chain structures given in Figure 40 is at best crude because no account is taken of the molecular stereochemistry, which is certainly bound to influence the electrooxidative activity. Except for glucitol, all other structures are capable of forming lactones (internal esters) from the carboxylic acids and hemiacetals (O-H addition across the carbon-oxygen double bond) from the aldehydes. As mentioned earlier (Figure 4) the most stable forms of glucose are the hemiacetal ring structures in which no aldehyde is directly present. Even so, glucose does exhibit reactivity associated with an aldehyde under many circumstances. Data collected in the H-region show that the three structures (1, 2, and 3 of Figure 40) having the primary alcohols at the 6 carbon exhibit a single anodic peak here, while those with carboxylic acid groups (4 and 5) exhibit inhibition of the hydrogen desorption. This suggests that the primary alcohol group is the principal participant in the H region electrooxidation. In the DL region at ambient temperature, the only structure failing to show some

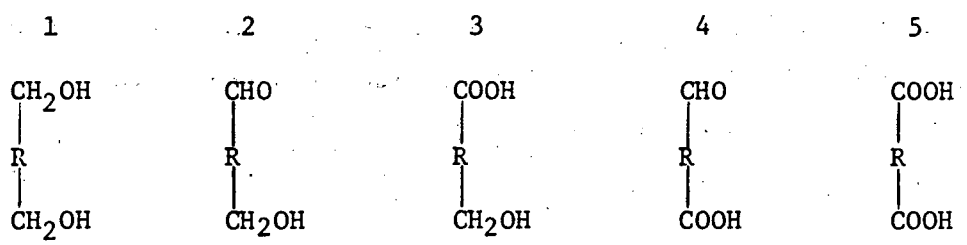

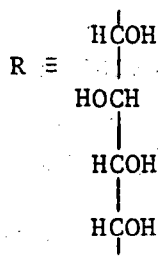

1 ≡ D-Glucitol

2 ≡ D-Glucose

3 ≡ D-Gluconic Acid

4 ≡ D-Glucuronic Acid

5 ≡ D-Glucaric Acid

Figure 40. GLUCOSE AND ITS DERIVATIVES SHOWN TO EMPHASIZE THE DIFFERENCES IN TERMINAL CARBON GROUPS

electrooxidative activity was the dicarboxylic acid (5), glucaric acid indicating the need for an oxidizable group at a terminal carbon. Glucose and glucuronic acid both exhibited a DL electrooxidation at about +90 mV versus MSE of comparable magnitude, which implicates the common aldehyde group that they contain. Glucitol, glucose, and gluconic acid all show electrooxidation in the DL region, suggesting that primary alcohol oxidation can also occur. Thus multiple reactions can presumably take place in the DL region, and selectivity is poor. This is supported as well by the elevated temperature data in which glucose, gluconic acid, and glucitol display very similar current potential behavior and CO_2 gas evolution, which indicates further oxidative reaction. In addition, an anodic peak in the DL region was found in the glucaric acid scan at this temperature possibly implicating the occurrance of secondary alcohol groups. This conclusion is supported by previous work on alcohols in which the rates of secondary alcohols were appreciable only at higher temperatures while primary alcohols were more easily electrooxidized.[107]

In the Pt-O region of the cyclic voltammograms recorded at ambient temperature, only glucose exhibited a distinct anodic peak. The results of all the other compounds were found to display only a more rapid current increase to electrolyte breakdown. Assignment of the glucose aldehyde or anomeric (#1) carbon electrooxidation to that observed in Pt-O region would be suggested if it were not for the results of glucuronic acid, which also has the terminal aldehyde group but little activity in the Pt-O region. Perhaps the lactone formation of the glucuronic acid causes an unfavorable sterochemical situation that inhibits the aldehyde electrooxidation.

Cyclic voltammograms on platinized Pt were recorded for glucose, gluconic acid, and glucaric (Structures 2, 3, and 5 in Figure 40) acid in strong alkaline (6.1M KOH). Glucose and gluconic acid gave nearly identical cyclic voltammograms in this electrolyte with the exception that gluconic acid retained the electrooxidation in the Pt-O region even at the high temperature. Radically different results were found in the case of glucaric acid in this electrolyte; up to six peaks covering the entire potential range of the electrolyte and very large current densities were detected. These varied results in alkaline electrolyte are thought to suggest that chemical degradation products are playing the dominate role in the observed electrochemical activity.

The important conclusions can be drawn from these comparisons: 1) electrooxidation beyond gluconic acid is possible in both acid and base at DL region potentials, 2) a mechanism exists by which oxidation to CO_2 can occur without oxidation of both terminal carbons to carboxylic acids, and 3) the electrooxidations in the DL region are quite nonspecific — a number of parallel reactions are possible.

Electrooxidation of Dextrin

Dextrin is the carbohydrate mixture obtained by hydrolysis of starch. Cyclic voltammograms were recorded with dextrin on platinized Pt in acidic (1.00M H_2SO_4) and alkaline (6.1M KOH) electrolytes to demonstrate that pure monosaccharides, like glucose, are not necessary for electrooxidation to take place. In addition, the reducing power of dextrin is not as great as glucose as evidenced by its inability to reduce Fehling's solution.[108] As usual, two temperatures were surveyed.

The cyclic voltammograms in acid electrolyte with and without dextrin are shown in Figure 41 for the two temperatures. The results were very similar to glucose results in that a electrooxidation occurred both in the double layer and "Pt-O" regions of the Pt electrode. Current densities were also comparable to those found for glucose.

The cyclic voltammetry results for dextrin in the alkaline electrolyte are shown in Figure 42. Although the results at 22°C were similar to glucose in that oxidations occurred in all three regions of the Pt electrode, only single distinct peaks were found with dextrin whereas glucose showed two. The higher temperature voltammogram (Figure 42b) was also similar to glucose with the major feature being a very broad peak centered in the double-layer region. Unlike glucose, however, dextrin maintained a strong oxidation in the "Pt-O" region as well. These data show that hydrolzed carbohydrate polymers provide an anodically electroactive mixture.

Electrooxidation of Lignosulfonic Acid Salts

A less extensive electrochemical survey than that conducted for the carbohydrates was made for the other major biomass constituent described in Task 1, the lignins. Lignin residues derived from the sulfite pulping process are the salts of lignin sulfonic acids. In the sulfite pulping process the natural lignin, like that illustrated in Figure 3, is fragmented into units of

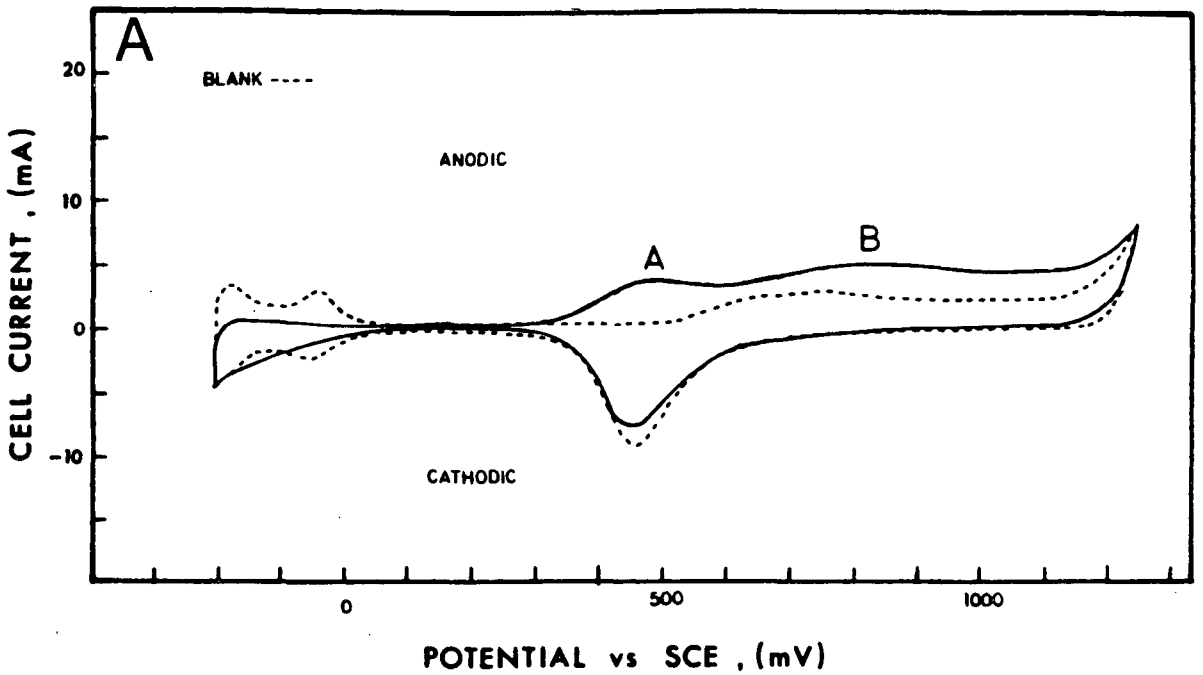

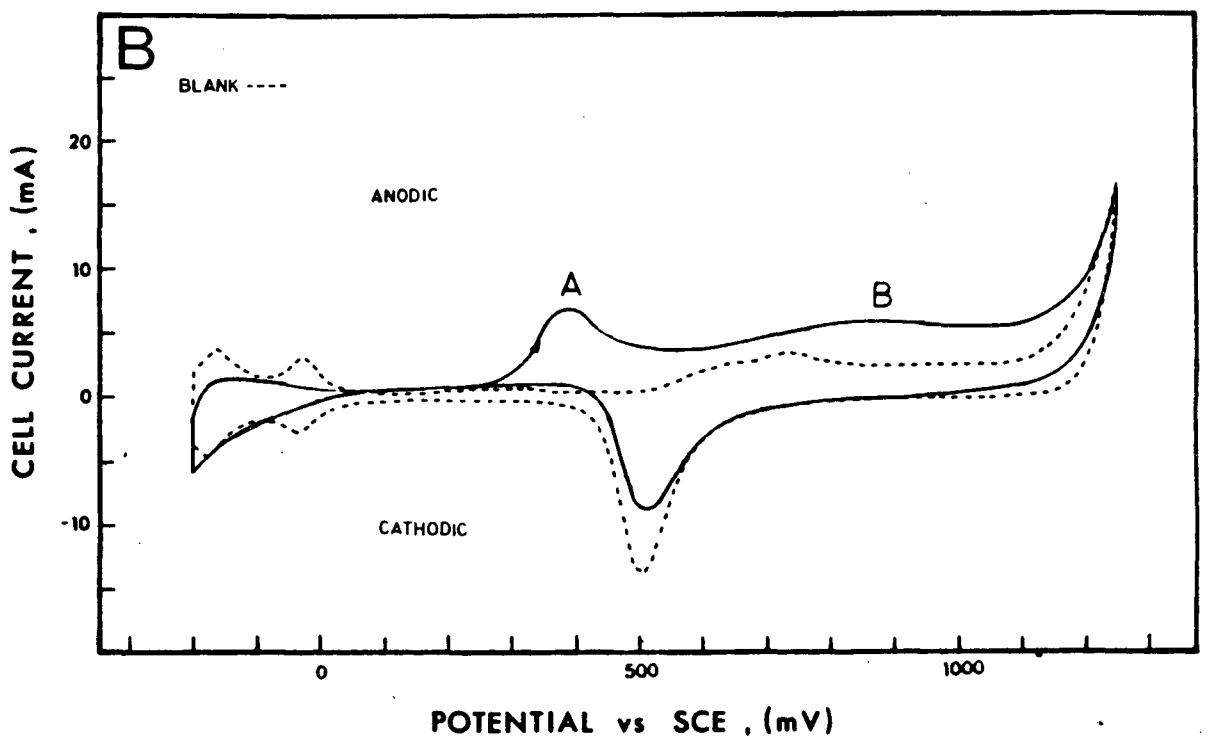

Figure 41. COMPARISON OF CYCLIC VOLTAMMOGRAMS WITH (Solid Line) AND WITHOUT (Dashed Line) 100 g/L DEXTRIN PRESENT. EXPERIMENTAL CONDITIONS: ELECTROLYTE, 1.00M H_2SO_4; WORKING ELECTRODE, PLATINIZED Pt (801 cm^2); SCAN RATE, 5 mV/s; TEMPERATURE, (a) 24°C AND (b) 61°C.

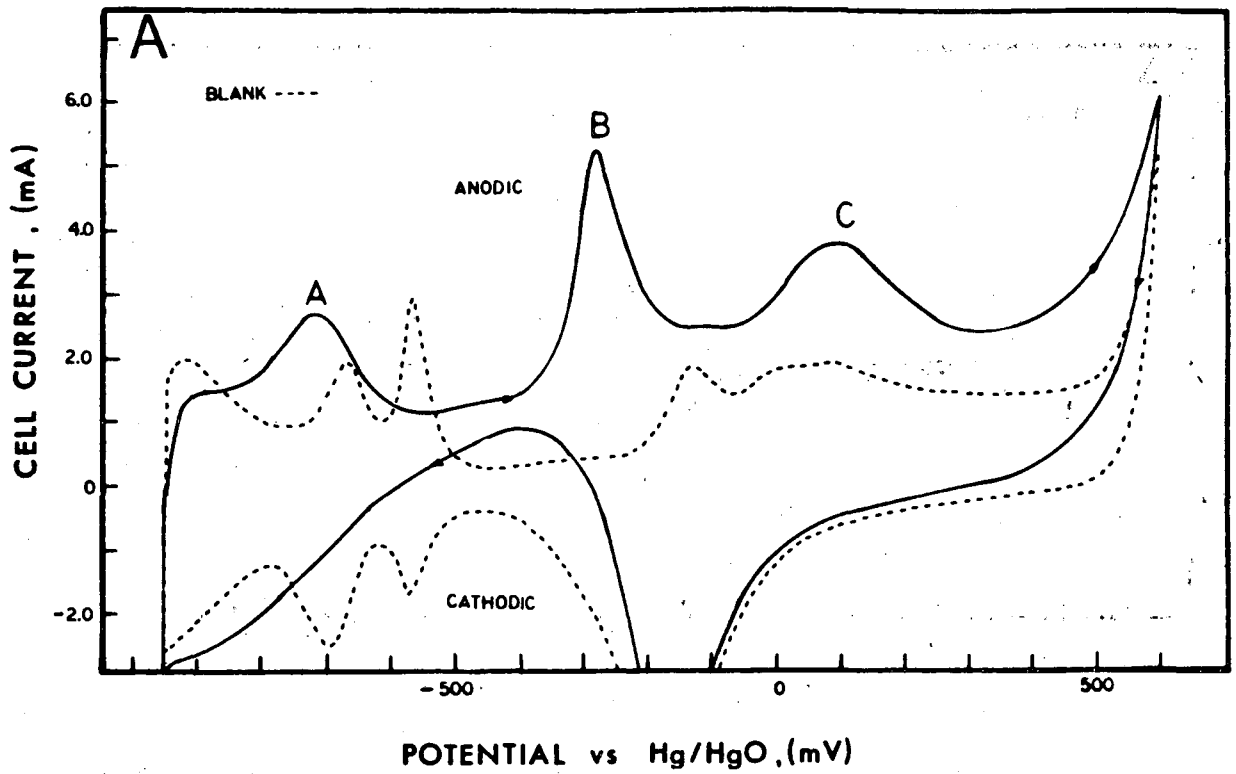

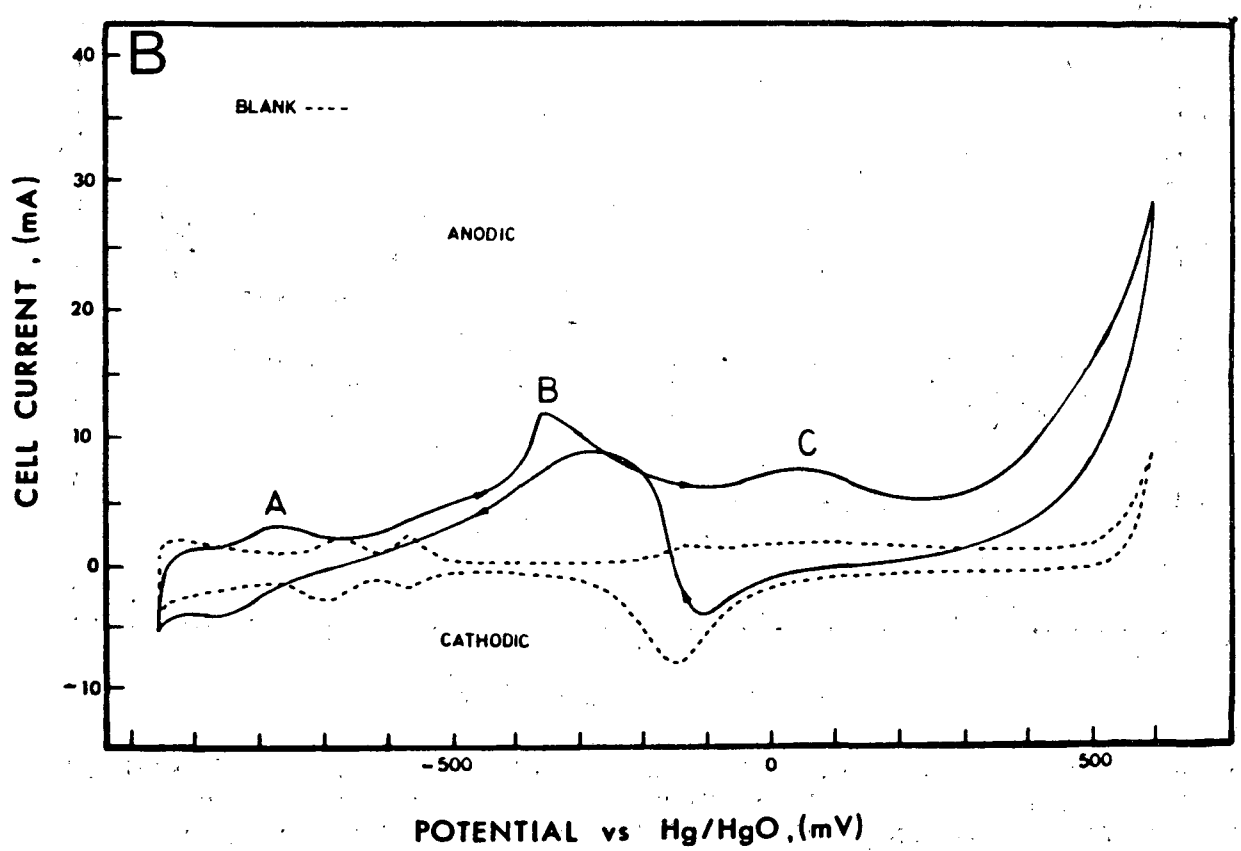

Figure 42. COMPARISON OF CYCLIC VOLTAMMOGRAMS WITH (Solid Line) AND WITHOUT (Dashed Line) 100 g/L DEXTRIN PRESENT. EXPERIMENTAL CONDITIONS: ELECTROLYTE, 6.1M KOH; WORKING ELECTRODE, PLATINIZED Pt (764 cm^2); SCAN RATE, 5 mV/s; TEMPERATURE, (a) 22°C AND (b) 62°C.

relatively large molecular weights in the range from 2000 to 5000 and sulfonated. The added ionic sulfonate groups then solubilize the lignin fragments in aqueous solutions of all pH's. Information was collected on the five lignosulfonic acid salts listed in Table 15, which gives a limited number of their properties. The first four salts in Table 15 were provided by the Crown-Zellerbach pulp and paper company, and the last one was from the commercial chemical vendor, Pfaltz and Bauer (P&B). The majority of the data were obtained with the P&B lignosulfonic acid, Na salt while the others were investigated under a limited number of conditions in order to identify whether the small differences in prior histories could possibly affect the electrooxidative activity.

Table 15. LIGNOSULFONIC ACID SALTS AND SELECTED PROPERTIES

Material	Type of Salt	Sugars, wt %	pH	Ash, wt %
Orzan A	NH_4^+	6	4	3
Orzan S	Na^+	19	6	17
Orzan LS	Na^+	0	11	28
Product 1120	Ca^{2+}	3	7	20
Pfaltz & Bauer	Na^+	—	—	—

Cyclic voltammetry was used to collect data on shiny and platinized Pt, glassy carbon, and Pb anodes. Experimental procedures were identical to those previously discussed for the glucose investigation. In most instances cyclic voltammograms were recorded at two temperatures, as has been the custom. The concentration of lignosulfonic acid salt was always 100 g/L.

Platinum Anode — Shiny

All the lignosulfonic acid salts listed in Table 15 were surveyed for electrooxidative activity on the shiny Pt anode. Data for the P&B lignosulfonic acid were obtained in acidic, near-neutral, and basic electrolytes (Nos. 1, 5, and 7 of Table 4) while the others were restricted to acid only (1.00M H_2SO_4). The cyclic voltammogram of 100 g/L P&B lignosulfonic acid, Na salt in 1.00M H_2SO_4, is shown in Figure 43 at 24°C. Electrooxidative activity at potentials more negative than oxygen evolution is clearly evident for this lignosulfonic acid. The electrooxidation, which appeared almost entirely in the Pt-O region, consisted of two broad peaks with the first beginning near

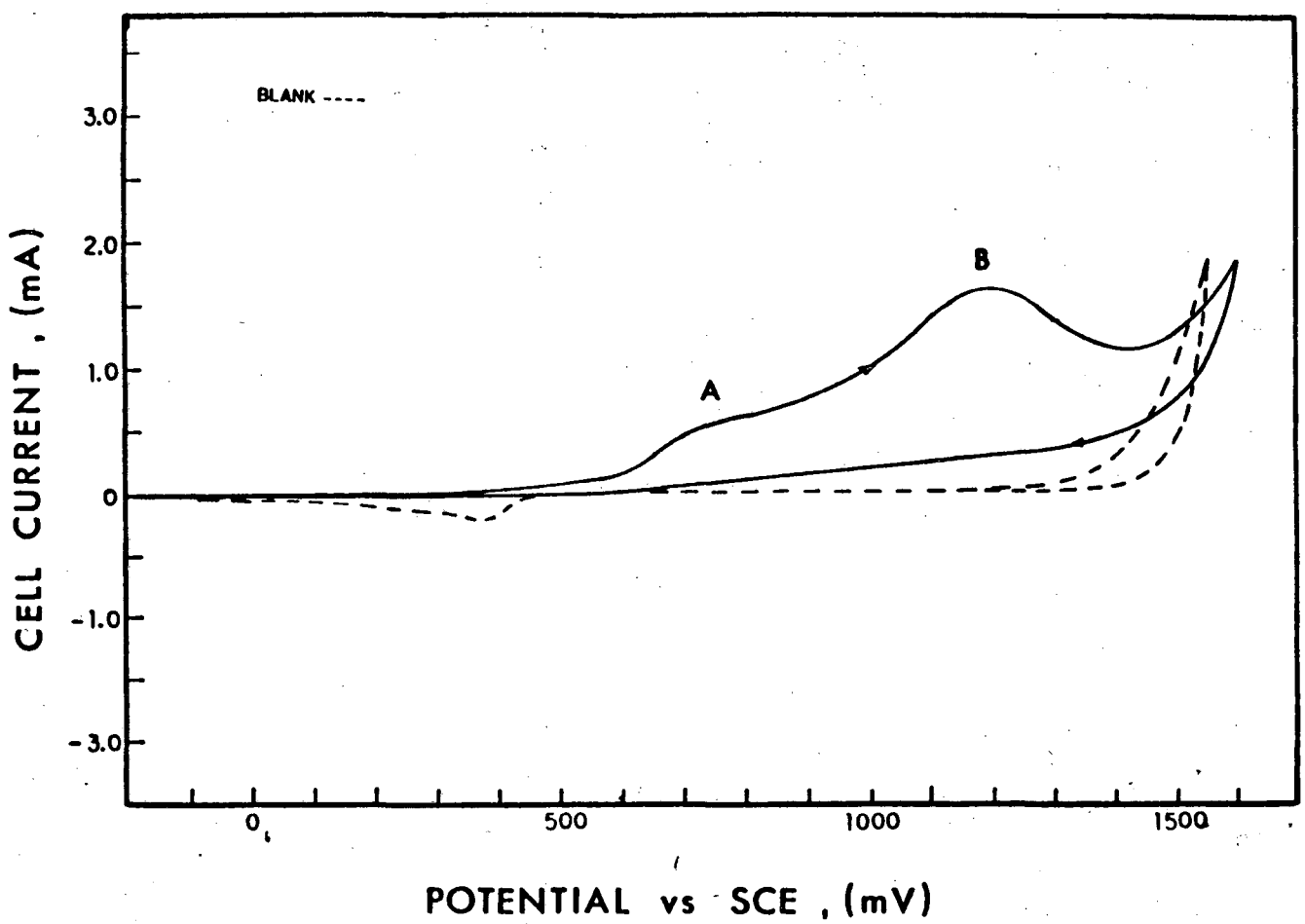

Figure 43. COMPARISON OF CYCLIC VOLTAMMOGRAMS WITH (Solid Line) AND WITHOUT (Dashed Line) 100 g/L LIGNOSULFONIC ACID, Na SALT. EXPERIMENTAL CONDITIONS: ELECTROLYTE, 1.00M H_2SO_4 (pH = 0.0); WORKING ELECTRODE, SHINY Pt (1 cm^2); SCAN RATE, 5 mV/s; TEMPERATURE, 24°C.

the potential where the "Pt-oxide" layer begins to form. The potentials of the initial shoulder, Peak A in Figure 43, and the broad second peak, B, along with their current densities are given in Table 16. The four other lignosulfonic acid salts provided by Crown-Zellerbach gave qualitatively similar cyclic voltammograms in that two anodic peaks in the Pt-O region were always observed. Figure 44a gives a comparative cyclic voltammogram for Orzan LS, and Table 16 lists the peak potentials and current densities for the two peaks of all the lignosulfonic acid salts for further comparison at both ambient and elevated temperature. The only deviation in this pattern was a small reversible wave observed in the DL region for the Ca salt (Product 1120). Slight differences in the relative magnitudes of the two peaks were observed.

Increased temperature was found to leave the peak pattern unchanged, and only current density increases of about a factor of three were detected. (See Figure 44b and Table 16.) The data indicate that the different lignosulfonic acid salts are essentially equivalent. Based upon current densities calculated from real platinum area, these values are about 100 times larger than those found with glucose.

Electrochemical oxidation of P&B lignosulfonic acid was also observed over a wide range of potentials in the near-neutral phosphate buffer. Figure 45 shows the single broad feature of the electrooxidation at ambient temperature. Qualitatively, raising the temperature to 65°C had no effect. At 24°C the maximum current density of 0.18 mA/cm^2 occurred at +479 mV versus SCE; at 65°C a value of 0.23 mA/cm^2 was found at +328 mV versus SCE. The increase in temperature caused a negative shift in potential for the maximum current density with little increase in its magnitude.

The cyclic voltammograms of P&B lignosulfonate obtained in strong alkaline electrolyte, 6.1M KOH, are shown in Figure 46 at 26°C and 64°C. Again, electrooxidation of the lignosulfonate occurred over a wide range of potential with the cyclic voltammogram at ambient temperature (Figure 46) being similar in appearance to those recorded in acid electrolyte, which had an initial plateau region followed by a more distinct peak. Unlike the previous two electrolytes, qualitative changes in the cyclic voltammograms occurred when the temperature was increased in alkaline electrolyte. (See Figure 46.) At the higher temperature, Figure 46b, a double peak appeared initially followed by a sharp rise at about the peak potential (B in Figure 46a) found

Table 16. PEAK POTENTIALS AND CURRENT DENSITIES FOR THE LIGNOSULFONIC ACID SALTS LISTED IN TABLE 15

Lignosulfonic Acid Salt	Peak Designation	$E_{p,a}$ vs. SCE, mV	$i_{p,a}$, mA/cm^2
	23° to 28°C		
Pfaltz and Bauer	A (Fig. 43)	+713	0.45
	B (Fig. 43)	+1208	1.56
Orzan A	A	+708	0.65
	B	+1150	1.55
Orzan S	A	+770	0.63
	B	+1150	1.55
Orzan LS	A (Fig. 44a)	+750	0.88
	B (Fig. 44a)	+1050	1.15
Product 1120	A	+765	0.68
	B	+1145	1.68
	C	+450	0.18
	62° to 65°C		
Pfaltz and Bauer	A	+720	1.30
	B	+1200	4.27
Orzan A	A	+750	1.60
	B	+1070	4.15
Orzan S	A	+725	1.48
	B	+1055	4.13
Orzan LS	A (Fig. 44b)	+730	2.15
	B (Fig. 44b)	+975	3.63
Product 1120	A	+745	1.95
	B	+1070	5.08

* Experimental Conditions: Working electrode, shiny Pt; electrolyte, 1.00M H_2SO_4/100 g/L lignosulfonic acid salt; scan rate, 5 mV/s.

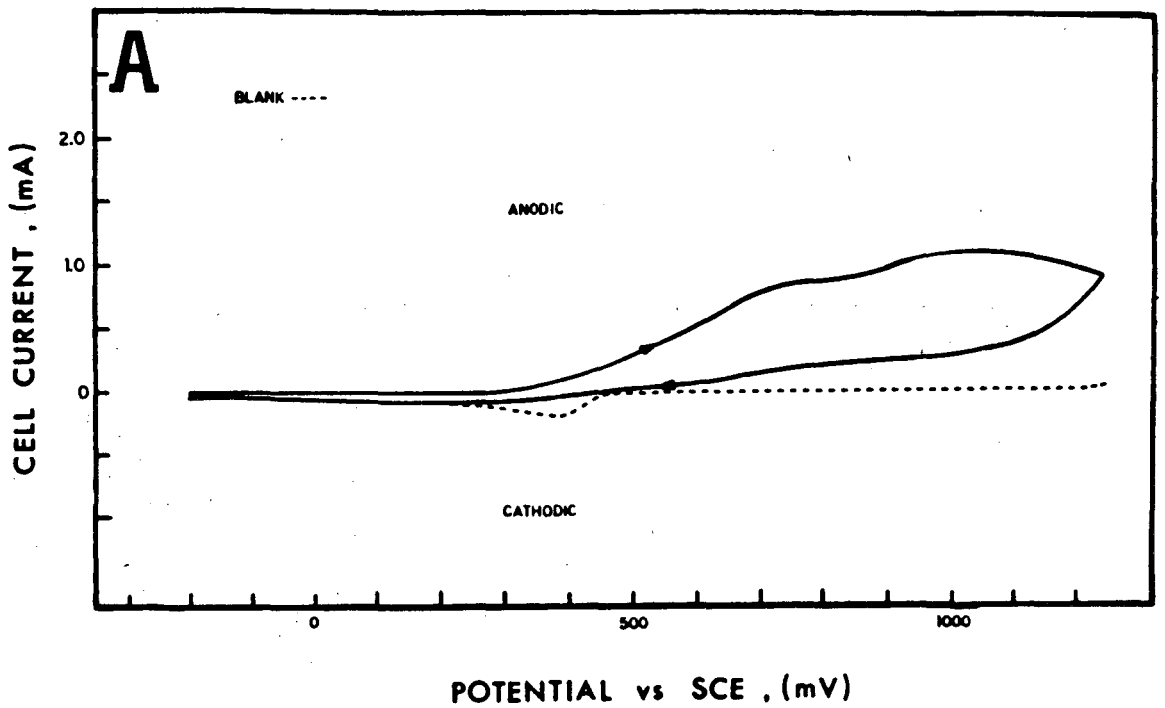

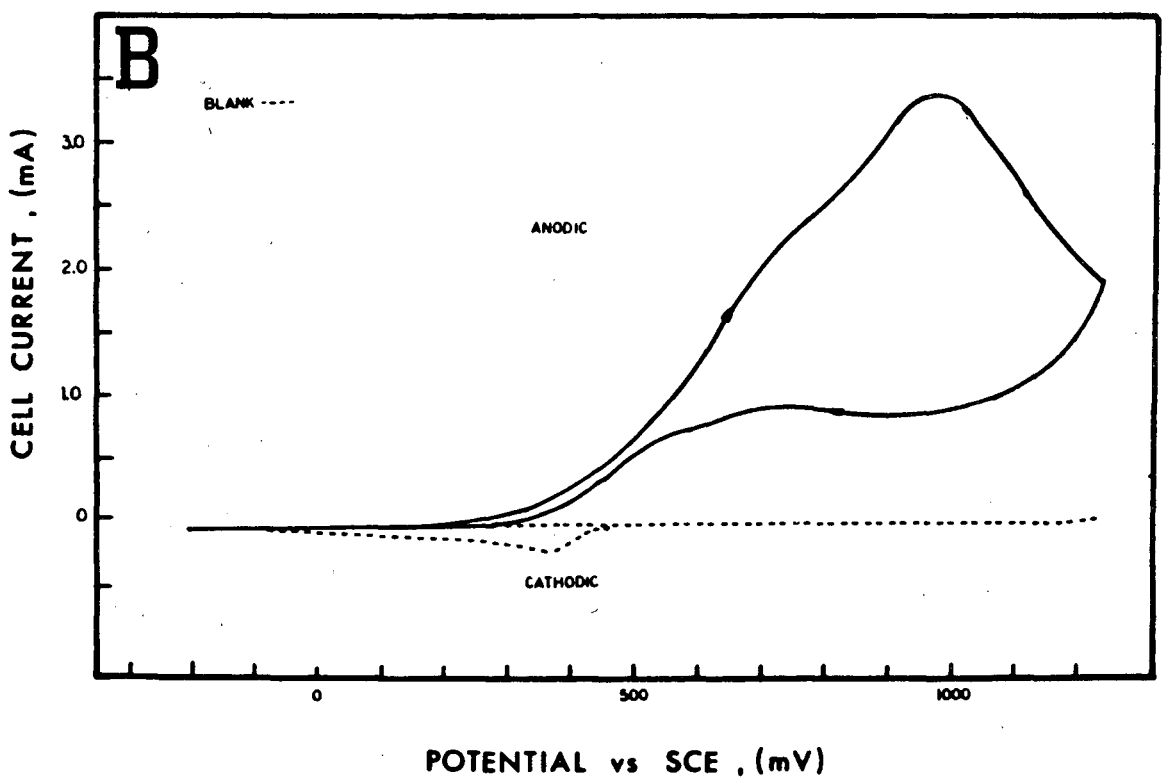

Figure 44. COMPARISON OF CYCLIC VOLTAMMOGRAMS WITH (Solid Line) AND WITHOUT (Dashed Line) 100 g/L LIGNOSULFONIC ACID, Na SALT (Orzan LS) PRESENT. EXPERIMENTAL CONDITIONS: ELECTROLYTE, 1.00M H_2SO_4; WORKING ELECTRODE, SHINY Pt (1 cm^2); SCAN RATE, 5 mV/s; TEMPERATURE, (a) 23°C AND (b) 62°C.

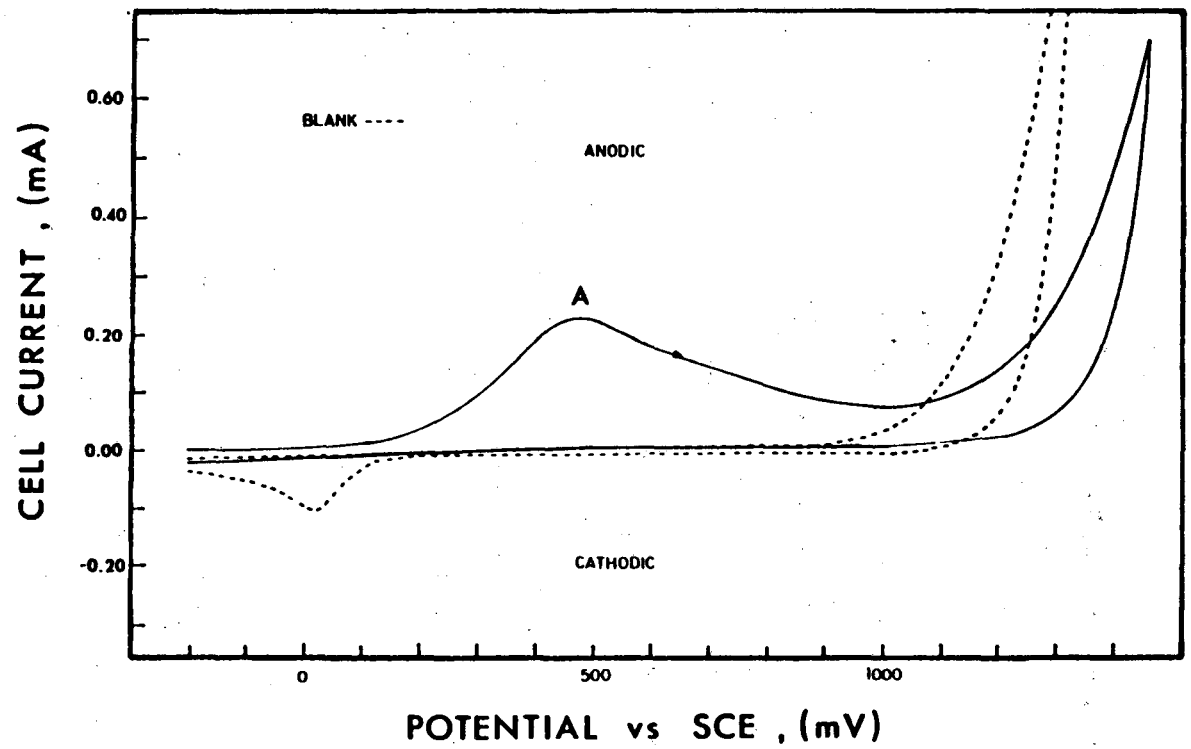

Figure 45. COMPARISON OF CYCLIC VOLTAMMOGRAMS WITH (Solid Line) AND WITHOUT (Dashed Line) 100 g/L LIGNOSULFONIC ACID, Na SALT PRESENT. EXPERIMENTAL CONDITIONS: ELECTROLYTE, 0.50M NaH_2PO_4/0.50M Na_2HPO_4 (pH = 6.6); WORKING ELECTRODE, SHINY Pt (1 cm^2); SCAN RATE, 5 mV/s; TEMPERATURE, 24°C.

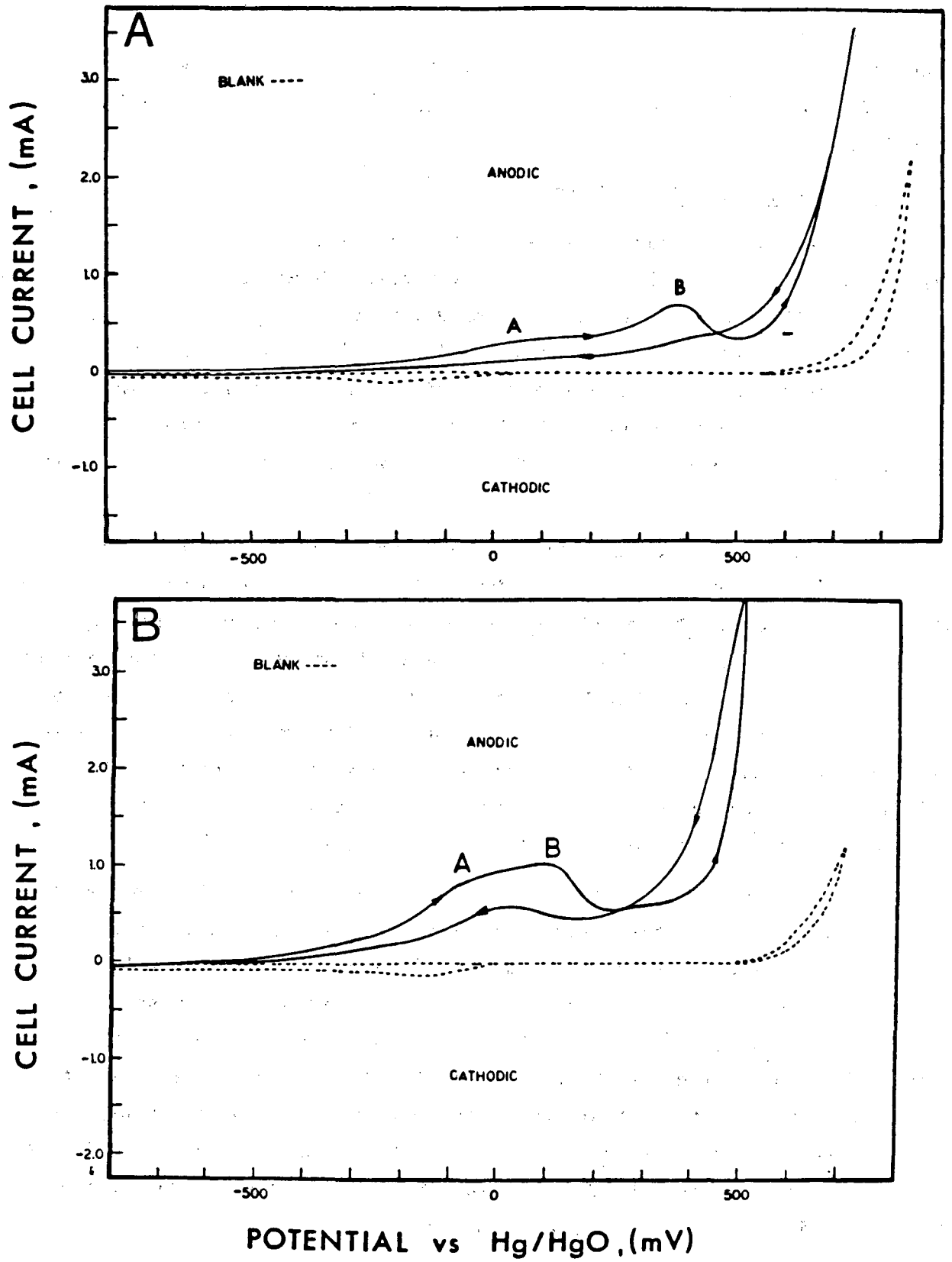

Figure 46. COMPARISON OF CYCLIC VOLTAMMOGRAMS WITH (Solid Line) AND WITHOUT (Dashed Line) 100 g/L LIGNOSULFONIC ACID, Na SALT PRESENT. EXPERIMENTAL CONDITIONS: ELECTROLYTE, 6.1M KOH (pH =14.8); WORKING ELECTRODE, SHINY Pt (1 cm^2); SCAN RATE, 5 mV/s; TEMPERATURE, (a) 26°C AND (b) 64°C.

at ambient temperature. Table 17 lists the average potentials and current densities for the features designated in Figure 46. Current densities again attained values near 1 mA/cm^2 and were influenced only slightly by the temperature increase.

Platinum Anode — Platinized

Although the true current densities for the lignosulfonic acid were much higher than those found for glucose, higher currents are desirable for practical bulk electrolyses. The electrochemically active area per unit area of electrode can be increased by roughening its surface, thereby increasing the current density based on electrode geometric area. As is well known, platinizing a platinum electrode is a simple way to accomplish this roughening, and this procedure was used widely in the investigation of glucose to increase the total currents observed.

The electrochemical oxidation of P&B lignosulfonic acid in 1.00M H_2SO_4 was, therefore, investigated on platinized Pt by cyclic voltammetry, and the results are given in Figure 47 for two temperatures. Pretreatment I was used. Few distinguishing features were observed except for a small peak at the most negative potential, Peak C in Figure 47, which was not in evidence on the shiny Pt electrode. Because there were no distinct features over most of the potential range, the gradual current increase was characterized by tabulating the current densities at the potentials of the peaks observed using the shiny Pt as well as the initial small peak (Table 18).

Although electrochemical differences in the lignosulfonic acid salts in Table 15 were expected to be small based upon the shiny Pt data, cyclic voltammograms were recorded on platinized Pt in 1.00M H_2SO_4 for all the Crown-Zellerbach materials as well in order to verify that nothing unusual occurred. In fact, all the lignosulfonic acid salts in Table 15 gave qualitatively the same cyclic voltammograms, and Table 18 compares the real and geometric current densities at two potentials of the gradually increasing cyclic voltammograms. Quantitatively, the only unusual feature was the lack of current increase for the P&B material when the temperature was increased as was observed for the other lignosulfonic acid salts.

The platinized Pt electrodes used here had an area approximately 600 times larger than the shiny Pt electrode. Using the platinized Pt area and

Table 17. CYCLIC VOLTAMMETRIC POTENTIALS ($E_{p,a}$) AND CURRENT DENSITIES ($i_{p,a}$) FOR THE ELECTROOXIDATION OF LIGNOSULFONIC ACID, Na SALT IN 6.1M KOH ON SHINY PLATINUM*

Oxidation Designation	$E_{p,a}$ vs Hg/HgO, mV	$i_{p,a}$, mA/cm^2
	26°C (46a)	
A	+80	0.48
B	+375	0.90
	64°C (46b)	
A	−60	0.85
B	+105	1.05
Potential of B (46a)	+375	1.45

* Electrolyte: 100g lignosulfonic acid, Na salt/L; 6.1M KOH (pH = 14.8).

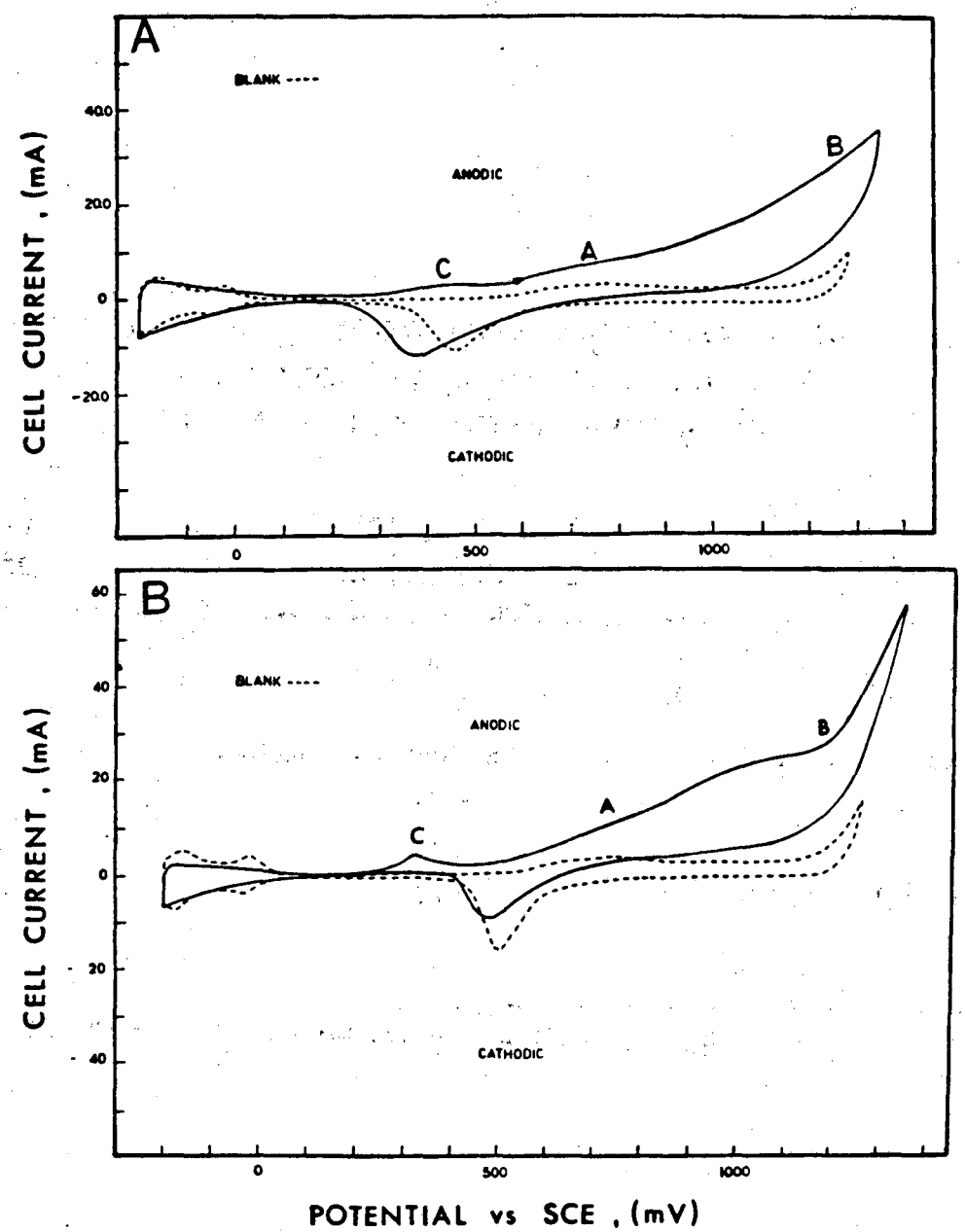

Figure 47. COMPARISON OF CYCLIC VOLTAMMOGRAMS WITH (Solid Line) AND WITHOUT (Dashed Line) 100 g /L LIGNOSULFONIC ACID, Na SALT PRESENT. EXPERIMENTAL CONDITIONS: ELECTROLYTE, 1.00M H_2SO_4 (pH = 0.0); WORKING ELECTRODE, PLATINIZED Pt (1200 cm^2); SCAN RATE, 5 mV/s; TEMPERATURE, (a) 24°C AND (b) 65°C

Table 18. REAL AND GEOMETRIC CURRENT DENSITIES FOR THE LIGNOSULFONIC ACIDS AT +725 AND 1210 mV VS. SCE AT 26° AND 62°C

Substance	Geometric $i_{p,a}$ @ 725 mV vs. SCE, mA/cm^2	Real $i_{p,a}$ @ 725 mV vs. SCE, $\mu A/cm^2$	Geometric $i_{p,a}$ @ 1210 mV vs. SCE, mA/cm^2	Real $i_{p,a}$ @ 1210 mV vs. SCE, $\mu A/cm^2$
		26°C		
Pfaltz and Bauer	5.00	4.2	21.0	17.5
Orzan S	1.75	2.77	13.8	21.8
Orzan LS*	2.50	3.96	15.2	24.2
Orzan A	3.50	5.64	12.1	19.8
Product 1120*	2.00	3.17	17.8	28.1
		62°C		
Pfaltz and Bauer	6.50	5.4	21.0	17.5
Orzan S	6.00	9.51	33.2	52.7
Orzan LS*	6.75	10.70	27.5	43.6
Orzan A (Scan 1)	8.50	13.71	25.5	41.1
Orzan A (Scan 2)	9.25	14.92	29.8	48.0
Product 1120*	6.75	10.70	34.8	55.1

* These samples contained precipitates and were less than 100g/l.

INSTITUTE OF GAS TECHNOLOGY

61060

scaling the current based on real current densities determined form shiny Pt (Table 16), the geometric current densities given in Table 18 are several hundred times smaller than this scaling predicts. The experimental, real current densities are therefore much lower on the platinized Pt than on the shiny Pt. This effect of area was investigated further by recording cyclic voltammograms of 100 g/L P&B lignosulfonic acid, Na salt/0.50M H_2SO_4 solutions on platinum electrodes with different roughness factors. (The roughness factor is the proportionality constant relating real area to the geometric area.)

Table 19 lists the results of the current densities, both real and geometric, for Pt electrodes with varying roughness factors at two potentials. For all electrodes except the shiny Pt, cyclic voltammograms with increasing currents similar to Figure 47 were observed. Although there is considerable scatter in the data, electrode roughening (platinizing) is not particularly effective for increasing total currents. Increasing real area by a factor of 1000 only results in about 10-fold increase in current. Real current densities appear to change little among the platinized sample of differing area, at least compared to the shiny Pt electrode.

The reason for this inability to scale the geometric current density with area is believed to result from the large size of the lignosulfonic acid fragments, which have molecular weights between 2000 and 5000.[13] Figure 48 schematically illustrates the relationship between the lignosulfonic acid fragment and the platinized Pt electrode. The roughness of the platinized Pt is on a smaller scale than the size of the lignosulfonic acid fragments, which makes most of the area inaccesible to it. Whereas a smaller molecule like glucose may reach into the valleys and make full use of Pt area, the lignosulfonic acid can take advantage only of the peaks in the electrode surface, and little is gained by platinizing. The inability to increase the currents appreciably for lignosulfonic acid by platinizing is disappointing.

Lead Anode

Cyclic voltammograms were obtained from (P&B) lignosulfonic acid in 1.00M H_2SO_4 on a 1-cm^2 Pb anode at 23° and 62°C. Figure 49 shows the cyclic voltammogram recorded at 23°C. No current of any kind, not even a Pb surface reaction, was detected until potentials well past those necessary for O_2 evolution in the absence of the lignin. Such behavior is indicative of strong

Table 19. EFFECT OF Pt ELECTRODE ROUGHNESS FACTOR ON THE CYCLIC VOLTAMMETRY GEOMETRIC AND REAL CURRENT DENSITIES FOR ELECTROOXIDATION OF LIGNOSULFONIC ACID[a]

Expt. No.	Electrode Geometric Area, cm^2	Roughness Factor	Real Area, cm^2	Geometric $i_{p,a}$ @ 725 mV vs. SCE, mA/cm^2	Real $i_{p,a}$ @ 725 mV vs. SCE, $\mu A/cm^2$	Geometric $i_{p,a}$ @ 1210 mV vs. SCE, mA/cm^2	Real $i_{p,a}$ @ 1210 mV vs. SCE, $\mu A/cm^2$
1	1.00[c]	2.7	2.7	0.40	148	1.69	626
2	1.00[c]	2.7	2.7	0.50	185	1.44	533
1	1.54	184	281	0.89	4.9	2.60	14.2
2	1.54	184	281	0.36	2.0	1.53	8.4
1	1.00	631	631	1.5	2.4	12.00	19.0
1	1.00	1200	1200	5.0	4.2	21.00	2.9

a Experimental Conditions: Electrolyte, 0.50M H_2SO_4/100g/l lignosulfonic acid, Na salt (Pfaltz and Bauer); temperature, 25 ± 3°C; scan rate 5 mV/sec.

b Real area determined by hydrogen desorption method.

c Shiny Pt.

INSTITUTE OF GAS TECHNOLOGY

61060

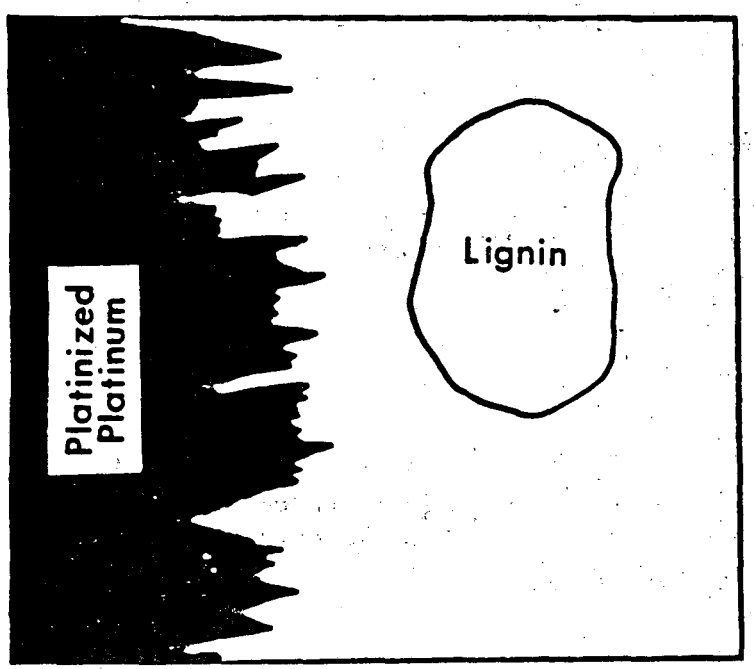

Figure 48. SCHEMATIC ILLUSTRATION OF A LIGNIN FRAGMENT APPROACHING A PLATINIZED Pt ELECTRODE

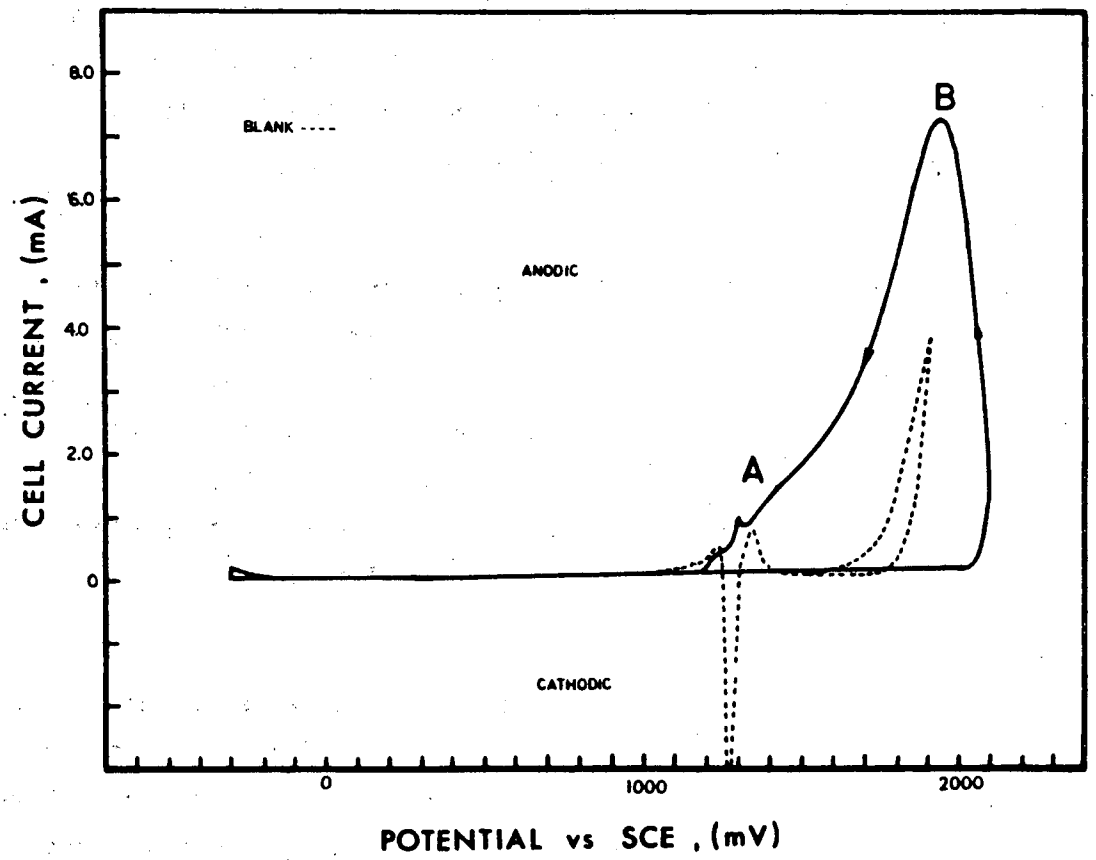

Figure 49. COMPARISON OF CYCLIC VOLTAMMOGRAMS WITH (Solid Line) AND WITHOUT (Dashed Line) 100 g/L LIGNOSULFONIC ACID, Na SALT (Pfaltz & Bauer) PRESENT. EXPERIMENTAL CONDITIONS; ELECTROLYTE, 0.50M H_2SO_4; WORKING ELECTRODE, Pb (1 cm^2); SCAN RATE, 5 mV/s; TEMPERATURE, 23°C

adsorption of the lignin material on the Pb electrode surface, which inhibits the Pb surface reactions and O_2 evolution. Such adsorption has been reported in the literature.[109] As Figure 49 shows, once a potential is reached at which current is passed, the passive layer appears to be broken and current flows to significant values even on the return scan. The anode potential at which current flows is, however, quite positive being on the order of 2.0 V versus RHE. Increasing the temperature yields the same qualitative results but the currents decrease. However, these currents may be a function of the reversal potential, which were not the same.

Vitreous Carbon Anode

Only a single cyclic voltammogram was recorded with (P&B) lignosulfonic acid on a vitreous carbon (Atomergic V25) electrode. The electrolyte composition was 1.00M H_2SO_4 plus 100 g/L lignosulfonic acid, Na salt. At a scan rate of 5 mV/s and 23°C, a single, broad, weak peak was observed beginning at +600 mV versus SCE and peaking at +1350 mV versus SCE with a current density of 1 mA/cm^2. This magnitude of current is on the same order of magnitude as those found with Pt electrodes under similar conditions.

Conclusions

The results obtained for the lignosulfonic acid salts, clearly indicate that they exhibit electrooxidative activity at potentials more negative than oxygen evolution. The potentials, however, where reaction occurs were rather positive (+900 mV or greater versus RHE) and only modest current densities of a few milliamperes per square centimeters were observed. The reactivity in near-neutral electrolyte was the smallest, with that in strongly acidic and basic electrolytes being about equal. Anode surface roughening and increased temperature had only a small effect on the electrooxidative current detected. The very limited anode variation indicated Pt as the preferred anode material. Only minor quantitative differences were observed between the results of the various lignosulfonic acid salts investigated. The data suggest that lignins may have limited electrochemical reactivity because the major portion of the lignin molecular fragment is inaccessable to the electrode.

Electrooxidation of Other Lignin Materials

Two samples derived from the kraft pulping process were supplied by the Crown-Zellerbach pulp and paper company, and they were briefly investigated. The samples provided were kraft lignin and raw black liquor.

Kraft Lignin

The pulping in the kraft process is performed in strongly alkaline solution, and the lignin fragment's solubility arises from neutralization of the phenol type hydrogens to form ionized phenoxide groups. Acidification can reprotonate the phenoxide groups, which causes a loss in solubility and precipitation. The kraft lignin investigated here was a material precipitated from the black liquor with H_2SO_4 in just such a manner.

The cyclic voltammograms of kraft lignin were recorded on shiny Pt in an electrolyte of 6.1M KOH containing 100 g/L kraft lignin. As usual, data were collected at two temperatures, the results of which are shown in Figure 50. As can be seen from the figure, several distinct oxidations of the lignin occur at potentials more positive than about —100 mV versus Hg/HgO with real current densities of several tenths of a milliampere per square centimeter. Little increase in current density occurred with increased temperature, typical of the lignin sulfonic acid salts investigated.

The cyclic voltammograms recorded with the lignosulfonic acid samples under identical conditions exhibited electrooxidation in the same general potential regime and had slightly larger current densities. However, the structure of the voltammetric peaks was entirely different.

The normal Pt electrode Pretreatment (No. I) of anodic and cathodic cycling was found to be inadequate for the kraft lignin. After the first scan, subsequent cyclic voltammograms showed reduced currents and resolution. Washing the electrode with an organic solvent like acetone prior to the electrochemical pretreatment allowed reproducible scans to be obtained. Implication from this observation is that an organic substance is adhering to the electrode surface, perhaps through anodic polymerization. The aromatic structure (Figure 3) of lignin makes stable free-radical formation likely,[60] and polymerization of the radicals may then be expected. Such polymerization has been observed with lignin model compounds and would naturally be a hindrance to continued electrochemical activity.

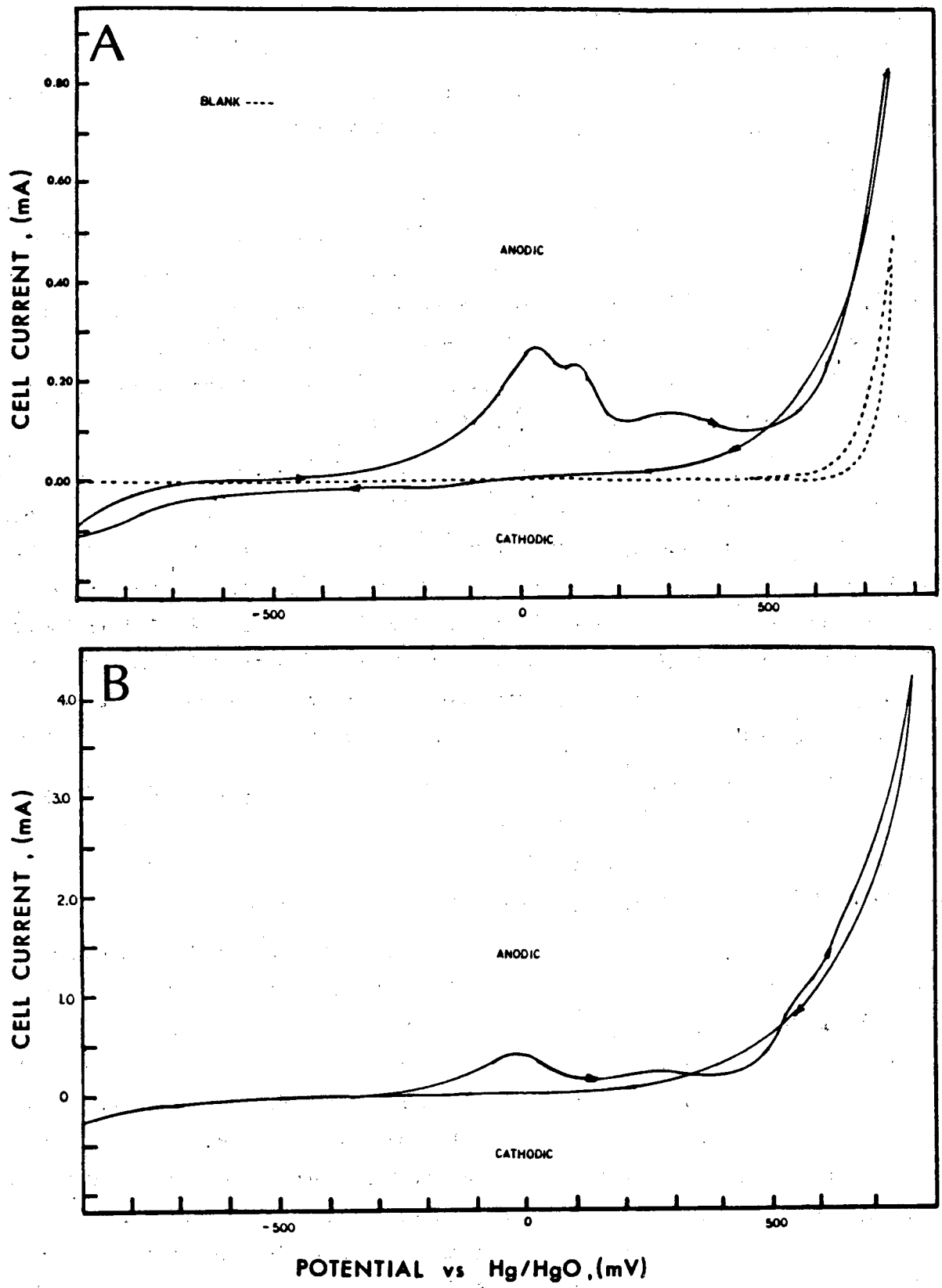

Figure 50. COMPARISON OF CYCLIC VOLTAMMOGRAMS WITH (Solid Line) AND WITHOUT (Dashed Line) 100 g/L KRAFT LIGNIN. EXPERIMENTAL CONDITIONS: ELECTROLYTE, 6.1M KOH; WORKING ELECTRODE, SHINY Pt ($1\ cm^2$ Geometrical); SCAN RATE, 5 mV/s; TEMPERATURE, a) 24°C AND b) 64°C

Black Liquor

Kraft black liquor is the spent liquid remaining after pulping and is composed of a large collection of substances, the largest fraction of which is kraft lignin. Table 20 lists the constituents of a typical sample as given by Sjostrom[13] showing the heterogeneous nature of the liquor.

Cyclic voltammograms were recorded on a platinized Pt electrode with a scan rate of 5 mV/s and a temperature of 23°C. An initial cyclic voltammogram was obtained immediately on arrival and then again the next day after exposure to air during the night. These cyclic voltammograms are shown in Figure 51.

In the scan recorded immediately on arrival, some sort of electrooxidation occurred over nearly the entire range of potential available to the electrolyte. The oxidation began at about —400 mV versus Hg/HgO and maintained currents between 5 and 10 mA/cm^2 (geometrical) up to +1000 mV versus Hg/HgO. The current then rose to a peak of 25 mA/cm^2 (geometrical) at +1450 mV versus Hg/HgO before anodic breakdown occurred.

After a light exposure to air, much of the oxidation disappeared. Initial oxidation did not begin until about +200 mV versus Hg/HgO with currents between 5 and 10 mA/cm^2 (geometrical) appearing over the potential range from +200 to +1300 mV versus Hg/HgO. The current then rose to the anodic breakdown. The alkali lignin in kraft pulping effluent is known to air oxidize, which presumably accounts for the differences in the cyclic voltammograms in Figure 51.

Further investigation of the degradation was made by recording a cyclic voltammogram 54 days after receipt. Additional reduction in electrooxidative activity was observed, and a scan very similar to that of the kraft lignin was obtained. This observation suggests that the stable species in the black liquor is akin to the species obtained by acid precipitation, the kraft lignin.

Conclusions. With the limited experimental data available on the black liquor and the kraft liquor derived from it, not a great deal can be concluded. Although a peak structure was observed in the cyclic voltammogram of the kraft lignin (Figure 50), its potential versus RHE and the current density magnitude were very similar to those seen for the lignosulfonic acid salts. Thus one type of lignin does not appear to be preferred over the other. The

Table 20. TYPICAL COMPOSITION OF THE ORGANIC MATERIAL IN PINE KRAFT SPENT LIQUOR[13]

Component	Content (% of dry solids)	Composition (% of hydroxy acids)
Lignin	47	
Hydroxy acids	28	
Lactic		15
2-Hydroxybutanoic		5
2,5-Dihydroxypentanoic		4
Xyloisosaccharinic		5
α-Glucoisosaccharinic		15
β-Glucoisosaccharinic		36
Others		20
Formic Acid	7	
Acetic acid	4	
Extractives	5	
Other compounds	9	

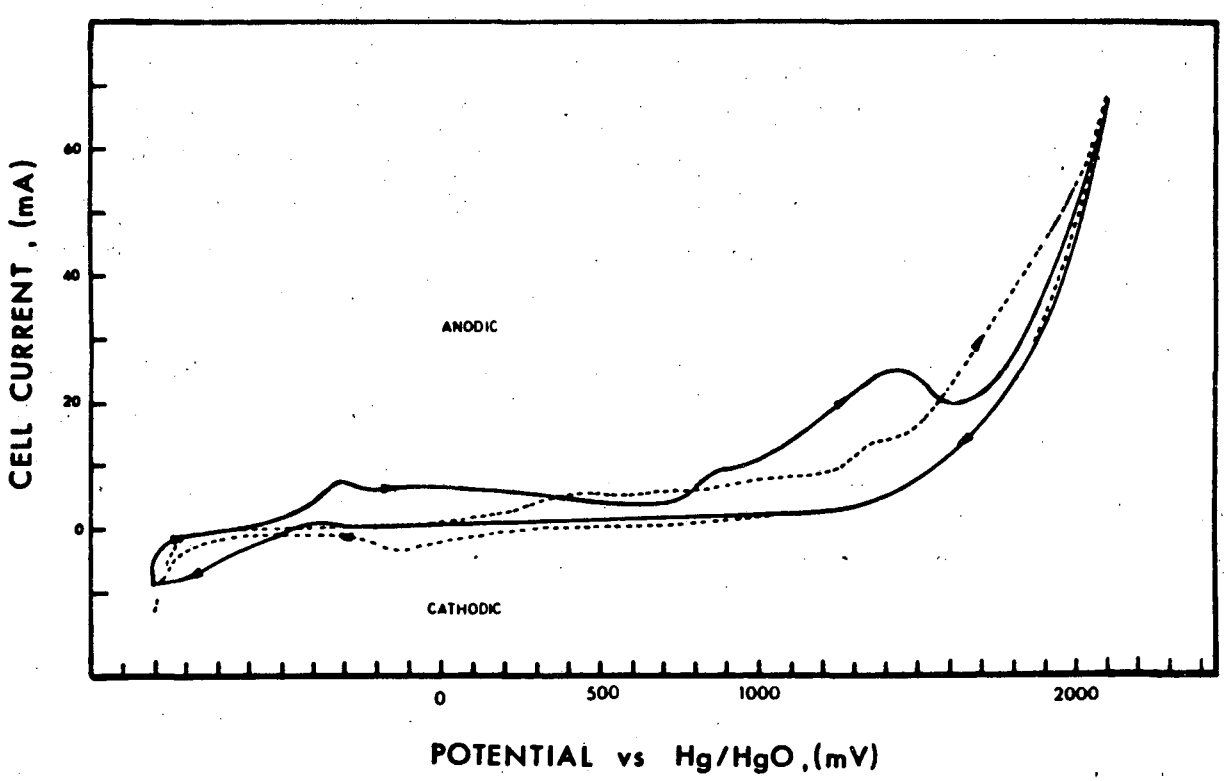

Figure 51. CYCLIC VOLTAMMOGRAMS OF WEAK BLACK LIQUOR ON SHINY Pt (1 cm^2) IMMEDIATELY AFTER RECEIPT (Solid Line) AND AFTER EXPOSURE TO THE ATMOSPHERE FOR ~20 HOURS (Dashed Line); SCAN RATE, 5 mV/s; TEMPERATURE, 23°C.

black liquor exhibited initial currents greater than the other lignins, but this activity declined with time and reached values commensurate with the other lignin samples investigated. This behavior suggests that degradable, nonlignin components are responsible for the larger current densities initially observed or that the oxidizable groups on the lignin are degraded with time and processing.

TASK 3. CHARACTERIZATION OF ANODIC OXIDATIONS

This task is directed at determining the properties of the sustained electrooxidation of the biomass materials identified in Task 2 that exhibited oxidation. In addition, chemical analysis of samples prepared by sustained electrooxidation or bulk electrolysis allows the identification of the reaction products being generated.

Nearly all the experiments conducted in this task were performed to investigate the properties of glucose electrooxidation, and the vast majority of these were conducted with the platinized Pt anode. In platinized Pt work, constant current (chronopotentiometry) and constant potential (chronoamperometry and bulk electrolysis) electrolyses were performed. Chemical analysis of electrolyzed solutions was investigated by high-pressure liquid chromatography (HPLC) and gas chromatography/mass spectrometry (GC/MS) of derivatized samples. Sustained electrooxidation of glucose on lead ruthenate and nickel anodes was also briefly explored.

Lignin electrolysis with a Pt anode was briefly touched upon in this task.

Electrooxidation of Glucose

Most of the electronic equipment and procedures employed in this task were identical to those described in Task 2. A PAR Model 179 Digital Coulometer plug-in was used in conjunction with potentiostat when it was necessary to count the amount of charge passed during an electrolysis. Various electrochemical cells were used and will be described as needed.

Platinum Anode — Platinized

Chronoamperometry. In the chronoamperometric experiment the current is monitored as a function of time during constant potential electrolysis. Any decline in current with time or limiting current may be identified in this manner. Passivation problems may also be discovered.

The platinized Pt working electrodes (1.54 cm^2 geometric area) were constructed by fastening a Pt disk to a piece of glass tubing with Teflon shrink tubing. After platinization, it was mounted horizontally in the electrolytic cell containing 250 mL of electrolyte, a graphite counter with glass fit separator, and a SCE reference. The real electrode area was determined as

previously described, and Pretreatment I was used. Current-time curves were recorded for the oxidation of 0.50M glucose on platinized Pt in 1.00M H_2SO_4 under variable conditions of anode potential, temperature, and mass transport. Anode electrolysis potentials investigated were +450 and +950 mV versus SCE, which were chosen to be approximately 50 mV more positive than the peak potentials for the two oxidations observed in the cyclic voltammogram at 23°C (Figure 6). Data were collected at ambient (23°C) and elevated (68° ± 3°C) temperatures with and without stirring.

Under all conditions, an initial rapid decline occurred which developed into a gradual decline after approximately 5 minutes. Figure 52 illustrates this behavior for the elctrooxidation of glucose at +450 mV versus SCE, a temperature of 68° ± 3°C, and with or without stirring over a period of 50 minutes. At no time was a true steady-state current attained. For both temperatures and at both potentials, the simple stirring by a magnetic stirring bar had little effect. A slight increase in current seemed to occur initially when stirred, but after 10 minutes, it was lower than in the unstirred electrolytes.

Table 21 lists the total charge passed in an hour and the current density at 10 minutes, which represents the current densities in the slowly changing region under the conditions investigated. Current densities at the two different potentials were effectively the same while the 45°C temperature increase caused increases of about an order of magnitude. These current densities are far below values that would be calculated on the basis of direct oxidation of α- and β- D-glucopyranose in the bulk electrolyte. The total number of glucose molecules involved in the oxidation was not great, as may be seen in Table 21. If a two-electron oxidation is assumed, at most only 0.1 mol % of the glucose was oxidized.

The continuous decline in current suggests electrode passivation. There appears to be two parts to the passivation: 1) a rapid initial component in the first 5 minutes and 2) a longer term decay that follows. Lack of a positive influence on the current by stirring indicates that current declines are not caused by mass transport.

Chronopotentiometry. In the chronopotentiometric experiment the potential was monitored as a function of time during constant current electrolysis. It most closely mimics electrolyzer operation in that the

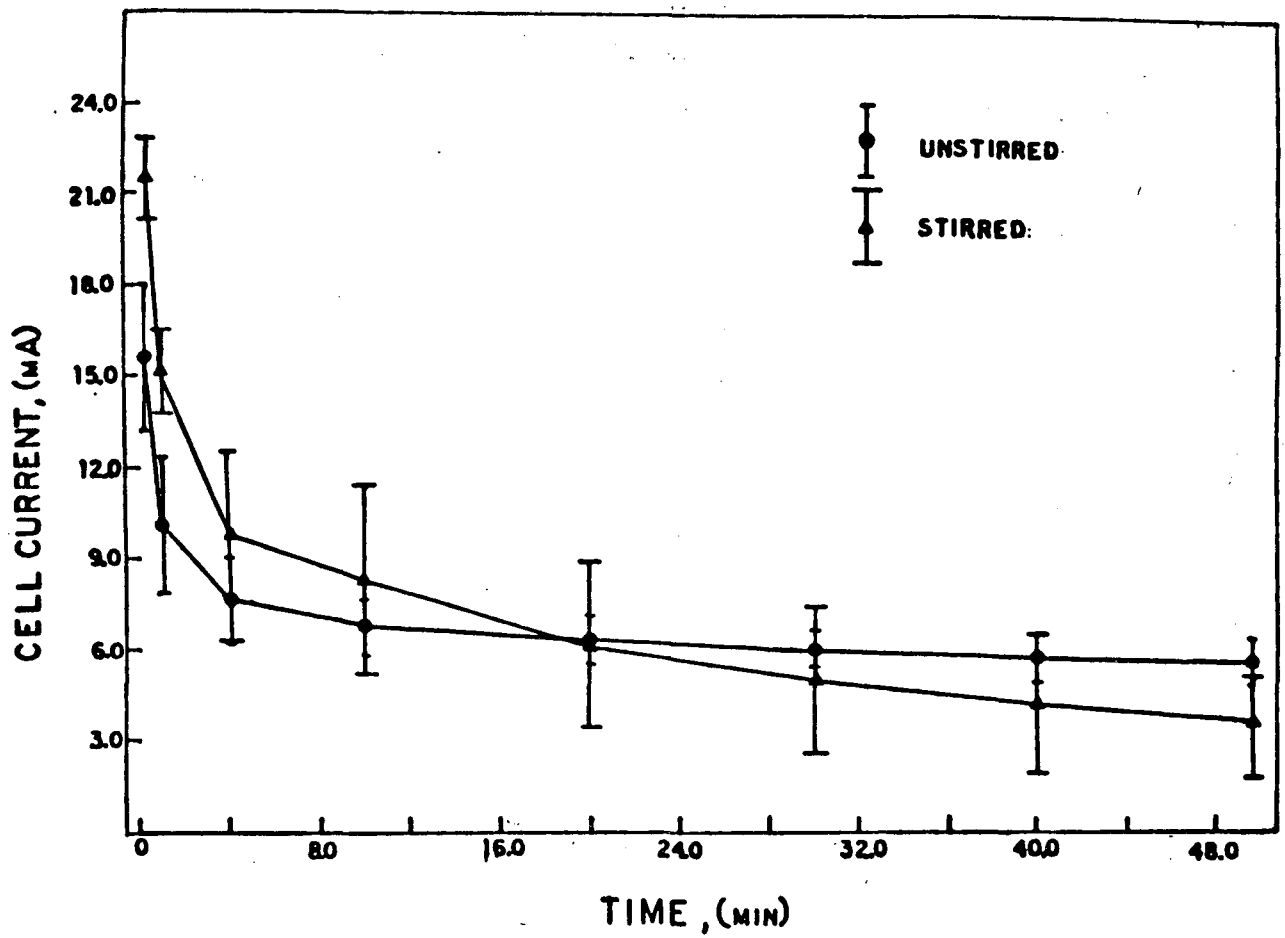

Figure 52. CHRONOAMPEROGRAM OF GLUCOSE OXIDATION AT +450 mV VERSUS SCE. EXPERIMENTAL CONDITIONS: ELECTROLYTE, 0.50 GLUCOSE/1.00M H_2SO_4; ANODE, PLATINIZED PLATINUM (428 cm^2); TEMPERATURE, 68 ± 3°C; ERROR BARS INDICATE STANDARD DEVIATION FOR 3 MEASUREMENTS.

Table 21. CHRONOAMPEROMETRY RESULTS: CHARGE PASSED PER 60 MIN AND SELECTED CURRENT DENSITY UNDER VARYING CONDITIONS ON PLATINIZED PLATINUM ANODE

Anode Potential vs. SCE, mV	Temp. °C	Stirring[b]	Electrons[c] Passed in 60 min, μmol	Current Density at 10 min, $\mu A/cm^2$
+450	23	No	25	1.8
+450	23	Yes	21	1.7
+450	65	No	187	13.6
+450	68	No	297	16.1
+450	70	No	223	17.8
+450	72	Yes	145	12.3
+450	69	Yes	307	26.9
+450	70	Yes	202	18.7
+950	24	No	45	3.2
+950	23	Yes	33	2.1
+950	68	No	225	16.0
+950	70	Yes	134	10.7

[a] General experimental conditions: Anode, Platinized Pt (428 cm^2); Electrolyte, 0.50M Glucose/1.00M H_2SO_4.

[b] Stirring provided by magnetic stir bar.

[c] For comparison, total moles glucose present equal 100 mmol.

reaction rate (current) is fixed while allowing the potential to take on the value necessary to maintain the desired rate. The general behavior of the potential time curve is as follows. If a fixed electrochemical reaction is taking place during the constant current electrolysis, the potential will remain essentially constant until the species at the electrode being reacted is consumed, at which time a rapid rise in potential to a value required to react the next available species occurs. A plateau structure similar to battery charging curves may often be obtained. Gradual rises in a plateau potential will occur as the concentration of the reacting species is depleted at the surface and concentration overpotential is increased.

The cell used was the same as that described for the chronoamperometry. Reaction rates between 1 and 100 mA/cm^2, geometrical, (~1 and 100 $\mu A/cm^2$, actual) for glucose oxidation were investigated in acid, neutral, and basic electrolytes, Nos. 1, 5, and 7 of Table 4. Emphasis was placed on the acidic electrolyte, 1.00M H_2SO_4. Because of the substantial temperature dependence of the glucose oxidation previously identified in cyclic voltammetry results, data were collected at ambient temperature and 65°C.

In the acid electrolyte over the range of experimental conditions explored, rather diverse behavior was observed in the potential-time curves. At the large reaction rate (100 mA/cm^2, geometrical), the potential increased rapidly up to the value found without glucose, and oxygen evolution was observed. A slight decrease in potential, about 100 mV, was detected at 65°C.

At lower reaction rates, distinct plateau structures in the potential-time curves were recorded. The potential plateaus appeared at potential values corresponding to the peaks observed in the cyclic voltammograms. Thus two glucose oxidation plateaus were identified that correspond to two of the cyclic voltammogram peaks, as can be seen from Figure 6 for example. The most negative potential plateau is of the greatest interest, and it was explored most thoroughly. This first potential plateau, in nearly all cases, exhibited large potential oscillations. Figure 53 illustrates typical behavior observed. This type of oscillatory behavior has been previously observed in the electrooxidation of other organic materials like formic acid[110] and glucose as well.[28] Its appearance has been related to passivation behavior of the Pt electrode. Reproducibility for this low potential plateau was not great either quantitatively or qualitatively, perhaps due to electrode

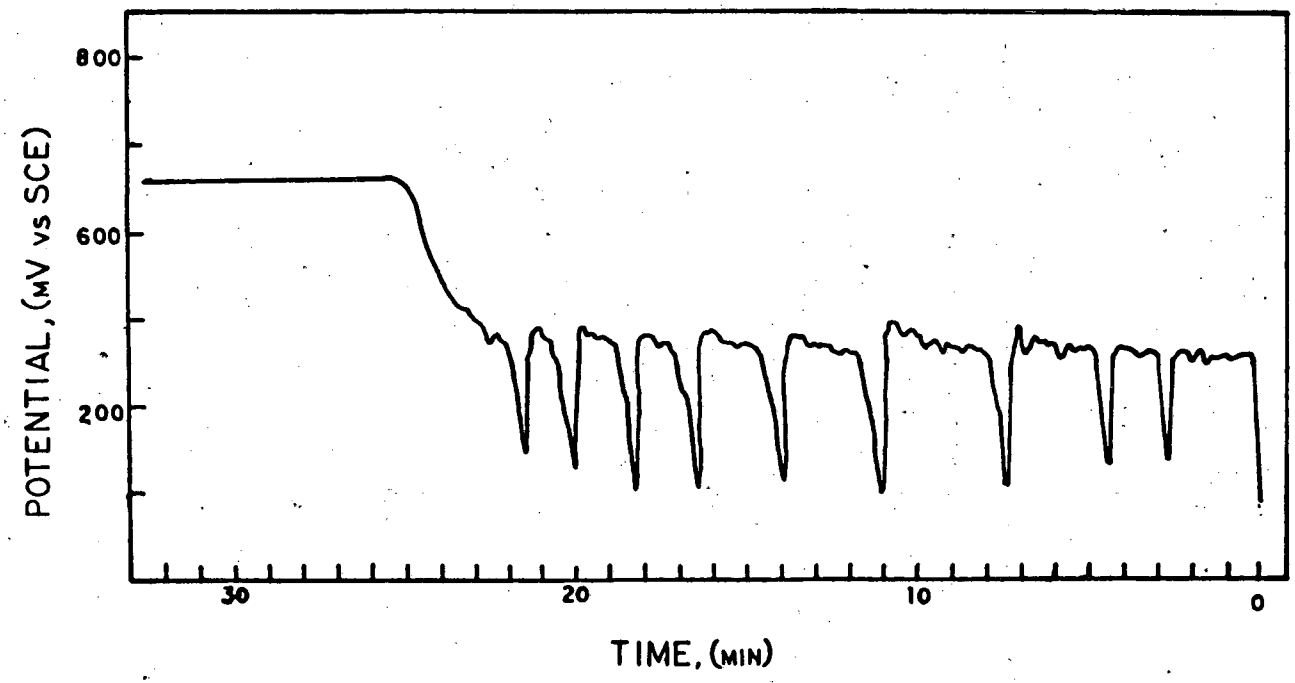

Figure 53. POTENTIAL-TIME CURVE FOR THE OXIDATION OF GLUCOSE IN ACID AT A CONSTANT CURRENT OF 5 mA. EXPERIMENTAL CONDITIONS: ELECTROLYTE, 0.50M GLUCOSE/0.50M H_2SO_4; ANODE, PLATINIZED PLATINUM (1034 cm^2); TEMPERATURE, 24°C

pretreatment effects. Table 22 gives the results of four chonopotentiograms curves that were generated under conditions as identical as possible.

The capacity of this first plateau was a sharp function of current or reaction rate. Table 23 lists the capacities found at ambient temperature for a range of currents. Low current densities favored increased capacity; increased temperature also increased the capacity of this plateau. If the electrolysis was terminated after passing totally through the low potential plateau, stirred for 10 minutes, and restarted, the potential returned to the low potential value and passed through it again. Table 24 presents such a series of data.

Although a decline in plateau capacity appears to be occurring with each run, the values are not outside the range found for the four "fresh" glucose solutions listed in Table 22. These chronopotentiometric data suggest a mechanism where the electrochemical species is being formed rather slowly by some nonelectrochemical step prior to electron transfer. At any rate, the capacity under any of the circumstances investigated was very much smaller than the amount of glucose present. Compare 250 mmol of glucose with the capacities in Tables 22 through 24.

At the second potential plateau at ~710 mV versus SCE, the potential could be maintained for capacities up to several percent of the moles of glucose at which time electrolysis was terminated. Thus, this reaction is believed to result from direct oxidation of bulk glucose.

Although limited experimentation was conducted at the higher temperature, 65°C, increased capacitance at the more negative potentials was clearly the trend. At the 1 mA rate a plateau was maintained at 140 mV versus SCE for 21.5 minutes, at which time the experiment was terminated. This potential lies below that found at ambient temperature. (See Table 23.) When electrolysis was maintained at the 10 mA rate, no plateau structure was observed. The initial working electrode potential was, however, quite negative. A slow rise followed, indicative of less reaction selectivity, which might be expected at the higher temperature. Table 25 tabulates the potential at selected times.

At ambient temperature no depolarizing effect at negative potentials was observed for a 10 mA rate (Table 23); increased temperature clearly increases the depolarizing capacity of the glucose.

Table 22. 5-mA CHRONOPOTENTIOMETRY OF "FRESH" GLUCOSE SOLUTIONS[a]

Run No.	Max. 1st Plateau Potential vs. SCE, mV[b]	Min. 1st Plateau Potential vs. SCE, mV[b]	2nd Plateau Potential vs. SCE, mV	No. of Oscilla-tions	Length of 1st Plateau, min	Capacity of 1st Plateau, μmol of electrons
1	340 ± 40	40 ± 40	710	9	25.4	78.9
2	340 ± 50	50 ± 50	710	9	28.8	89.5
3	320 ± 80	100 ± 50	710	16	41.8	130.0
4	350 ± 60	90 ± 50	710	13	33.6	104.4
Ave	337 ± 55	70 ± 48	710	12	32.4(7.1)[c]	100.7(22.2)

a Experimental Conditions: Electrode, platinized Pt (1034 cm^2); Electrolyte, 0.50M Glucose/0.50M H_2SO_4 (250 ml); Temperature, 25 ± 2°C.

b Potential given is the middle plateau value and the errors are the extreme.

c Number in parentheses is std. dev.

Table 23. COMPARISON OF LOW POTENTIAL PLATEAU DATA FOR VARIABLE CURRENT[c]

Galvanostatic Current, mA	Plateau Potential vs. SCE, mV	Length of Plateau, min	Capacity, μmol of electrons
1.00[a]	+275 ± 75	750	466
3.00	+330 ± 50	107	200
5.00[b]	+337 ± 50	32	101
7.00	+360 ± 50	2.8	12
10.00	No plateau at the lowest potential		

a Average of 2 runs.

b Average of 4 runs.

c Experimental Conditions: Working electrode, platinized Pt (1034 cm^2); Electrolyte, 0.50M Glucose /1.00M H_2SO_4 (500 ml) Temperature, 25 ± 2°C.

Table 24. CONSECUTIVE 5-mA CHRONOPOTENTIOMETRY IN THE SAME GLUCOSE SOLUTION[c]

Run[b] No	Max. 1st Plateau Potential vs. SCE, mV[c]	Min. 1st Plateau Potential vs. SCE, mV[c]	No. of Oscillations	Length of 1st Plateau, min	Capacity of 1st Plateau, μmol of electrons
3A	320 ± 80	100 ± 50	16	41.8	130.0
3B	350 ± 50	100 ± 100	15	35.2	109.4
3C	340 ± 40	100 ± 60	12	23.6	73.4

a Experimental Conditions: electrode, platinized Pt (1034 cm^2); electrolyte, 0.50M glucose/1.00M H_2SO_4; temperature, 25 ± 2°C.

b Run consectively with 10 minutes stirring between runs.

c Potential given is the middle plateau value and the errors as the extreme.

Table 25. POTENTIALS AT SELECTED TIMES DURING THE ELECTROLYSIS OF GLUCOSE IN H_2SO_4 ON PLATINIZED PLATINUM AT 65°C

Time, h		Potential vs. SCE, mV[b]
Initial		+210
1.0		280
2.0		440
4.0		530
9.0		800
17.0	(terminated)	740

a Experimental Conditions: Electrode, platinized Pt (1034 cm^2); electrolyte, 0.50M glucose/1.00M H_2SO_4 (250 mL).

b Blank without glucose goes to 1340 mV vs. SCE.

In the alkaline electrolyte at 25°C and a reaction rate of 10 mA/cm^2, geometrical (9.7 μA/cm^2, real), three plateau regions were observed in the potential-time curve. The three plateau potentials coincide nicely with the potential found for the three peaks observed in the cyclic voltammogram in Figure 12. The plateau capacities are given in Table 26. The first two, more negative potential plateaus had limited capacities, but the potentials were very attractive. Plateau D would appear to arise from direct oxidation of bulk glucose as indicated by its capacity, which would require participation of a substantial fraction of glucose molecules. During Plateau BC, seven potential oscillations between the potential values of Plateaus A and BC occurred.

After increasing the temperature to 65°C, the depolarizing effect was extended at the negative potentials for the 10 mA reaction rate. The potentials in the potential-time curve observed, again, followed closely those found in the cyclic voltammogram at this temperature in Figure 12b. The electrode potential began at —800 mV versus Hg/HgO rising to —575 mV in 2 minutes and to —350 mV in 10 minutes. A potential plateau was reached after 24 minutes. Oscillations occurred between —200 and —500 mV versus Hg/HgO for 26.6 hours at an average frequency of about 1 cycle/minute. After this period, the potential remained at —150 mV versus Hg/HgO without oscillation for another 15.1 mmoles of electrons passed. Under these conditions, this indicates that the reaction occurring at —150 mV versus Hg/HgO can be sustained.

When the reaction rate was increased to 100 mA (~350 μA/cm^2), the electrode potential rose relatively quickly to a value near +650 mV versus SCE. This potential can be sustained up to capacities of over a 100 mmoles (200 mmoles of glucose present).

In the phosphate buffer, no depolarizing effect was detected at room temperature even at the 1 mA/cm^2 (geometric) rate. Raising the temperature to 65°C generated a small oscillating plateau between the potentials of —350 and +160 mV versus SCE and with a capacity of 560 μmoles of electrons.

The plateau structures indicate that specific reactions are most likely taking place, and their potentials match nicely with peaks observed in the cyclic voltammograms recorded under the same experimental conditions. The capacities of the most negative plateau were quite small and function of

Table 26. PLATEAU DATA OF THE POTENTIAL-TIME CURVE FOR THE ELECTROOXIDATION OF 0.50M GLUCOSE ON PLATINIZED Pt IN 6.1M KOH AT 10 mA/cm^2 (Geometrical) AND 25°C

Plateau Designation[d]	Potential vs. Hg/HgO, mV	Length of Plateau, h	Charged Passed, mmol of electrons[b]
A	-875	0.59	0.22
B,C	-225[a]	1.6	0.60
D	+400	>19.1[a]	>7.13

[a] Terminated after 19.1 hours of electrolysis.

[b] 250 mmoles of glucose in electrolyte.

[c] Maximum potential of oscillation which appear in this plateau.

[d] Designations from Figure 12a.

reaction rate (current). Thus the electrochemical active specie's concentration is small as it is consumed rather easily at a rate much faster than would occur for bulk electrooxidation of glucose. This implies that the electrochemically active specie is derived from glucose at a rate slower than the rates of oxidation used. The appearance of potential oscillations during these plateaus was indicative of electrode passivation behavior. Again the near-neutral electrolyte was least active, and increased temperature was beneficial.

Bulk Electrolysis and Product Analysis. As discussed in the introduction, an aspect of considerable importance besides depolarization is the organic oxidation products generated at the anode. To accomplish this, bulk electrolyses in which the amount of charge passed is comparable to the amount of glucose present is necessary, and subsequent separation and chemical analysis of the electrolyzed samples must be performed. Unfortunately, the program permitted only an extremely limited effort in this area. The bulk electrolysis of glucose was investigated in platinized Pt in 1.00M H_2SO_4 only. All the electrolyses were conducted under controlled potential conditions, as opposed to controlled current, thereby allowing close regulation of the possible reactions.

Because the chronoamperometry discovered that current-time curves recorded at constant anode potential declined rapidly to impractical values during bulk electrolysis, especially at ambient temperature, various ways were sought to increase the current sufficiently for the passage of an exceptable amount of charge over a practical time period. Standard measures like designing an electrolysis cell with a large ratio of anode surface to electrolyte volume and increased temperature were considered. However, it was previously noted that for the constant potential electrolysis at the electrooxidation in the DL region, changes in anode potential could reactivate the currents after the decline had occurred. Any potential change, whether negative, positive, or open-circuit, seemed to do. This type of behavior was also identified in the chronopotentiometry where the capacity of the most negative plateau could be regenerated by placing the anode at open circuit for a brief period. This behavior suggested that pulsed electrolysis where the potential is pulsed to a more negative potential could be beneficial in maintaining the electrolysis at a reasonable rate.

The amount of charge passed per fixed time for a constant potential electrolysis at +450 mV versus SCE and for two pulsed electrolyses where the potential was shifted to the double layer (+50 mV) and hydrogen potential (—150 mV) regions of the Pt electrode are compared in Table 27. Recording the charge during the pulsed electrolysis was done bimodally to allow capacitance and surface reaction charge to cancel and leave only Faradaic charge. Table 27 shows that the periodic potential shifting to potentials where no reaction occurs is very beneficial, allowing greater than an order of magnitude increase in charge passed per unit time. This type of variable potential electrolysis was used to increase the rate of reaction.

Initial attempts at bulk electrolysis were performed in a simple pyrex H-cell with an anolyte volume of 20 mL and a large flag Pt anode (4 cm^2 geometric and 2480 cm^2 real). The currents observed were rather disappointing. Even with an area ~10 times larger than previously observed for the 200 mL reaction vessel, the currents were smaller, indicating a difficulty in scaling the reaction. After electrolysis at +450 mV versus SCE reduced the currents to a negligible value, a cyclic voltammogram showed that the anodic peak at +450 mV versus SCE was absent. Pretreatment of the electrode by the normal anodizing cathodizing procedure resulted in the return of the anodic peak at +450 mV versus SCE, suggesting poisoning of the electrode towards this reaction.

Because the simple H-cell was not particularly satisfactory nor adaptable to running electrolyses at elevated temperatures, a tubular all-Teflon cell was constructed. The anolyte volume was 10 mL and cathode/anode chamber separation was provided by a Nafion 390 membrane in the acid electrolyte. A small reflux column was attached to the outlet of the anode chamber to control evaporation at the higher temperatures. In addition, the purge gas was exited through a standard CO_2 trap consisting of a $Mg(ClO_4)_2$ drier followed by Ascarite for capture of the CO_2. In this manner, the possibility of any CO_2 evolution could be monitored. Tests of the apparatus indicated that the sensitivity was within 1 mg of CO_2 or 0.023 mmole. For elevated temperature electrolysis, the electrolysis cell assembly was immersed in a water bath with controlled temperature. This cell design proved satisfactory.

The bulk electrolyses of 0.50M glucose in 1.00M H_2SO_4 on platinized Pt were performed without difficulties, and their associated data are given in Table 28.

Table 27. CHARGE PASSED IN 1.0 HOURS BY VARIOUS ELECTROLYSIS SCHEMES FOR THE ELECTROOXIDATION OF GLUCOSE

Type of Electrolysis[a]	Charge Passed In 1.0 Hour, Coulombs
Constant Potential @ +450 mV vs. SCE	1.2
Pulsed,[b] 100 sec @ +450 mV and 10 sec @ +50 mV vs. SCE	38.0
Pulsed, [b] 100 sec @ +450 mV and 10 sec @-150 mV vs. SCE	55.0

a Experimental Conditions: Electrode, platinized Pt (280 cm^2); electrolyte, 1.00M H_2SO_4/0.50M glucose; volume, 200 mL.

b Charge recorded in a bimodal fashion allowing capacitive and surface reaction charge to be cancelled.

Table 28. RESULTS OF GLUCOSE ELECTROLYSES IN 1.00M H_2SO_4 ON PLATINIZED Pt[a]

Electrolysis No.	Potential Applied vs. SCE	Electrode Area, cm^2	Temp., °C	Time of Electrolysis, h	Electrons Passed, mmol	CO_2 Evolved, mmol	Glucose Remaining, mmol[b]
Constant Potential Electrolysis							
9	+450 mV	750	69	15.6	0.48	0.02	0.5
Pulsed Potential Electrolysis							
3	+450 mV for 110 sec −150 mV for 10 sec	1400	23	63	1.61	0.46	3.6
5	+450 mV for 110 sec −150 mV for 10 sec	1333	65	15.2	5.58	0.44	2.6
10	+450 mV for 110 sec −150 mV for 10 sec	3049	67	22.8	10.07	1.45	3.2
6	+450 mV for 110 sec +50 mV for 10 sec	1016	68	15.4	2.86	0.22	2.8
12	+950 mV for 110 sec +50 mV for 10 sec	2019	66	48.0	32.25	2.76	<.004

a Experimental Conditions: Electrolyte, 10 ml 0.50M glucose (5.00 mmol)/1.00M H_2SO_4 (pH = ∩.0); electrode, platinized Pt (3.24 cm^2 geometrical).

b Determined by HPLC.

As shown in Table 28, four different electrolysis potential schemes were used. The first was simple constant potential electrolysis (No. 9). The rest of the electrolyses employed two potentials. The first potential, maintained for 110 seconds was at the oxdiation potential of the peaks detected in the cyclic voltammogram, either +450 or +950 mV versus SCE. After this period at the electrolysis potential, the potential was shifted for a 10-second period to either a potential in the Pt double-layer region, +50 mV versus SCE, or the Pt hydrogen region, —150 mV versus SCE, where no electrolysis should occur. The purpose of this pulsed potential was to increase the rate of electrolysis.

Comparison of the constant potential electrolysis (No. 9) with either pulsed electrolysis Nos. 5 or 6 shows the increased rate of electrolysis which is afforded by the variable potential scheme. The effect of temperature is shown by comparison of electrolysis No. 3 (23°C) and 5 (65°C). The increased temperature allows the oxidation to proceed at much higher average rates, making the time required for an electrolysis acceptable. Stepping to the more negative potential, —150 mV versus SCE, increases the rate of electrooxidation. (Compare Electrolysis Nos. 5 and 6.)

Blanks treated identical to the electrolyzed samples but without any passage of current exhibited negligible decline in the glucose concentration as measured by HPLC, indicating that negligible chemical degradation occurs during the course of the electrolyses.

A somewhat unexpected result was the observed evolution of significant amounts of CO_2 during the electrolysis. This was unusual in that most reports in the literature do not indicate any carbon-carbon bond cleavage at electrode potentials as negative as those used here.[25-32] Because the presence of significant amounts of CO_2 is believed to be unusual, and chemical degradation might be possible at the higher temperature, a blank was obtained by passing purge gas through the cell under the experimental conditions at 65°C given in Table 28 for a period of 22.5 without electrolyzing. Less than 0.0003 g weight change in the Ascarite occurred, verifying that the production of CO_2 was real.

The analytical procedures explored for the electrolyzed samples were direct HPLC and GC/MS of trimethylsilyl derivatized samples. In general, these procedures gave excellent results with standards of simple sugars, but when applied to the sugar acids, particularly in actual samples, serious

difficulties developed. As these acids are expected oxidation products, steps were required to rectify the situation. Considerable effort was devoted to the development of analytical techniques needed for the particular samples generated in the bulk electrolyses.

Because samples can be analyzed directly by HPLC, its use was thought to be desirable if only a few components were contained in the samples. If this were the case, retention times would provide an adequate identifier of the compound. Sample analysis indicated that many comounds were present which made GC/MS analysis preferrable. HPLC was used, however, to quantitate the amount of glucose remaining after electrolysis. The electrolysis samples under investigation are given in Table 28 where the remaining glucose may be found.

The GC/MS analysis of the glucose and its oxidative derivatives requires derivatization before analyses can be performed. Solid test samples gave excellent results but difficulty was encountered in derivatizing the aqueous electrolyte. In particular, the acids derivable from glucose were difficult to derivatize. In fact, it was never possible to detect glucaric acid when derivatized from the aqueous/H_2SO_4 solution. The following derivatization procedure was adopted for GC/MS analyses.[111-114] The solutions were first lactonized using HCl. Excess water was removed by freeze-drying, and the remaining sample was then derivatized using Trisil-Z (Pierce Chemical) to form trimethylsilyl compounds.

Samples from Electrolyses Nos. 5, 10, and 12 (Table 28) were subjected to this analysis. Qualitatively, similar results were obtained in all three samples. GC signals were detected for compounds expected from glucose oxidation with little specificity. Compounds detected and identified by library MS and/or comparison of standards included gluconic acid along with its 1,5 and 1,4 lactones and glucuronic acid and its 6,2 and 6,3 lactones. As CO_2 was clearly generated, shorter carbon chain species were expected, such as oxidation products of arabinose or xylose. No standards of acids and lactones of these compounds were available nor were results contained in the NIH/EPA mass spectra library. However, the samples clearly contained smaller mass compounds that appeared at retention times commensurate with the arabinose and xylose. These signals are believed to be the five carbon sugar acids or lactones.

Considerable effort was expended trying to quantitate the amounts of the materials present, but the determination of detector response factors from standards varied widely depending on derivatization. Consequently, not even a rough quantitation could be made.

These results do show that the electrooxidation of glucose under the conditions used does not exhibit great specificity. In fact, oxidative attack appears to occur at several sights. These sights include the carbon No. 1, which yields gluconic acid and lactones, and carbon No. 6, which yields glucuronic acid and lactones. In addition, chain degradation results. Greater formation of gluconic acid appeared to occur at the higher electrolysis potential of +950 mV versus SCE (Electrolysis No. 12), while greater chain degradation seemed to result at the lower electrolysis potential of +450 mV versus SCE (Electrolysis Nos. 5 and 10).

Lead Ruthenate Anode

The Teflon-bonded lead ruthenate electrode described in Task 2 was employed for this electrolysis experiment. The preliminary electrolysis was performed with the lead ruthenate electrode to see whether the gas evolved contained CO_2. It was thought that CO_2 may be evolving because rapid gas evolution occurred at what was considered to be a rather negative electrode potential for O_2 evolution. To detect the presence of CO_2, the N_2 purge gas was run through trap of 0.5M NaOH saturated with $Ba(OH)_2$. The electrolyte composition was 0.50M H_2SO_4/1.00M glucose maintained at room temperature. With the electrode at 1100 mV versus SCE, a current of ~70 mA was maintained, which evolved gas. After only a few minutes, a strong positive test for CO_2 was detected by the precipitation of $BaCO_3$. Thus, the lead ruthenate electrode is capable of oxidizing the glucose at least partially to CO_2 at significant rates. Continued gas evolution caused blistering of the Teflon-bonded electrode, indicating that if CO_2 is to be evolved a different electrode design will be required.

Electrooxidation of Lignosulfonic Acid

Limited chronopotentiometry was performed with P&B lignosulfonic acid, Na salt (100 g/L) in 1.00M H_2SO_4 on shiny Pt (1.3 cm^2) at 24°C. Current densities of 0.77 and 7.69 mA/cm^2 were investigated in stirred electrolytes. Electrolyzing at the 7.69 mA/cm^2 rate, the initial depolarization detected at 1000 mV versus SCE was lost in approximately 2 minutes, at which time the

potential had reached the value of 1420 mV versus SCE characteristic of the steady-state value obtained in the absence of the lignosulfonic acid. Continued electrolysis of the lignin solution past 2 minutes resulted in even more positive electrode potentials and 1680 mV versus SCE was attained within 10 minutes, indicating a passivation of the electrode. At the lower rate of 0.77 mA/cm^2, greater depolarization occurred with an initial potential of 600 mV versus SCE than with 1400 mV when lignosulfonic acid was not present. However, this depolarizing effect also did not continue for very long as the potential increased steadily to 1420 mV versus SCE in only 72 minutes. These results and the cyclic voltammetry results that showed the requirement of an organic cleaning of the electrode suggest that under the conditions studied an organic passivating film is produced on the Pt electrode when the lignin is electrooxidized in aqueous electrolyte.

TASKS 4 AND 5

Task 4. Selection of Separation and Purification Techniques for Oxidized Reaction Products

Tasks 2 and 3 did not progress far enough to proceed to Task 4.

Task 5. Determination of Technical and Economic Viability for Pulp and Paper Industry

Data from Tasks 2 and 3 were insufficient to make a determination of economic viability.

2H/RPE/bio-elec2

SUMMARY

The biomass-derivable materials selected for investigation were chosen from the most abundant carbohydrates and lignins. In particular, glucose, its derivatives, and its polymers were considered to be representative of the carbohydrate group and were explored. Lignins selected were those derived from the two principal pulping processes, sulfite and kraft.

A major task, and that on which the greatest effort was expended was the identification of experimental conditions under which the selected biomass materials exhibited anodic electrochemical activity along with the potentials and reaction rates (current densities) of the electrooxidations that occurred. Cyclic voltammetry was the principal survey method used, although steady-state current-voltage curves were also utilized when necessary. The experimental parameters varied were electrolyte (pH), anode material, and temperature.

This variation in experimental conditions resulted in a great diversity of electrochemical behavior for the biomass materials selected, making generalizations difficult. However, all the biomass materials examined showed some anodic activity under some set of experimental conditions at potentials prior to oxygen evolution. In fact, only a very few conditions showed no activity at all. The electrooxidations observed were always very irreversible.

Glucose was the material investigated most extensively. Glucose current-potential data were collected from experimental conditions derived from 7 electrolytes covering pH's from strong acid to strong base, 10 anode materials, and 2 temperatures. This variation of experimental parameters yielded an enormous qualitative and quantitative diversity in electrochemical behavior of glucose. Under many conditions, more than one electrooxidative reaction was signified in the data, indicating parallel and/or consecutive reactions of glucose. For example, as many as 6 anodic peaks were identified on platinum anodes. The electrooxidations of glucose observed under varying experimental conditions appeared over a large potential range from +200 to +1200 mV versus RHE and exhibited current densities from a few mircoamperes to several hundred milliamperes per square centimeter. The general order of increased glucose electrooxidative activity relating to electrolyte pH was alkaline > acid > neutral. This order of reactivity parallels the chemical

reactivity of glucose in these electrolytes. Significant current increases were detected upon increasing the temperature from 23° to 65°C; this increase was from 3 to 10 times the ambient temperature current.

The largest rates of glucose electrooxidation were found with Pd, Ni, and lead ruthenate anodes, which gave current densities for glucose electrooxidation near 100 mA/cm^2 while various forms of Pt, Pb, vitreous carbon, Rh, and ruthenized T gave lesser current densities. Roughening the Pt electrode by platinizing was effective in increasing current densities per electrode area to acceptable levels and the underpotential deposition of Pb, Tr, and Bi increased real current densities on Pt by an order of magnitude.

This voltammetry work clearly showed that electrooxidative activity of glucose abounds at potentials more negative than oxygen evolution and could, in principal, be used as a depolarization agent for the generation of H_2. The experimental factor exhibiting the greatest control over the glucose electrooxidation parameters of potential and current appears to be the anode material which highlights the fact that a highly catalytic reaction is involved. Several anode materials exhibited short-term reaction rates of appreciable magnitude, as mentioned above, but further work is required in order to establish longer term stability of the currents. The data suggest that cells generating H_2 that were depolarized with glucose and presumably other carbohydrates could operate in the range of 600 to 1000 mV.

The diversity of results in the voltammetry data point to the possibility of achieving reaction specificity based on anode material.

Investigation of glucose electrooxidation on the Pt anode was found to be highly dependent upon anode pretreatment, which determines the anode's initial surface condition. Thus, any comparison of glucose voltammetry data requires a rather exact knowledge of the Pt anode's prior history.

Electrooxidation of glucose beyond the gluconic acid stage in the DL region (+300 to +800 mV versus RHE) was shown to occur. Evidence of this was the ability to electrooxidize the partially oxidized glucose derivatives gluconic acid, glucuronic acid, and glucaric acid. In addition, gas was observed to evolve in this region, and bulk electrolysis showed the gas to be CO_2, indicating oxidative carbon-carbon bond cleavage. CO_2 evolution was also detected with the lead ruthenate anode, suggesting that complete electro-

oxidation of the carbohydrates to CO_2 and removal from solution may be possible.

Chromatographic analysis of electrolyzed glucose solutions on Pt indicated that the electrooxidation on this anode was very nonspecific. Numerous anticipated electrooxidation products were identified. Further constant current and constant potential electrolyses indicated that poisoning of the Pt electrode occurred. Substantial regeneration of anode activity was possible by employing potential changes.

The heterogeneous carbohydrate mixture, dextrin, exhibited very nearly the same behavior as glucose under the conditions investigated, suggesting that hydrolyzed carbohydrate mixtures also provide an anodically active media.

Lignin electrooxidation was explored principally on the Pt anode. All the lignins exhibited some electrooxidation at any of the pH's investigated although, like glucose, acid or alkaline showed greater activity than neutral electrolyte. Real current densities on Pt were larger for the lignins than for glucose, typically on the order of a few milliamperes per square centimeter, and appeared at only potentials in the Pt-O region (>800 mV versus RHE). Unlike the carbohydrates, roughening (platinized) or heating had only minor effects on the lignin currents detected.

Two potential problems relating to lignin electrooxidation were identified.

1. The large molecular weight of the lignin fragments makes electrochemical accessibility of the major portion of lignin difficult and may, therefore, keep currents small.

2. The aromatic nature of the lignin may stabilize free radicals that may cause unwanted polymerization of the material.

REFERENCES CITED

1. Coughlin, R. W. and Farooque, M., "Hydrogen Production from Coal, Water and Electrons," Nature 279, 301 (1979).

2. Farooque, M. and Coughlin, R. W., "Electrochemical Gasification of Coal (Investigation of Operating and Variables)," Fuel 59, 705 (1979).

3. Coughlin, R. W. and Farooque, M., "Electrochemical Gasification of Coal — Simultaneous Production of Hydrogen and Carbon Dioxide by a Single Reaction Involving Coal, Water and Electrons," Ind. Eng. Chem. Process Des. Dev. 19, 211 (1980).

4. Coughlin, R. W. and Farooque, M., "Consideration of Electrodes and Electrolytes for Electrochemical Gasification of Coal by Anodic Oxidation," J. Appl. Electrochem. 10, 729 (1980).

5. Okada, G., Guruswamy, V., and Bockris, J. O'M., "On the Electrolysis of Coal Slurries," J. Electrochem. Soc. 128, 2097 (1981).

6. Senftle, F. W., Patton, K. M. and Heard, Jr. I., "Electrolytic Oxidation of Anthracite," Fuel 60, 1131 (1981).

7. Appleby, A. J. and Pinchon, B., "Electrochemical Aspects of the H_2SO_4-SO_2 Thermoelectrochemical Cycle for Hydrogen Production," Int. J. Hydrogen Energy 11, 347 (1981).

8. Lu, P. W. T., Garcia, E. R. and Ammon, R. L., "Recent Developments in the Technology of Sulphur Dioxide Depolarized Electrolysis," J. Appl. Electrochem. 11, 347 (1981).

9. St. John, M. R., Furgala, A. J. and Sammells, A. F., "Hydrogen Generation from Glucose Depolarized Water Electrolysis," J. Electrochem. Soc. 128, 1174 (1981).

10. Lehninger, A. L., Biochemistry, Ch. 11. New York: Worth, 1970.

11. Pigman, W. and Horton, D., "1. Introduction: Structure and Stereochemistry of the Monosaccharides," in Pigman, W. and Horton, D., eds., The Carbohydrates, Chemistry and Biochemistry, Vol. IA. New York: Academic Press, 1972.

12. Schaffer, R., "2. Occurence, Properties, and Preparation of Naturally Occurring Monosaccharides (Including 6-Deoxy Monosaccharides Sugars)," ibid.

13. Sjostrom, E., Wood Chemistry. London: Academic Press, 1981.

14. Goldstein, I. S., "Chemicals form Cellulose," in Goldstein, I. S., ed., Organic Chemicals from Biomass, Ch. 6. Boca Raton, Florida: CRC Press, 1981.

15. Timell, T. E., "Wood Hemicelluloses: Part I and II," Adv. Carbohyd. Chem. 19, 247 (1964) and 20, 410 (1965).

16. Wilke, K. C. B., "The Hemicelluloses of Grasses and Cereals," Adv. Carbohyd. Chem. 36, 215 (1979).

17. Whistler, R. L. and Richards, E. L.,"Hemicelluloses," in Pigman, W., Horton, D. and Herp, A., Eds., The Carbohydrates, Chemistry and Biochemistry, Vol IIA. New York: Academic Press, 1970.

18. Fedoronko, M., "The Electrochemistry of Carbohydrates and Their Derivatives," Adv. Carbohyd. Chem. Biochem. 29, 107 (1974).

19. Weinberg, N. L. and Weinberg, H. R., "Electrochemical Oxidation of Organic Compounds," Chem. Rev. 68, 449 (1968).

20. Karabinos, J. V., "Anodic Oxidation of Sugars," Rev. Euclides 14, 211 (1954).

21. Bockris, J. O'M., Piersma, B. J. and Gileadi, E., "Anodic Oxidation of Cellulose and Lower Carbohydrates," Electrochim. Acta. 9, 1329 (1964).

22. Hay, G. W. and F. Smith, "Electrolysis of Low Molecular Weight Carbohydrates in Non-Aqueous Media. I. The Products of Electrolysis of Monosaccharides," Can. J. Chem. 47, 417 (1969).

23. Isbell, H. S., Frush, H. L. and Bates, F. J., "Manufacture of Calcium Gluconate by Electrolytic Oxidation of Dextrose," Ind. Eng. Chem. 24, 375 (1932).

24. Fink, C. G. and Summers D. B., "Electrolytic Preparation of Calcium Gluconate and Other Salts of Aldonic Acids," Trans. Electrochem. Soc. 74, 625 (1938).

25. Appleby, A. J. and Van Drunen, C., "Anodic Oxidation of Carbohydrates and Related Compounds in Neutral Saline Solution," J. Electrochm. Soc. 118, 95 (1971).

26. Yao, S. J., Appleby, A. J. and Wolfson, S. K. Jr., "Anomeric Effects in the Electrodic Oxidation of Carbohyrates," Z. Physik. Chem. Neue Folge 82, 15 (1972).

27. Yao, S. J. et al., "Anodic Oxidation of Carbohydrates and their Derivatives in Neutral Saline Solution," Nature 224, 921 (1969).

28. Rao, M. L. B. and Drake, R. F., "Studies of Electrooxidation of Dextrose in Neutral Media," J. Electrochem. Soc. 116, 334 (1969).

29. Skou, E., "The Electrochemical Oxidation of Glucose on Platinum. I. Oxidation in 1M H_2SO_4," Electrochem. Acta. 22, 313 (1977).

30. Skou, E. M., "The Inhibition of the Electrochemical Oxidation of Glucose at Platinum at pH = 7.4 by Chloride Ions," Acta. Chem. Scand. 27, 2239 (1973).

31. Ernst, S., Heitbaum, J. and Hamann, C. H.,"The Electrooxidation of Glucose in Phosphate Buffer Solutions. Part I: Reactivity and Kinetics Below 350 mV/RHE," J. Electroanal. Chem. 100, 173 (1979).

32. Ernst, S., Heitbaum, J. and Hamann, C. H., "The Electrooxidation of Glucose in Phosphate Buffer Solutions: Kinetics and Reaction Mechanism," Ber. Bunsenges. Phys. Chem. 84, 50 (1980).

33. Gebhardt, U., Rao, J. R. and Richter, G. J., "A Special Type of Raney-Alloy Catalyst Used in Compact Biofuel Cells," J. Appl. Electrochem. 6, 127 (1976).

34. Giner, J. and Malachesky, P., "Anodic Oxidation of Glucose." Proceedings of the Artificial Heart Program Conf., Washington, D.C., June 9-13, 1969.

35. Gough, D. A., Anderson, F. L., Giner, J. Cotton, C. K. and Soeldner, J. S., "Effect of Coreactants on Electrochemical Glucose Oxidation," Anal. Chem. 50, 941 (1978).

36. Marincic, L., Soeldner, J. S., Cotton, C. K. Giner, J. and Morris, S., "Electrochemical Glucose Oxidation on a Platinized Platinum Electrode in Krebs-Ringer Solution I. Potentiodynamic Studies," J. Electrochem. Soc. 126, 43 (1979).

37. Lerner, H., Giner, J., Soeldner, J. S. and Cotton, C. K., "Electrochemical Glucose Oxidation on a Platinized Platinum Electrode in Krebs-Ringer Solution II. Potentiostatic Studies," J. Electrochem. Soc. 126, 237 (1979).

38. Marincic, L., Soeldner, J. S., Giner, J., and Cotton, C. K., "Electrochemical Glucose Oxidation on a Platinized Platinum Electrode in Krebs-Ringer Solution III. Effect of Urea," J. Electrochem. Soc. 126, 1687 (1979).

39. deMele, M. F. L., Videla, H. A. and Arvia, A. J., "503-Comparative Study of the Electrochemical Behaviour of Glucose and Other Compounds of Biological Interest," Bioelectrochem. Bioenerg. 9, 469 (1982).

40. deMele, Videla, H. A. and Arvia, A. J., "Potentiodynamic Study of Glucose Electrooxidation at Bright Platinum Electrodes," J. Electrochem. Soc. 129, 2207 (1982).

41. Pigman, W. and Anet, E. F. L. J., "Mutarotations and Actions of Acids and Bases," Ch. 4 in Pigman, W. and Horton, D., eds., The Carbohydrates, Chemistry and Biochemistry, Vol IA. New York: Academic Press, 1972.

42. Feather, M. S. and Harris, J. F., "Dehydration Reactions of Carbohydrates," Adv. Carbohyd. Chem. Biochem. 28, 161 (1973).

43. Pigman, W. and Isbell, H. S., "Mutarotation of Sugars in Solution: Part I," Adv. Carbohyd. Chem. 23, 11 (1968); Isbell, H. S. and Pigman, W., "Mutarotation of Sugars in Solution: Part II," Adv. Carbohyd. Chem. Biochem. 24, 13 (1969).

44. Theander, O., "Acids and Other Oxidation Products," Ch. 23 in Pigman, W., Horton, D. and Wander, J. D., Eds., The Carbohydrates, Chemistry and Biochemistry, Vol. IB. New York: Academic Press, 1980.

45. Pearl, I. A., The Chemistry of Lignin. New York: Marcel Dekker, 1967.

46. Sarkanen, K. V. and Ludwig, C. H., Eds., Lignins — Occurrence, Formation, Structure, and Reactions. New York: Wiley-Interscience, 1971.

47. Goheen, D. W., "Chemicals from Lignin," Ch. 8 in Goldstein, I. S., Ed, Organic Chemicals from Biomass. Boca Ration, Florida: CRC Press, 1981.

48. Gould, R. F., Ed., Lignin Structure and Reactions, ACS Adv. Chem. Series No. 59. Washington D.C.: Am. Chem. Soc., 1966.

49. Brauns, F. E., The Chemistry of Lignin. New York: Academic Press, 1952.

50. Bailey, A. and Brooks, H. M., "Electrolytic Oxidation of Lignin," J. Am. Chem. Soc. 68, 445 (1945).

51. Demin, V. A., Davydov, V. D. and Gogomolov, B. D., "Study of the Electrochemical Oxidation of Lignin," Kim. Drev. 2, 41 (1979).

52. Korytheseva, V. F., Vodzinskii, Yu, V. and Skvortsov, N . P., "Voltammetric Oxidation of Lignins at a Graphite Electrode. 2. Electrooxidation Currents of Lignin," Kim. Drev. 1, 87 (1979).

53. Kovalenko, E. K., Shifron, E. M. and Raskin, N. M., "Electrochemical Oxidation of the Natural Polymer Lignin," Novosti Elektrokhim. Org. Soedin, Tezisy Dokl. Vses. Soveshch. Elektrockhim. Org. Soedin. 8, 24-25 (1973).

54. Kovalenko, E. I., Smirnov, V. A. and Shalimov, V. N., "Influence of the Anode Material and Electrolysis Time on the Course of Electrochemical Oxidation of Hydrolytic Lignin," J. Appl. Chem. U.S.S.R. 50, 1741 (1977).

55. Forostyan, Yu. N., Forostyan, E. I. and Soroka, I. I., "Reactions of Hydrolysis Lignin of Softwood Under Electrolytic Oxidation Conditions," Kim. Prir. Soedin 3, 408 (1976).

56. Steelink, C. and Britton, W. E., "The Electrochemical Oxidation of Lignin Model Compounds I. Oxidation of 3,5-dimethoxy-4-hydroxy-2-methylbenzyl Alcohol," Tetrahedron Lett. 33, 2869 (1974).

57. Britton, W. E. and Steelink, C., "The Electrochemical Oxidation of Lignin Model Compounds II. Oxidation of 3,5-dimethoxy-4-hydroxy acetophenone," Tetrahedron Lett. 33, 2873 (1974).

58. Chabaud, B., Sundholm, F. and Sundholm, G., "Anodic Oxidation of Some Pherrols Related to Lignin - II. Oxidation of Isoeugenol Methylether and 4-Propylveratrole in Acetonitrile," Electrochim. Acta 23, 659 (1978).

59. Vermillion, F. J., Jr., and Pearl, I. A., "Anodic Reactions of Simple Phenolic Compounds," J. Electrochem. Soc. 111, 1392 (1964).

60. Sundholm, F. and Sundholm, G., "Anodic Oxidation as a Tool for Mechanistics Studies, Guaiacol and 4-Propyl Guaiacol in Aprotic Media," Holzforschung 36, 71 (1982).

61. Green J. W., "Oxidative Reactions and Degradations," Ch. 24 in Pigman, W., Horton, D. and Wander, J. D., Eds., The Carbohydrates, Chemistry and Biochemistry, Vol. IB. New York: Academic Press, 1980.

62. Sawyer, D. T. and Roberts, Jr. J. L., Experimental Electrochemistry for Chemists, p. 36. New York: John Wiley, 1974.

63. Gilman, S., "Measurement of Hydrogen Adsorption by the Multipulse Potentiodynamic (MPP) Method," J. Electroanal Chem. 7, 382 (1964).

64. Biegler, T., Rand, D. A. J. and Woods, R., "Limiting Oxygen Coverage on Platinized Platinum; Relevance to Determination of Real Platinum Area by Hydrogen Adsorption," J. Electroanal. Chem. 29, 269 (1971).

65. Gilman, S., "The Anodic Film on Platinum Electrodes," Electroanal. Chem. 2, 111 (1967).

66. Adams, R. N., Electrochemistry at Solid Electrodes, Ch. 7. New York: Marcel Dekker, 1960.

67. Isbell, H. S., "Enolization and Oxidation Reactions of Reducing Sugars," in Ch. 5 Carbohydrates in Solution, ACS Adv. Chem. Series No. 117. Washington D.C.: Am. Chem. Soc., 1971.

68. Forsskahl, I., "Reactions of D-Xylose and D-Glucose in Alkaline, Aqueous Solutions," Carbohyd. Res. 48, 13 (1976).

69. Izatt, R. M., Rytting, J. H., Hansen, L. D. and Christensen, J. J., "Thermodynamics of Proton Dissociation in Dilute Aqueous Solution. V. An Entropy Titration Study of Adenosine, Pentoses, Hexoses, and Related Compounds," J. Am. Chem. Soc. 88, 2641 (1966).

70. Christensen, J. J., Rytting, J. H. and Izatt, R. M., "Thermodynamics of Proton Dissociation in Dilute Aqueous Solution. Part XV. Proton Dissociation from Several Monosaccharides at 10 and 40°C," J. Chem. Soc. (B), 1646 (1970).

71. Giner, J., "Electrochemical Reduction of CO_2 on Platinum Electrodes in Acid Solutions," Electrochim. Acta 8, 857 (1963).

72. Giner, J., "The Anodic Oxidation of Methanol and Formic Acid and the Reductive Adsorption of CO_2," Electrochim. Acta 9, 63 (1964).

73. Brieter, M. W., "Voltammetric Study of the Inhibition of Methanol Oxidation on Platinum by CHloride Ion in Acid Solution," Electrochim. Acta 9, 827 (1964).

74. Snell, K. D. and Keenan, A. G., "Chloride Inhibition of Ethanol Electro-oxidation at a Platinum Electrode in Aqueous Acid solution," Electrochim. Acta. 26, 1339 (1981).

75. Wroblowa, H., Piersma, B. J. and Bockris, J. O'M., "Studies of the Mechanism of the Anodic Oxidation of Ethylene in Acid and Alkaline Media," J. Electroanal. Chem. 6, 401 (1963).

76. Heyns, K. and Paulsen, H., "Selective Catalytic Oxidation of Carbohydrates Employing Platinum Catalysts," Adv. Carbohyd. Chem. 17, 169 (1962).

77. Dirkx, J. M. H. and Vander Baan, H. S., "The Oxidation of Glucose with Platinum on Carbon as atalyst," J. Catalysis 67, 1 (1981).

78. DeWit, G., DeVlieger, J. J., Kock-vanDalen, A. C., Heus, Rl, Laroy, R., Van Hengstun, A. J., Kieboam, A. P. G. and Van Bekkum, H., "Catalytic Dehydrogenation of Reducing Sugars in Alkaline Solution," Carbohyd. Res. 91, 125 (1981).

79. Dirkx, J. M. H., Vander Baan, H. S. and Van den Broek, J. M. A. J. J., "The Preparation of D-Glucaric acid by the Oxidation of D-Gluconic Acid Catalysed by Platinum on Carbon," Carbohyd. Res. 59, 63 (1977).

80. Dirkx, J. M. J. and Vander Baan, H. S., "The Oxidation of Gluconic Acid with Platinum on Carbon as Catalyst," J. Catalysis 67, 14 (1981).

81. Gileadi, E. and Piersma, B., "The Mechanism of Oxidation of Organic Fuels," Mod. Aspects Electrochem. 4, 47 (1966).

82. Brieter, M. W., "Adsorption of Organic Species on Platinum Metal Electrodes," Mod. Aspects Electrochem. 10, 161 (1975).

83. Wieckowski, A., Andreev, V. N., Zelenay, R. Sobkowski, J. and Kazarinov, V. E., "Effect of Surface Preparation Technique on the Composition of Methanol Adsorption Products," Sov. Electrochem. 16, 570 (1980).

84. W. E. O'Grady, S. Srinivasan, and R. F. Dudley, Eds. The Electrocatalysis of Fuel Cell Reactions. Princeton N. J.: The Electrochemical Society, Inc., 1979.

85. Adzic, R. R., Simic, D. N., Despic, A. R. and Drazic, D. M,. "Electrocatalysis by Foregin Metal Monolayers: Oxidation of Formic Acid on Platinum," J. Electroanal. Chem. 65, 587 (1975).

86. Spasojevic, M. D., Adzic, R. R. and Despic, A. R., "Electrocatalysis on Surfaces Modified by Foreign Metal Adatoms: Oxidation of Formaldehyde on Platinum," J. Electroanal. Chem. 109, 261 (1980).

87. Takamura, K. and Sakamoto, M., "Catalytic Effects of Metal Submonolayers Formed by Faradaic Adsorption on the Anodic Oxidation of Ascorbic Acid at a Platinum Electrode," J. Electroanal. Chem. 113, 273 (1980).

88. Adzic, R. R., O'Grady, W. E. and Srinivasan, S., "Oxidation of HCOOH and CH_3OH on Platinum Modified by Foreign Metal Adatoms in 85% Phosphoric Acid," J. Electrochem. Soc. 128, 1913 (1981).

89. Adzic, R. R., "Some Recent Developments in Electrocatalysis on Surfaces Modified by Foreign Metal Adatoms," in W. E. O'Grady, P. N. Ross Jr., and F. G. Will, Eds., Electrocatalysis, pp. 309-322. Pennington, N.J.: The Electrochemical Society, 1982.

90. Motoo, S. and Shibata, M., "Electrocatalysis by Ad-Atoms. Part IX A Fast Parallel Path for Formaldehyde Oxidation on a Platinum Electrode by Oxygen Adsorbing Ad-Atoms," J. Electroanal. Chem. 139, 119 (1982).

91. Sakamoto, M. and Takamura, K., "Catalytic Oxidation of Biological Components on Platinum Electrodes Modified by Adsorbed Metals. Anodic Oxidation of Glucose," J. Electroanal. Chem. Bioelectrochem. Bioenerg. 9, 571 (1982).

92. Tilak, B. V., Lu, P. W. T., Colman, J. E. and Srinivasan, S. "Electrolytic Production of Hydrogen," Ch 1 in Bockris, J. O.'M., Conway, B. E., Yeager, E. and White, R. E., Eds., Comprehensive Treatise of Electrochemistry, Vol 2. New York: Plenum Press, 1981.

93. Fleischmann, M. Korinek, K. and Pletcher, D., "The Oxidation of Organic Compounds at a Nickel Anode in Alkaline Solution," J. Electroanal. Chem. 31, 39 (1971).

94. Vertes, G., Horanyi, G. and Nagy, F., "Oxidation on the Nickel Hydroxide Electrode, I. Principals of the Study," Acta Chim. Acad. Sci. Hung. 67, 145 (1971).

95. Horanyi, G., Vertes, G. and Nagy, F., "Oxidation on the Nickel Hydroxide Electrode, II. Some Problems of the Practical Application of the Electrode With Special Reference to the Oxidation of Di-O-Isopropylidenesorbose," Acta. Chem. Acad. Sci. Hung. 67, 357 (1971).

96. Vertes, G., Horanyi, G. and Nagy, F., "A New Method for the Electrochemical Oxidation of Alcohols," Tetrahedron 28, 37 (1972).

97. Robertson, P. M., "On the Oxidation of Alcohols anbd Amines at Nickel Oxide Electrodes: Mechanistic Aspects," J. Electroanal. Chem. 111, 97 (1980).

98. Fleischmann, M., Korinek and Pletcher, D., "The Kinetics and Mechanism of the Oxidation of Amines and Alcohols at Oxide-Covered Nickel, Silver, Copper, and Cobalt Electrodes," J. Chem. Soc. Perkin II, 1396 (1972).

99. Trasatti, S., Ed., Electrodes of Conductive Metallic Oxides, Part A and B. New York: Elsevier, 1980 and 1981.

100. Horowitz, H. H., Horowitz, H. S. and Longo, J. M., "Electro-Organic Oxidations on Lead Ruthenate," in W. E. O'Grady, R. N. Ross Jr., and F. G. Will, Eds., Electrocatalysis, Proc. Vol. 82-2, Pennington, N.J.: The Electrochemical Society, 1982.

101. Horowitz, H. S., Longo, J. M. and Haberman, J. J., "$Pb_2[M_{2-x}Pb_x]O_{7-y}$ Compounds Wherein M is Ru, Ir, or Mixtures Thereof, and Method of Preparation," U.S. Patent 4,124,539, Nov. 7, 1978.

102. Trasatti, S. and Lodi, G., "Oxygen and Chlorine Evolution at Conductive Metal Oxides," Ch. 10 in Trasatti, S., Ed., Electrodes of Conductive Metallic Oxides, Part A and B. New York: Elsevier, 1980 and 1981.

103. Denton, D. A., Harrison, J. A. and Knowles, R. I., "The Oxygen Evolution Reaction on RuO_2-TiO_2 Electrodes," Electrochim. Acta 26, 1197 (1981).

104. Caldwell, D. L., "Production of Chlorine," Ch. 2 in Bockris, J. O'M., Conway, B. E., Yeager, E. and White, R. E., Eds., Comprehensive Treatise of Electro-Chemistry, Vol. 2. New York: Plenum Press, 1981.

105. Yeo, R. S., Orehotsky, J., Visscher, W. and Srinivason, S., "Ruthenium-Based Oxides as Electrocatalysts for Oxygen Evolution in Acid Electrolytes," J. Electrochem. Soc. 128, 1900 (1981).

106. Paturau, J. M., By-Products of the Cane Sugar Industry. New York: Elsevier, 1969.

107. Raicheva, S. N., Christov, M. V. and Sokolova, E. F., "Effect of Temperature on the Electrochemical Behavior of Aliphatic Alcohols," Electrochem. Acta 26, 1669 (1981).

108. The Merck Index, 9th ed., p. 2911, Rathway, N.J.: Merk & Co., 1976.

109. Sharpe, T. F., "The Adsorption f Lignosulphate onto Lead Surfaces - I. Adsorption on Lead Powder and Lead Sulphate," Electrochim. Acta 14, 635 (1969).

110. Wojtowicz, J., Marincic, N., and Conway, B. E., "Oscillatory Kinetics in the Electrochemical Oxidation of Formate and Ethylene," J. Chem. Phys. 48, 4333 (1968).

111. Verhaar, L. A. Th. and deWitt, H. G. J., "The Gas Chromatographic Determination of Polyhydroxy Monocarbonic Acids Obtained by Oxygenation of Hexosesin Aqueous Alkaline Solutions," J. Chromatog. 41, 168 (1969).

112. Sweeley, C. C., Bentley, R., Makita, M. and Wells, W. W., "Gas-Liquid Chromatography of Trimethylsilyl Derivatives of Sugars and Related Substances," J. Am. Chem. Soc. 85, 2497 (1963).

113. Petersson, G., "Mass-Spectrometry of Aldonic and Deoxyaldonic Acids as Trimethylsilyl Derivatives," Tetrahedron 26, 3413 (1970).

114. Petersson, G., Samuelson, O., Anjou, K., and vonSydow, E., "Mass Spectrometric Identification of Aldonolactones as Trimethylsilyl Esters," Acta. Chem. Scand. 21, 1251 (1967).

This report was done with support from the Department of Energy. Any conclusions or opinions expressed in this report represent solely those of the author(s) and not necessarily those of The Regents of the University of California, the Lawrence Berkeley Laboratory or the Department of Energy.

Reference to a company or product name does not imply approval or recommendation of the product by the University of California or the U.S. Department of Energy to the exclusion of others that may be suitable.

TECHNICAL INFORMATION DEPARTMENT
LAWRENCE BERKELEY LABORATORY
UNIVERSITY OF CALIFORNIA
BERKELEY, CALIFORNIA 94720